

Energy Research and Development Division  
FINAL PROJECT REPORT

**SUPPORT FOR THE WESTERN  
COOLING EFFICIENCY CENTER**

Prepared for: California Energy Commission  
Prepared by: Western Cooling Efficiency Center  
University of California, Davis



**WCEC**  
WESTERN COOLING EFFICIENCY CENTER

**UCDAVIS**  
UNIVERSITY OF CALIFORNIA

JULY 2015  
CEC-500-2015-072

**PREPARED BY:**

***Primary Author(s):***

Mark Modera, PI  
Curtis Harrington  
Nasim Tajmand  
David Grupp

Western Cooling Efficiency Center  
University of California, Davis  
215 Sage Street, Suite 100  
Davis CA 95616  
Phone: 530-752-0799 | Fax: 530-754-7672  
<http://wcec.ucdavis.edu>

***Contract Number: 500-08-042***

***Prepared for:***

**California Energy Commission**

Matthew Fung  
***Contract Manager***

Virginia Lew  
***Office Manager***  
***Energy Efficiency Research Office***

Laurie ten Hope  
***Deputy Director***  
***ENERGY RESEARCH AND DEVELOPMENT DIVISION***

Robert P. Oglesby  
***Executive Director***

**DISCLAIMER**

This report was prepared as the result of work sponsored by the California Energy Commission. It does not necessarily represent the views of the Energy Commission, its employees or the State of California. The Energy Commission, the State of California, its employees, contractors and subcontractors make no warranty, express or implied, and assume no legal liability for the information in this report; nor does any party represent that the uses of this information will not infringe upon privately owned rights. This report has not been approved or disapproved by the California Energy Commission nor has the California Energy Commission passed upon the accuracy or adequacy of the information in this report.

## **ACKNOWLEDGEMENTS**

The Western Cooling Efficiency Center wishes to thank the many researchers, post-doctoral candidates, graduate and undergraduate students who participated in the programs sponsored under this interagency agreement. Without them, this series of projects could not have been completed. Yet with the experience they gained through this effort, they became better-trained engineers, better prepared to enter the professional workforce with practical, professional experience, and able to more immediately contribute in their chosen field. And based on their experiences with this project, they have a far more developed ability to bring experience in energy efficiency, and efficiencies in particular, to their new roles.

The Western Cooling Efficiency Center wishes to thank the California Energy Commission for its foresight in establishing this project as a broad, flexible interagency agreement with a flexible, responsive oversight structure. Its structure allowed the Western Cooling Efficiency Center to follow a variety of technologies and processes; the vast majority of them were successful, with their funding taken on by private sources or other sponsoring agencies, freeing up funds to pursue new leads and providing far greater benefit to the state than the amounts invested by the California Energy Commission. For the few ideas that proved disappointing, the Western Cooling Efficiency Center was able to quickly reroute those funds toward other, more productive lines of research with no administratively-imposed down-time. The nature of this project allowed the Western Cooling Efficiency Center to develop long-term staff continuity that allowed the Center to follow promising developments from research to demonstrations and, in notable cases, to the intellectual property and technology transfer phases. Additionally, the contract's flexibility allowed the center to rapidly commence projects on new ideas, well faster than is normally the case. Moreover, its innovative oversight structure helped reinforce existing Western Cooling Efficiency Center ties to industry, and kept projects under this contract focused on ideas most beneficial to the citizens of California.

## PREFACE

The California Energy Commission Energy Research and Development Division supports public interest energy research and development that will help improve the quality of life in California by bringing environmentally safe, affordable, and reliable energy services and products to the marketplace.

The Energy Research and Development Division conducts public interest research, development, and demonstration (RD&D) projects to benefit California.

The Energy Research and Development Division strives to conduct the most promising public interest energy research by partnering with RD&D entities, including individuals, businesses, utilities, and public or private research institutions.

Energy Research and Development Division funding efforts are focused on the following RD&D program areas:

- Buildings End-Use Energy Efficiency
- Energy Innovations Small Grants
- Energy-Related Environmental Research
- Energy Systems Integration
- Environmentally Preferred Advanced Generation
- Industrial/Agricultural/Water End-Use Energy Efficiency
- Renewable Energy Technologies
- Transportation

*Support for Western Cooling Efficiency Center* is the final report for the Western Cooling Efficiency Center project (contract number 500-08-042) conducted by The University of California at Davis, Western Cooling Efficiency Center. The information from this project contributes to Energy Research and Development Division's Buildings End-Use Energy Efficiency Program.

For more information about the Energy Research and Development Division, please visit the Energy Commission's website at [www.energy.ca.gov/research/](http://www.energy.ca.gov/research/) or contact the Energy Commission at 916-327-1551.

## ABSTRACT

This report includes the research and results from the Western Cooling Efficiency Center's work under an interagency agreement from the California Energy Commission. The research period spans almost six years of work, from June 2009 to March 2015. This comprehensive report contains findings from four of the most recent projects completed by the Western Cooling Efficiency Center under the interagency agreement, and a prospectus of previously completed research projects. Also included are results and links to academic/research papers created from the Western Cooling Efficiency Center's work under the interagency agreement, and a brief mention of continuing support for some of these projects under new sponsors.

**Keywords:** Energy Efficiency, HVAC, air conditioning, thermal, envelope, water, water-use, rooftop unit, coefficient of performance, heating, ventilation, geothermal, ground, source, heat, pump, cooling, cool, rainwater, aerosol, adhesive, building, home, residential, commercial, industrial, evaporative, direct, indirect

Please use the following citation for this report:

Modera, Mark; Harrington, Curtis; Tajmand, Nasim; Grupp, David. UC Davis Western Cooling Efficiency Center, 2015. *Support for the Western Cooling Efficiency Center*. California Energy Commission. Publication number: CEC-500-2015-072

# TABLE OF CONTENTS

|   |            |
|---|------------|
| <b>Acknowledgements</b> .....   | <b>i</b>   |
| <b>PREFACE</b> .....  | <b>ii</b>  |
| <b>ABSTRACT</b> .....   | <b>iii</b> |
| <b>TABLE OF CONTENTS</b> .....  | <b>iv</b>  |
| <b>LIST OF FIGURES</b> .....  | <b>vii</b> |
| <b>LIST OF TABLES</b> .....   | <b>xi</b>  |
| <b>EXECUTIVE SUMMARY</b> .....  | <b>1</b>   |
| Introduction .....  | 1          |
| Project Purpose.....  | 1          |
| Project Results .....   | 1          |
| Project Benefits .....  | 1          |
| Project Purpose.....  | 1          |
| Project Process and Results.....  | 2          |
| Project Benefits .....  | 2          |
| Project Purpose.....  | 3          |
| Project Process and Results.....  | 3          |
| Project Benefits .....  | 4          |
| Project Purpose.....  | 4          |
| Project Results .....   | 4          |
| <b>CHAPTER 1: Building Envelope Sealing using an Adhesive Mist</b> .....  | <b>6</b>   |
| 1.1 Problem Statement .....   | 6          |
| 1.2 Previous Research .....   | 6          |
| 1.2.1 Initial Laboratory Testing .....                                    | 6          |
| 1.2.2 First Field Test: Stockton, California (Habitat for Humanity) ..... | 7          |
| 1.2.3 Laboratory Testing Refinements after First Field Test.....          | 8          |
| 1.2.4 Field Test After Previous Laboratory Refinements.....               | 9          |
| 1.2.5 Field Test: Honda Smart Home.....                                   | 10         |

|  |   |           |
|--|---|-----------|
| 1.3  | Current Research (2014).....  | 13        |
| 1.3.1  | Laboratory Testing: Particle Size Testing .....   | 13        |
| 1.3.2  | Field Testing: Current Multi-Nozzle Air Based Injector System.....  | 15        |
| 1.3.3  | Field Testing: 6 Large Homes in Clovis, California .....  | 16        |
| 1.4  | Conclusion and Path Forward .....   | 27        |
| <b>CHAPTER 2: Studies in Rainwater Collection and Storage for Evaporative Cooling.....</b> |   | <b>29</b> |
| 2.1  | Water quality in an above ground rainwater cistern.....   | 29        |
| 2.1.1  | Quantifying roof runoff volume .....  | 30        |
| 2.1.2  | Methods, Procedures, and Facilities.....  | 31        |
| 2.1.3  | Results and discussion .....  | 34        |
| 2.1.4  | Conclusion.....   | 38        |
| 2.2  | Experimental results of different water quality in evaporatively cooled condenser with a copper coil..... | 39        |
| 2.2.1  | California Water Quality Analysis by Water District and Climate zone .....                                | 39        |
| 2.2.2  | Systematic testing of influential water quality parameters.....   | 41        |
| 2.2.3  | Experimental Setup.....   | 42        |
| 2.2.4  | Water chemistry analysis.....   | 44        |
| 2.2.5  | Initial results .....   | 45        |
| 2.2.6  | Recommendations for Follow-up Experiments.....  | 51        |
| <b>CHAPTER 3: New Techniques for Ground Source Heat Pumps (GSHP) .....</b>                 |   | <b>52</b> |
| 3.1  | Problem Statement.....  | 52        |
| 3.2  | GSHP Technologies .....   | 52        |
| 3.3  | Demonstration: Directional Earth Bore Exchanger at Rio Mondego.....                                       | 54        |
| 3.3.1  | Thermal Analysis .....  | 55        |
| 3.4  | Demonstration: Large Diameter Earth Bore Exchanger Demonstration: Honda Smart Home 61                     |           |
| 3.5  | Demonstration: Large Diameter Earth Bore Exchanger at Capay, California.....                              | 62        |
| 3.5.1  | System Design and Construction.....   | 63        |
| 3.5.2  | Thermal Analysis .....  | 65        |

|  |   |           |
|--|---|-----------|
| 3.5.3  | GSHP Performance Results in Various California Climate Zones.....                           | 69        |
| 3.5.4  | Conclusions and Recommendations .....   | 72        |
| <b>CHAPTER 4: Improving Energy Efficiency in the Hospitality Sector (PCMs) .....</b> |   | <b>74</b> |
| 4.1  | Problem Statement.....  | 74        |
| 4.2  | Previous Research: Laboratory Apparatus, Thermal Cycling and Mechanical Cycling Tests ..... | 75        |
| 4.2.1  | Mechanical Cycling Tests.....   | 75        |
| 4.2.2  | Thermal Performance Tests - Laboratory .....  | 79        |
| 4.3  | Current Research: Thermal Performance Tests – Field .....                                   | 83        |
| 4.3.1  | Setup & Instrumentation.....  | 83        |
| 4.3.2  | Experimental Approach & Progress to Date .....  | 85        |
| <b>CHAPTER 5: Previously Completed Research Projects .....</b>                       |   | <b>89</b> |
| 5.1  | Evaporative Cooler Precooling .....   | 89        |
| 5.1.1  | Problem Statement.....  | 89        |
| 5.1.2  | Research Findings & Results .....   | 89        |
| 5.2  | Swimming Pools as Heatsinks for Unitary Air Conditioners.....                               | 91        |
| 5.2.1  | Problem Statement.....  | 91        |
| 5.2.2  | Research Findings & Results .....   | 92        |
| 5.3  | The Western Cooling Challenge .....   | 94        |
| 5.3.1  | Problem Statement.....  | 94        |
| 5.3.2  | Research Findings & Results .....   | 94        |
| 5.4  | Hybrid Evaporative/DX Cooling Equipment First Principles Modeling.....                      | 100       |
| 5.4.1  | Problem Statement.....  | 100       |
| 5.4.2  | Research Findings & Results .....   | 100       |
| 5.5  | Optimized Hybrid Evaporative Cooling (Water-Use Efficiency) .....                           | 103       |
| 5.5.1  | Problem Statement.....  | 104       |
| 5.5.2  | Research Findings & Results .....   | 104       |
| 5.6  | Fault Detection & Diagnostics.....  | 107       |
| 5.6.1  | Problem Statement.....  | 107       |

|                         |                                   |            |
|-------------------------|-----------------------------------|------------|
| 5.6.2                   | Research Findings & Results ..... | 107        |
| 5.7                     | Industry Support & Outreach ..... | 113        |
| <b>REFERENCES .....</b> |                                   | <b>114</b> |
| <b>GLOSSARY .....</b>   |                                   | <b>115</b> |

## **LIST OF FIGURES**

|  |    |
|--|----|
| Figure 1: Leakage Sealing Time Profiles for Lab Tests .....  | 7  |
| Figure 2: Initial Injector System Used a Single Air-based Nozzle.....  | 8  |
| with the Sealant Contained in the Box Below It. ....   | 8  |
| Figure 3: Comparison of Old Injector, New Injector and Old and New Sealant .....   | 9  |
| Figure 4 (left): Sealing Profile for Apartment Field Test (preinsulation phase) Figure 5 (right):<br>Sealing Profile for Different Apartment Field Test (after drywall)..... | 10 |
| Figure 6: Aerosol Seals from the Honda Smart Home.....   | 11 |
| Figure 7: Summary of Results from Aerosol Envelope Sealing.....  | 12 |
| Demonstration in Honda Smart Home .....  | 12 |
| Figure 8: (left) WCEC Engineer Inspects the Cascade Impactor (right) Impactor Plate after Test<br>with Deposition .....  | 13 |
| Figure 9: Cascade Impactor Test Apparatus .....  | 14 |
| Figure 10: Mass Median Diameter Calculated from Cascade Impactor Results at Different<br>Operating Conditions.....   | 15 |
| Figure 11: Leaks Sealed vs. Amount of Sealant Used .....   | 15 |
| Figure 12: New Sealing Method from Field Test vs. Previous Aerosol Method Field Tests.....   | 16 |
| Figure 13: Clovis Aerosol Test Housing Development and Stage of Construction the Homes<br>Were in Before Sealing. ....   | 17 |
| Figure 14: Showing Supply Ducts Covered to Prevent Dust from Entering Duct System.....   | 18 |
| Figure 15: Network Access Point Prepared for Aerosol Sealing Process.....  | 19 |
| Figure 16: Untaped Network Access Points on an Interior Wall with Significant Deposition .....   | 19 |
| Figure 17: Hole Near Ventilation Supply Duct.....  | 20 |
| Figure 18: Nozzles Placement for One of the Aerosol Envelope Sealing Installations .....   | 21 |
| Figure 19: Profiles for the Sealing Demonstrations.....  | 23 |
| Figure 20: Sealing Rate Profile for Each Sealing Demonstrations.....   | 25 |

|  |    |
|--|----|
| Figure 21: Laboratory Sealant Test Using Black-light Sensitive Dye (left), WCEC Student Researcher Installs Aerosol Distance Measurement Apparatus (right) ..... | 28 |
| Figure 22: Scale Formation on the Surface of the Copper Coil in an Evaporative Condensing Unit Supplied with Municipal Tap Water.....                            | 30 |
| Figure 23: Annual Average and Minimum Rainfall Supply from 1,800 ft <sup>2</sup> Roof .....  | 31 |
| Figure 24: Schematic of the Rainwater Cistern .....  | 32 |
| Figure 25: Water and Ambient Air Temperature Profile in Home’s Rainwater Cistern Davis, California.....  | 35 |
| Figure 26: Dissolved Oxygen, pH and Turbidity During Storage in the Rainwater Cistern .....  | 36 |
| Figure 27: Load and Decay Trend for Coliforms in the Rainwater Cistern.....  | 36 |
| Figure 28: Dissolved Organic Carbon, Nitrate and Ammonia in the Rainwater Cistern .....  | 37 |
| Figure 29: Tap and Collected Water and Six Month Stored Rainwater .....  | 39 |
| Figure 30: The Range Concentration of Total Calcium (mg/L) and Magnesium (mg/L) in California’s Tap Water by Climate Zone .....                                  | 40 |
| Figure 31: Water Treatment Parallel Testing Experimental Setup.....  | 42 |
| Figure 32: System Schematic of Single Small-Scale Test Chamber .....   | 43 |
| Figure 33: Elemental Composition of Copper Coil using Scanning Electron Microscopy .....   | 44 |
| Figure 34: Bleed Rates for Each Test.....  | 45 |
| Figure 35: Coil pH Values.....   | 46 |
| Figure 36: The Experimentally Measured Conductivity Values .....   | 47 |
| Figure 37: Average Dissolved Calcium Ion Concentration at Steady State for A (New coil, LH feed) and C (Old coil, LH feed).....                                  | 48 |
| Figure 38: Average Dissolve Calcium Ion Concentration at Steady State for B (New coil, HH feed), and D (Old coil, HH feed).....                                  | 48 |
| Figure 39: Average dissolved magnesium ion concentration at steady state.....  | 49 |
| for A (New coil, LH feed), and C (Old coil, LH feed).....  | 49 |
| Figure 40: Average Dissolve Magnesium Ion Concentration at Steady State for B (New coil, HH feed), and D (Old coil, HH feed).....                                | 49 |
| Figure 41: Conventional GSHP Install .....   | 52 |
| Figure 42: Directional Bore Earth Exchanger Install .....  | 53 |
| Figure 43: Large Diameter Bore Earth Exchanger Install .....   | 53 |

|  |    |
|--|----|
| Figure 44: Demonstration Home (left) horizontal GSHP pipes (right) .....   | 54 |
| Figure 45: Ground loop temperatures as a function of outside air temperature .....   | 55 |
| Figure 46: Entering Water Temperature and Leaving Water Temperature During the Peak Cooling and Peak Heating Day of the Year ..... | 56 |
| Figure 47: Amount of Heat Delivered in kWh.....  | 57 |
| Figure 48: Domestic Hot Water Production, Inlet Average Temperature and Consumption .....  | 57 |
| Figure 49: Heat Pump Input Energy by Component .....   | 58 |
| Figure 50: Heat Pump Input Energy by Mode.....   | 58 |
| Figure 51: Input Energy by Mode.....   | 59 |
| Figure 52: GSHP Total Heating and Cooling Delivered.....   | 59 |
| Figure 53: Efficiency of Installed System .....  | 60 |
| Figure 54: Proportion of Time Unit Spent in Each Mode .....  | 60 |
| Figure 55: Installation of the LDEB system at the Honda Smart Home in West Village, Davis and the completed home. ....             | 61 |
| Figure 55: Installation of the LDEB system at the Honda Smart Home in West Village, Davis and the completed home. ....             | 61 |
| Figure 56: Installation of the LDEB system at a home in Capay, California.....   | 62 |
| Figure 57: System design diagram for the large diameter earth bore exchanger at Capay, California.....                             | 63 |
| Figure 58: Measured Indoor Air Temperature (10/6/14) .....   | 65 |
| Figure 59: [CZ 12] System Temperatures (Peak Cooling Day).....   | 66 |
| Figure 60: [CZ 12] Condenser Operating Hours.....  | 67 |
| Figure 61: [CZ 12] Total Monthly Energy Use .....  | 68 |
| Figure 62: [CZ 12] Average Monthly COP .....   | 68 |
| Figure 63: Baseline to GSHP Energy Use Comparison.....   | 69 |
| Figure 64: [CZ 12] Baseline to GSHP Energy Cost Comparison .....   | 70 |
| Figure 65: Peak Reduction .....  | 71 |
| Figure 66: Annual Energy Cost Reduction.....   | 72 |
| Figure 67: PCM Laboratory Test Schematic .....   | 75 |

|   |    |
|---|----|
| Figure 68 (left): Microscope image of mPCMs after 100 thermal cycles shows no evidence of broken capsules .....                           | 76 |
| Figure 69 (right): Completed PCM Test Apparatus .....   | 76 |
| Figure 70 (left): Pump Impeller with Wax from Broken mPCMs .....  | 77 |
| Figure 71 (right): mPCMs in Powder Form Shown Before Mechanical Cycling (left) and the Clumps Found After Pumping (right) .....           | 77 |
| Figure 72: Relative Concentration vs Diameter of Nominal 20 micron mPCMs. ....  | 77 |
| Figure 73: Relative Concentrations of Nominal 5 Micron mPCMs After 80 and 128,900 Cycles. 78  | 78 |
| Figure 74: Relative Concentrations mPCMs at 330 and 18,420 Cycles .....   | 78 |
| Figure 75: Comparative Heat Transfer Rates for Clear Water and a 16% Mass.....  | 80 |
| Figure 76: Heat Transfer Rates Within the Melting Range of the 82°F mPCMs.....  | 81 |
| Figure 77: Pumping Power versus Heat Transfer Rate for 62°F mPCM Slurry and Clear Water.82  | 82 |
| Figure 78: Diagram for the PCM demonstration building.....  | 83 |
| Figure 79: Temperature Rise of Air Between Intake and Outflow.....  | 86 |
| Figure 80: Air Temperature Rise Against Intake Temperature for a 14% Concentration of mPCMs .....   | 87 |
| Figure 81: Fluid Supply and Return Temperatures for Clear Water. ....   | 88 |
| Boiler set-point temperature is 114 °F and flow rate is 5gpm.....   | 88 |
| Figure 82: Equivalent Performance Method .....  | 90 |
| Figure 83: Preliminary Test Result Page from One of the Precoolers Tested in the Laboratory Environment Chamber.....                      | 91 |
| Figure 84: Comparison of Predicted and Measured Pool Temperatures in Sacramento, California.....  | 92 |
| Figure 85: Modeled Average Cooling Energy Savings in CA CZs 2, 9, 10, 12, and 13.....   | 93 |
| Figure 86: Modeled Peak Cooling Energy Savings in CA CZs 2, 9, 10, 12, and 13.....  | 93 |
| Figure 87: Amount of Cooling Delivered by Each Stage of the Coolerado H80's Systems.....  | 95 |
| Figure 88: Energy Intensity Ratio for Trane Voyager DC Compared to Standard 1-Stage CAV RTU .....   | 97 |
| Figure 89: Coefficient of Performance as a function of Outside Air Temperature (Based on Sensible System Cooling. Higher is better) ..... | 99 |

|   |     |
|---|-----|
| Figure 90: Gal of Water Consumed Per Ton Hour of Sensible Indirect Evaporative System Cooling ..... | 99  |
| Figure 91: (left) Heat Exchanger Wall with Tapered Pins. (right) Plate with Cylindrical Pins. .     | 101 |
| Figure 92: Typical Pattern of Fluid Flow Past a Cylindrical Pin .....                               | 101 |
| Figure 93: Effects of Water on Pressure Drop .....  | 102 |
| Figure 94: Pressure Drop Difference Between Wet and Dry States .....                                | 103 |
| Figure 95: Water-Use Efficiency of the Technologies Explored. ....                                  | 105 |
| Figure 96: Prevalence of Various Fault Types in RTUs (NBI 2004).....                                | 110 |
| Figure 97: WCEC Tour .....  | 113 |

## LIST OF TABLES

|  |     |
|--|-----|
| Table 1: Testing Conditions Protocols.....   | 7   |
| Table 2: Characteristics of Each House Sealed.....                                     | 17  |
| Table 3: Summary of Sealing Results - Single-Point Depressurization Tests .....        | 22  |
| Table 4: Summary of Time Required to Complete the Sealing for Each Demonstration ..... | 24  |
| Table 5: Summary of Sealant Costs for Each Demonstration .....                         | 24  |
| Table 6: Methods for Water Quality Characteristics .....                               | 33  |
| Table 7: Metals Concentration in the Rainwater Cistern.....                            | 38  |
| Table 8: Water Quality Parameters.....   | 41  |
| Table 9: Make Up Water Characteristics.....  | 41  |
| Table 10: Summary of Aqueous Chemistry Results.....                                    | 50  |
| Table 11: Field Instrumentation .....  | 85  |
| Table 12: Faults that impact energy performance of RTUs.....                           | 108 |
| Table 13: Comparison of Capabilities for Several AFDD Technologies.....                | 112 |

# EXECUTIVE SUMMARY

## Introduction

The Western Cooling Efficiency Center (WCEC) was established in 2007 through a grant from the California Clean Energy Fund and in partnership with California Energy Commission Public Interest Energy Research Program. The WCEC partners with industry stakeholders to stimulate developing innovative cooling technologies that reduce electricity demand, and energy and water consumption in buildings.

This report is a compilation of research projects by the WCEC from June 2009-2015 and funded by an Interagency Agreement with the California Energy Commission. Included are the research and findings from four of the most current projects completed and a section that briefly highlights previous research under the interagency agreement.

### *Building Envelope Sealing Using Adhesive Mist*

#### Project Purpose

More than 30 percent of a single family home's heating, ventilating, and air-conditioning (HVAC) energy is wasted by air leaks (Sherman, 2007). Standard methods to seal building leaks are inconsistent, and take numerous hours to accomplish with variable levels of success. The WCEC created an innovative aerosolized adhesive mist to seal leaks in a fraction of the time compared to previous methods and with consistent results. This technology also provides the contractor immediate feedback on the sealing progress, removing the guesswork out of tightening building envelopes.

#### Project Results

WCEC tested different sealants and injection methods in the laboratory and in more than 20 different single and multifamily residences. Currently, WCEC's technology can seal more than 80 percent of the available leaks in a 2,000+ square foot home in fewer than two hours. These results are significantly better than International Energy Conservation Code's (IECC) standard of 3 air-changes per hour (ACH) at 50 pascals pressure (ACH50) for leakage in single family homes.

#### Project Benefits

Sealing building air leaks significantly increases energy savings and reduces greenhouse gases, with savings estimates of more than 20 percent on HVAC energy costs, especially in colder climates (Emmerich et. Al, 2005). WCEC also estimates that with commercial equipment and trained installation personnel it will cost approximately \$355 to seal a large single-family home—less than what standard building practices cost and with a higher performance efficiency.

### *Studies in Rainwater Collection and Storage for Evaporative Cooling*

#### Project Purpose

Evaporative cooling is a very efficient method for cooling buildings in the majority of California's climate zones and can achieve more than 30 percent residential energy savings

during peak cooling hours. Unfortunately, evaporative technologies use water, a resource that is critical in California, to cool indoor air. This research investigated if evaporative cooling systems can use stored rainwater to transfer heat to the outside and if residences could generate sufficient water to provide their evaporative cooling system water requirements. The study also examined if stored rainwater increases or decreases the risks (scaling, corrosion, and biological growth) to residential evaporative cooling systems.

### **Project Process and Results**

The WCEC demonstrated on a Davis, California home that enough rainwater can be harvested during the wet season from the roof of a residential home to supply all the cooling demands for an evaporatively-cooled condenser system. Concerned about treating this water for bacteria before using in an evaporative cooling system, the harvested rainwater was stored in an outdoor cistern for six months before the cooling season. During that period, the WCEC tested bacteria levels at the top and bottom of the cistern and found the bacteria levels were many magnitudes lower than the EPA guideline standard for water quality in evaporative systems - separate treatment was not necessary before using in an evaporative cooler.

Using municipal water supplies and without proper maintenance, mineral deposits (scale) from water evaporation can develop and harm evaporative system components, shorting the lifespan of some evaporative system components. The study found that rainwater has significantly lower mineral concentrations than the majority of California's municipal water supplies. The difference was significant, with rainwater containing between 3-8 parts per million (ppm) calcium and 1-5 ppm magnesium compared to Davis tap water, with 16-72 ppm calcium and 6-130 ppm magnesium.

Since the mineral content of rainwater is so low, the research team also performed multiple laboratory tests on copper condenser coils to determine any potential damage caused by rainwater stripping copper from condenser coils. The pH in rainwater was of particular interest, because a more alkaline pH (< 3) could act as a solvent to strip copper from the coils. The pH of the rainwater samples from the shingle roof was in the near-neutral/mid-range of 6.9-7.3. The WCEC discovered that this near-neutral/mid range was from the shingles acting as a buffer, lowering the pH from an initially higher alkalinity to one that is more neutral and less likely to cause corrosion. The neutral pH combined with the reduced mineral content in rainwater compared to municipal water should result in greater overall longevity for evaporative systems and reduce aggressive bleed (or water releases) rates that use more water. Laboratory tests to confirm this hypothesis will be researched in the near future with funding from Southern California Edison.

### **Project Benefits**

Though the overall amount of water used to cool residential homes in California is small even in aggregate compared to other water consuming factors, water conservation at every level remains an important issue – small savings statewide add up. By combining the energy efficiency and greenhouse gas reduction benefits of evaporative cooling with near-free rainwater, Californians can reap economic benefits (especially at times of peak demand) without consuming additional water supplies

## **Project Purpose**

A ground source heat pump (GSHP) or a geothermal heat pump is a central heating and/or cooling system that uses the constant below ground temperature of soil or water to heat and cool a building. Like a cave, this ground temperature is warmer than the air above it during the winter and cooler than the air in the summer, making a GSHP extremely efficient and reducing heating and cooling costs to the consumer.

Traditional geothermal techniques require expensive drilling rigs that bore 200 feet vertically into the earth. New options such as the Directional Bore and the Large Diameter Earth Bore (LDEB) installations aim to reduce these costs by decreasing the drilling depth while maintaining an adequate heat exchange with the earth. Horizontal or directional boring, used mostly as an alternative to trenching when laying pipe or running underground conduit, can also be used to install ground source heat pumps and takes advantage of relatively inexpensive and easily transported horizontal boring equipment. Unlike vertical drilling, where a new setup is required for each bore, a Directional Bore can start all holes from a single central location, eliminating multiple setups. The Directional Bore system drills many shallow lanes across a plot of land creating more heat exchange surface area in less time and cost than the more conventional GSHP. The technique also allows ground source technology to be considered on parcels that would be too small for conventional vertical boring techniques by allowing the bores to be drilled under housing structures, landscaping, and other obstacles.

Large Diameter Bore Earth (LDBE) installations can cut drilling costs by reducing the drilling depth while maintaining an adequate amount of heat exchange with the earth. This innovative concept uses a 24 inch diameter 20 foot deep helix-shaped coil. Drilling for these shallow bore heat exchangers is quick, and less expensive than conventional techniques. Typically each bore may take less than an hour to drill, allowing around 8 to be completed in a typical work day. A day of work may yield around 150 linear feet of heat exchange depth but more capacity from the increase in effective surface area.

The WCEC explored these novel options with three different demonstrations in California.

## **Project Process and Results**

### *Demonstrating a Directional Earth Bore Exchanger at Rio Mondego*

The Rio Mondego project (a 1988, 3-bedroom single-family home with central heating and air) demonstrated a ground source heat pump system using Directional Boring technology. Overall, the system proved it was capable of high efficiencies, ranging from 10 – 20 energy efficiency rating (EER) for cooling in the summer and 3.5 to 6 coefficient of performance (COP) for heating in the winter<sup>1</sup>. Heat pump systems are generally capable of achieving high efficiencies. The measured efficiencies over the complete season for this particular system were 10.9 EER for

---

<sup>1</sup> Heat pump cooling efficiencies are given in terms of EER; whereas, the heating efficiencies are given in COP.

cooling and 3.9 COP for heating, relatively low if the extra energy recovery available from the desuperheater is not taken into account. The efficiency numbers are 12 EER and 4.6 COP if crediting the energy recovery. The low overall efficiency is most likely the consequence of an undersized or underperforming geo-exchange loop.

#### *Demonstrating Two Large Diameter Earth Bore Exchanger Projects*

Two LDEB techniques for building geo-exchange fields was installed at the Honda Smart Home at the UC Davis West Village Zero Net Energy community, testing two different field configurations. The Honda Smart Home is complete and tenants have recently moved in. Compiling data and analysis is currently ongoing.

#### *Demonstrating a Large Diameter Earth Bore Exchanger as a Storage Vessel*

This project used a system of uninsulated storage vessels buried underground at a home in Capay, California to store water cooled at night and later used during the day when building cooling loads are the highest. Implementating this system as a retrofit required only minor changes to an existing system. Modeling this system's performance across all climate zones shows energy savings of up to 14 percent.

#### **Project Benefits**

Research and demonstration at various sites has shown that energy savings up to 14 percent can be achieved by using new, lower cost ground heat exchanger technologies as alternatives to traditional geothermal systems. These systems save energy, and are significantly less expensive to install than traditional geothermal, cut drilling costs and time and are more compact so can be applied on more and varied property. Challenges remain though, and further research in some key areas would be beneficial in eliminating questions that still remain.

#### *Microencapsulated Phase Change Material*

#### **Project Purpose**

This project investigated adding microencapsulated phase change materials (mPCM) into water (hydronic) cooling and heating systems to reduce the pump energy required to circulate the fluid in the system. The mPCM technology consists of small two component particles containing a core material – the PCM – and an outer shell or capsule wall. The PCM is usually a waxy substance, which absorbs and releases heat to maintain a particular temperature. The thermal capacity of a hydronic system is determined by how fast the heat transfer fluid moves through the system, the potential amount of heat the fluid can hold, and the temperature differential across the heat exchanger. Adding mPCMs will increase the effective amount of heat the water can hold, allowing for a reduction in water flow rate while providing the same amount of heat transfer. Since the pumping power is roughly proportional to the cube of the flow rate, reducing the flow rate leads to significant power savings.

#### **Project Results**

This project consisted of laboratory testing and field testing of mPCMs in a hydronic system.

### *Laboratory Testing*

Laboratory testing included thermal cycling tests to determine the efficacy of the phase-change and the robustness of the mPCMs to handle the mechanical stresses after multiple cycles. This testing also helped to characterize the thermal carrying capacity of different sized mPCMs to determine the best balance between effective heat exchange and longevity. Laboratory results on the chosen size mPCM (20-micron) showed pump energy savings as high as 30 percent.

### *Field Testing*

A field performance test was conducted on a 200 square foot building located at the University of California Davis campus. Results for this test were unclear because of heavy temperature fluctuations experienced by the boiler chosen for this test. Water temperatures must remain close to the upper or lower end of the mPCM's melting range, with tolerances of only one to two degrees Fahrenheit (°F). It is imperative to develop a method of "tightening" boiler control of the water/slurry temperature.

### *Project Benefits*

Hydronic systems such as boilers, chillers or radiant systems make up a significant portion of energy consumption in California, especially in larger, industrial applications. The benefits in an ideal installation of this technology could deliver pump energy savings of up to 30 percent for a relatively modest investment in the mPCMs.

# **CHAPTER 1: Building Envelope Sealing using an Adhesive Mist**

## **1.1 Problem Statement**

Building shells are notorious for leaking, causing unintended air flows between conditioned and unconditioned spaces, which results in additional heating and cooling loads that the heating, ventilation, and air-conditioning (HVAC) equipment must remove. A significant effort has been made to reduce the leaks in building shells through current construction practices, but the problem remains one of high labor costs, constant vigilance and quality control. The WCEC has received funding from U.S. Department of Energy's Building America and the California Energy Commission's (Energy Commission) Public Interest Energy Research Program to investigate building shell sealing in both retrofit and new build applications. The objective of this research is to develop and demonstrate an automated and remote process that uses aerosolized sealant to simultaneously measure, find and seal leaks in a building. The process involves pressurizing a space with a fog of sealant particles that will travel to building leaks, and, as they seek to escape with the airflow, will adhere at the leakage sites and seal them.

## **1.2 Previous Research**

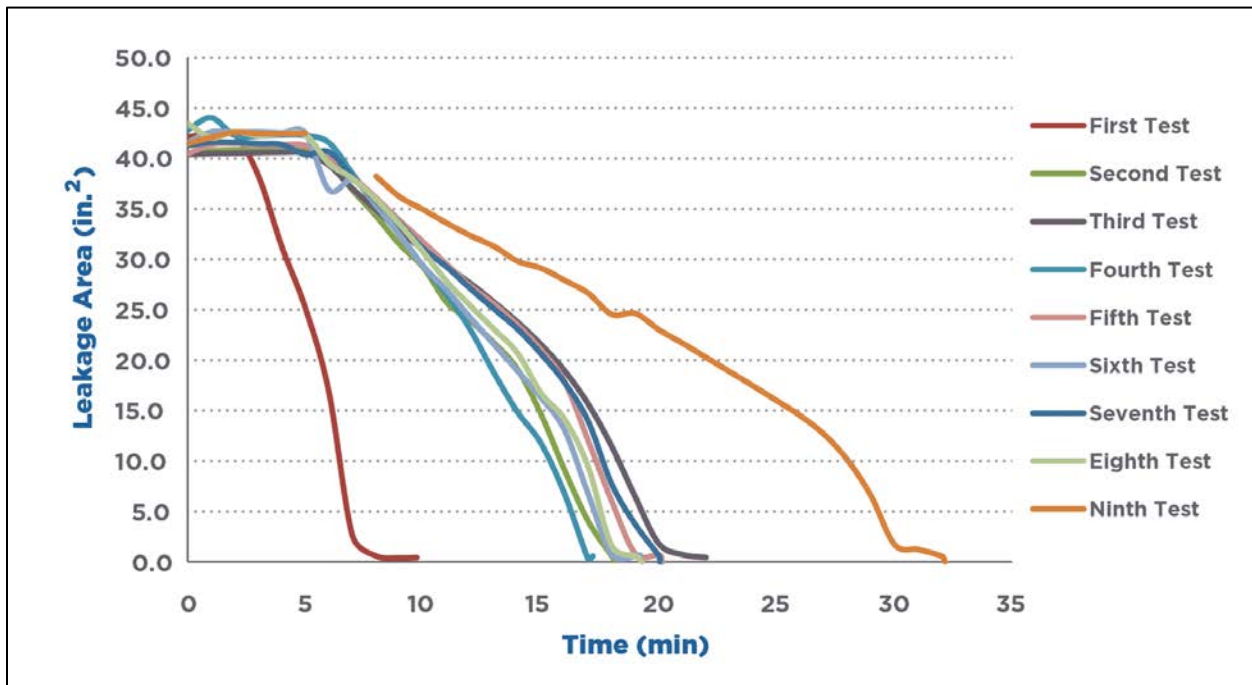
### **1.2.1 Initial Laboratory Testing**

The first round of funding for this project was restricted to small-scale laboratory tests of the sealing process. The WCEC constructed an 8 foot x 8 foot x 4 foot enclosure with leak panels distributed at various locations around the shell of the enclosure. Nine tests were performed in the test box, with all tests sealing the enclosure completely from about 42 square inches of leaks to less than 1 square inch. The objective of the tests was to determine the sensitivity of the sealing performance to various independent variables including: enclosure pressure, sealant flow rate, and particle size. Table 1 shows the conditions under which each test was performed. Figure 1 shows the leakage profiles for each of the nine tests in the enclosure. All tests successfully sealed the enclosure to nearly zero leakage in less than 30 minutes. Note that, at the beginning of each test, the sealant lines were first purged of water before sealant reached the injection nozzle, causing a slight delay at the beginning of each test, which for 25 cubic centimeters per minute (ccm) tests was about 5 minutes and for the 100 ccm test was about 2 minutes.

**Table 1: Testing Conditions Protocols**

| Test Number | Box Pressure (Pa)        | Sealant Injection Rate (ccm) | Sealant Dilution to Reduce Particle Size |
|-------------|--------------------------|------------------------------|--|
| 1           | No pressure/flow control | 100                          | No Dilution                              |
| 2           | 100                      | 25                           | No Dilution                              |
| 3           | No pressure/flow control | 25                           | No Dilution                              |
| 4           | 50                       | 25                           | No Dilution                              |
| 5           | 100                      | 25                           | No Dilution                              |
| 6           | 50                       | 25                           | No Dilution                              |
| 7           | 100                      | 25                           | No Dilution                              |
| 8           | 50                       | 25                           | No Dilution                              |
| 9           | 100                      | 25                           | 1 part sealant/1 part water              |

**Figure 1: Leakage Sealing Time Profiles for Lab Tests**



**1.2.2 First Field Test: Stockton, California (Habitat for Humanity)**

The Habitat for Humanity test was the first use of aerosol envelope sealing technology in a home. The Aerosol technology used for this test (Figure 2) utilized one air-based nozzle and an adhesive that was designed originally for sealing ducts, but modified to reduce nozzle clogging.

A blower door was used to pressurize the building during injection and to monitor leakage throughout the sealing process. The technology successfully sealed 50% of the leakage area that was available, after taping up the HVAC ductwork, double-hung windows (up to the outer edge), and door seams. A pre- and post-blower door test showed that the total building leakage

was reduced by 27%, and a third party Home Energy Rating System (HERS) test after construction was completed showed a 25% reduction in leakage compared to a similar home that was sealed by standard methods.

**Figure 2: Initial Injector System Used a Single Air-based Nozzle with the Sealant Contained in the Box Below It.**



### 1.2.3 Laboratory Testing Refinements after First Field Test

The first full-scale envelope sealing test demonstrated the need for multiple injection nozzles. The system used in the initial testing of the aerosol envelope sealing process was a modified commercial technology for sealing ducts with aerosol particles. This injection system uses a compressed air nozzle that requires a dedicated compressor to operate which limits the practical ability to expand the number of nozzles operating simultaneously. The WCEC has designed a new aerosol injection system that can operate five airless nozzles simultaneously with the option to expand to more if necessary. The new injection system uses compressed gas to pressurize liquid sealant to the appropriate operating pressure of the airless atomization nozzles, to ensure consistent particle sizes and reduce drip waste at the nozzle

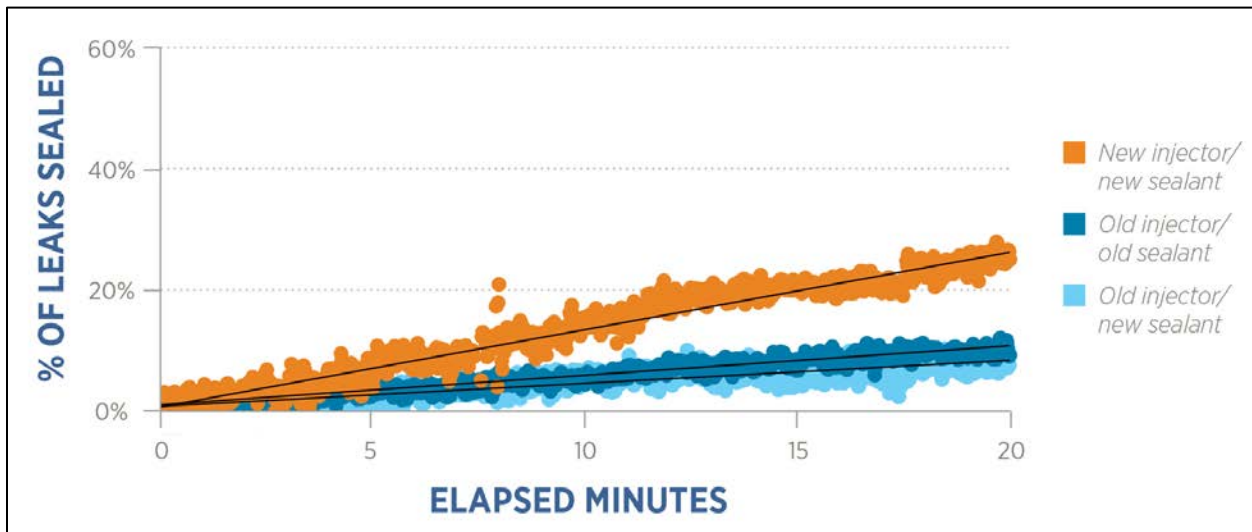
In addition to developing a new injection system, the WCEC worked with a large sealant manufacturer to test alternative sealants that are better suited for whole house applications of aerosol sealing. WCEC has successfully identified and tested a sealant that dries nontacky while also possessing the characteristics that allow it to be atomized and adhere to leaks. Tests are planned to assess the impact of different additives for improving the sealing effectiveness, maintaining tackiness throughout the sealing process, and strengthening the resulting seal.

Several full-scale tests of the aerosol envelope sealing process have been conducted in the last year which tested an alternative sealant, new nozzle injection system, and application protocols.

Figure 3 compares the sealing rates of the full-scale installations using, 1) existing duct sealing equipment and duct sealant, 2) existing duct sealing equipment and new sealant, and 3) recently develop aerosol injection system with the new sealant. Comparing tests using the old

injection system with the new and old sealant gives us an idea of the relative deposition efficiency. The slightly lower sealing rate when using the new sealant indicates that the new sealant has lower sealant deposition efficiency than the old sealant. This result is somewhat expected since the new sealant dries nontacky preventing particles that dry out before impacting a leak to stick. Figure 3 also shows that the new aerosol injection system using five injection nozzles has a much higher sealing rate nearly four times that of the old injection nozzle. When normalized by sealant injection flow rate; however, the new injection system has a lower sealing rate than the existing duct sealing system.

**Figure 3: Comparison of Old Injector, New Injector and Old and New Sealant**



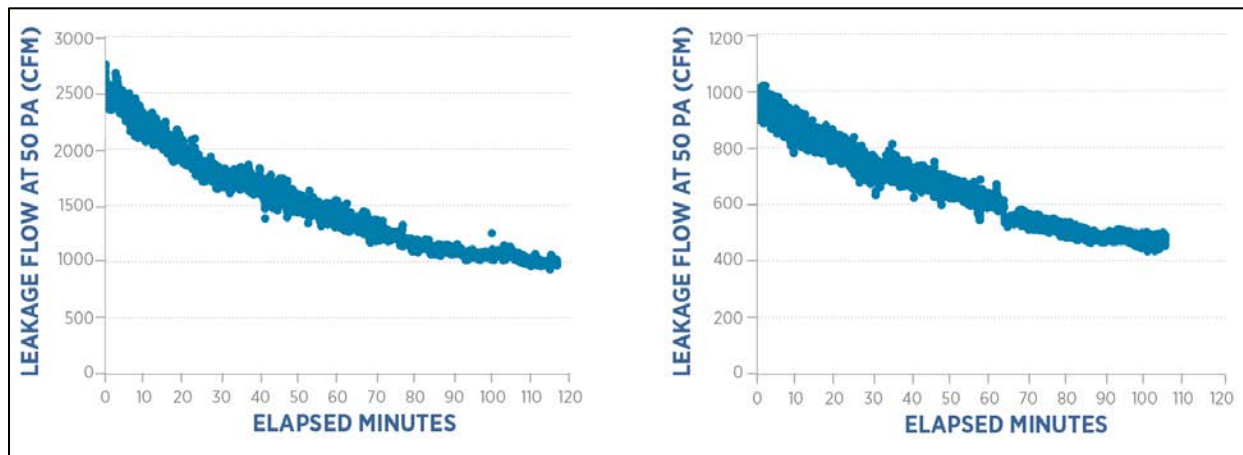
#### 1.2.4 Field Test After Previous Laboratory Refinements

The most recent full-scale applications tested the process in two multifamily apartments that were essentially identical but at different stages of construction. One test was performed at the preinsulation phase of construction before drywall was installed allowing the seal to form on the external surface of the unit while another test tested the unit after drywall was installed allowing the seal to form on the inside surface. Sealing the external wall would prevent outside air from entering the wall cavity effectively reducing the thermal exchange between the inside and outside walls; however, there is more leakage to seal and the leaks are typically bigger so the process takes more time and material.

Figure 4 shows the sealing profile for the full-scale sealing test of an apartment during the preinsulation and drywall phase of construction. The leakage normalized to 50 Pascals (Pa) started at 2,500 CFM and was sealed to about 1,000 cubic feet per minute (CFM) reducing unit leakage by 60%.

Figure 5 shows the sealing profile for the test in a similar apartment post-insulation and drywall installation. The leakage normalized to 50 Pa started much lower than the preinsulation test at about 950 CFM, with the unit sealed to below 500 CFM reducing leakage by 50%.

**Figure 4 (left): Sealing Profile for Apartment Field Test (preinsulation phase)**  
**Figure 5 (right): Sealing Profile for Different Apartment Field Test (after drywall)**



These tests show that the sealing rate of a leakier building is significantly higher than that of a tighter building. The preinsulation test sealed 1,500 CFM of leakage at 50 Pa in about 115 minutes while the test after drywall was installed sealed about 475 CFM in 105 minutes.

The amount of leakage after applying aerosol envelope sealing techniques is not the final leakage of the apartments since part of the process involves taping off doors, operable windows, and HVAC ducts. Ultimately the final leakage of these apartments will be tested by a third party HERS rater and compared in order to analyze the overall impact of sealing the buildings at the different stages.

### 1.2.5 Field Test: Honda Smart Home

The Honda Smart Home is a net-zero energy home built to showcase some of the most advanced strategies to reduce the carbon footprint of homes in the United States. The WCEC worked with the American Honda Motor Company to design mechanical systems for the home, as well as demonstrate the aerosol envelope sealing process to reduce building shell leakage for better ventilation control and lower infiltration loads for the building.

A demonstration of the aerosol envelope sealing process on the Honda Smart Home, a two-story single-family home, showed a reduction in building air leakage from 5.5 ACH when pressurized to 50 Pa (ACH50) to 1.0 ACH50. To put this in perspective, the International Energy Conservation Code (IECC) minimum requirement is 3.0 ACH50. This building was initially sealed using standard methods and the photos in Figure 6 clearly show where the aerosolized method sealed leaks that were not sealed properly by manual methods. The ultimate goal was to meet the very aggressive Passive House standard of 0.6 Pa (ACH50), which also requires that the air barrier be applied to the external envelope of the building.

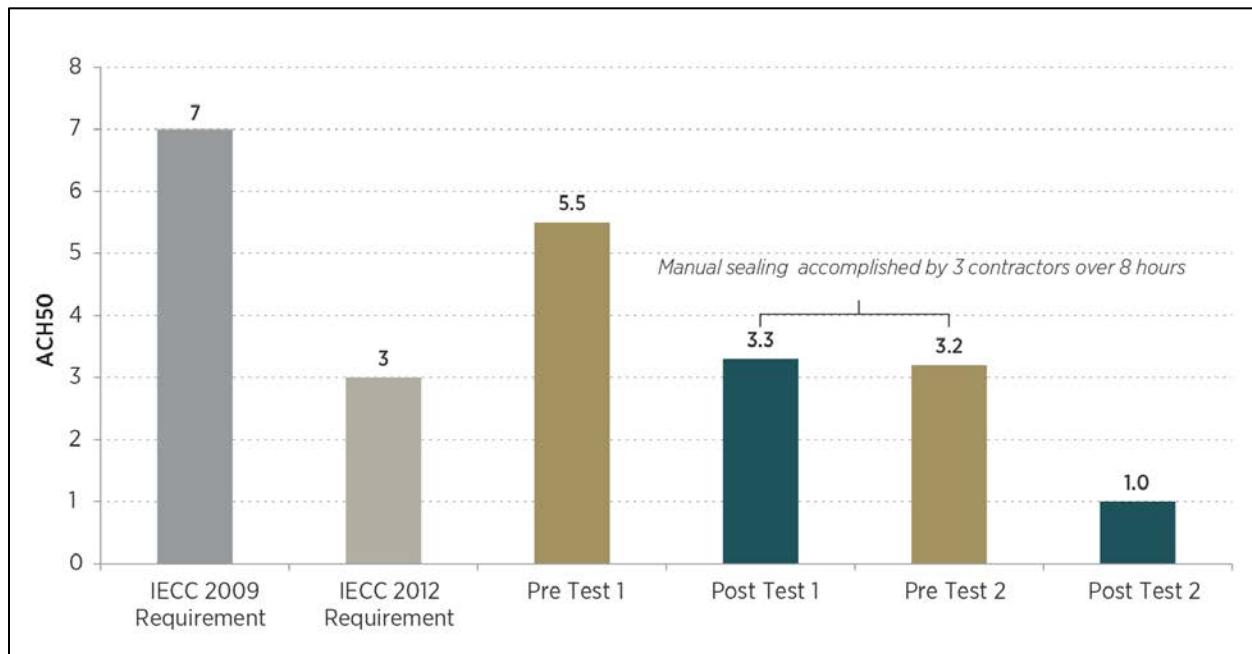
**Figure 6: Aerosol Seals from the Honda Smart Home**



The contractor used their standard methods to seal leaks larger than 0.25" in the smallest dimension. The time required to seal a leak with the aerosolized process has been shown to increase with the square of the size of the leak in the smallest dimension (e.g. it takes four-times longer to seal a leak that is 0.5" than to seal a leak that is 0.25").

Figure 7 summarizes the result of the demonstration showing three discrete phases in the sealing process. The first sealing demonstration used an airless nozzle injection system with five injection points using no temperature or humidity control which reduced the building leakage from 5.5 ACH50 to 3.3 ACH50. After the first demonstration, three contractors spent 24 man-hours attempting to further seal the building manually with expanding foam and caulk, resulting in an almost negligible impact on the overall tightness of the building shell. Finally, WCEC applied the aerosol envelope sealing process again, this time with air-atomization nozzles and with controlled temperature and humidity, and were able to further reduce the building leakage from 3.2 ACH50 to 1.0 ACH50. Figure 6 shows leaks sealed by the aerosol technology. The left side of the image shows leaks sealed with aerosols even after the manual sealing, and the right side shows a large leak around a beam sealed purely by aerosols.

**Figure 7: Summary of Results from Aerosol Envelope Sealing Demonstration in Honda Smart Home**



This demonstration provided a superb comparison of the performance between the airless and the air-atomization nozzles, as well as the impact of temperature and humidity control. WCEC found that while the airless atomization nozzles create a uniform particle size distribution, the air-atomization nozzles project the aerosol with more initial momentum, allowing the aerosol to fill the building space better and promote evaporation of water surrounding the sealant. Some evaporation of water contained in the sealant mixture is critical to allow the particles to adhere to leak sites. Too wet, and the particles will not all effectively stick to a surface, too dry and the sealant can lose tackiness before it can adhere to a leak. The two aerosol sealing tests also differed in that the first test using the airless system had five injector nozzles in the house while the air-atomization test only used one injector nozzle (the system was only capable of one injection site). The airless system used about five-times as much sealant to seal a similar amount of leakage, showing lower sealing performance than the air-atomization system.

In summary, this demonstration revealed the advantage of using the aerosol envelope sealing process over standard manual sealing methods. The results demonstrated that relying on manual sealing to achieve the level of air-tightness desired would have required a substantial amount of time and labor. WCEC also found that an air-atomization nozzle system is more promising than one that utilizes airless nozzles. WCEC found in subsequent demonstrations that the performance of the air-atomization system significantly improves as the process expands to multiple injection points since the single injector nozzle in this test had to be moved around the building.

## 1.3 Current Research (2014)

### 1.3.1 Laboratory Testing: Particle Size Testing

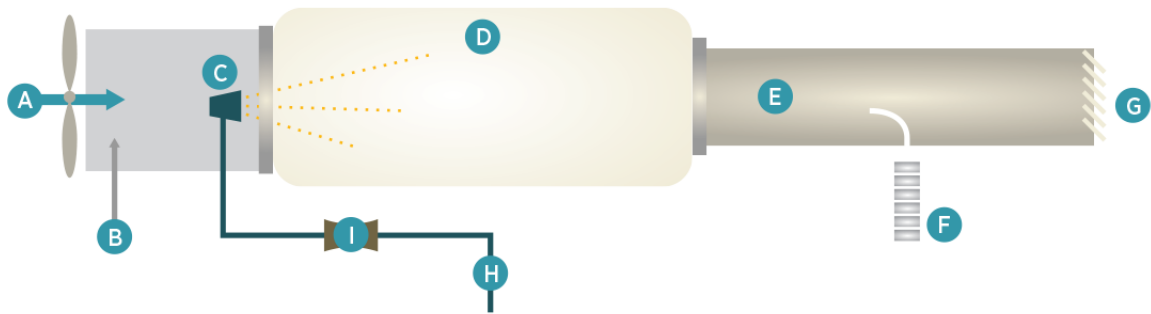
**Figure 8: (left) WCEC Engineer Inspects the Cascade Impactor (right) Impactor Plate after Test with Deposition**



Several cascade impactor tests were completed this year to measure particle size distribution from injection nozzles under different operating conditions (Figure 8). These tests will allow the WCEC to characterize the aerosol produced for envelope sealing applications improving our understanding of how to control the process, as well as provide information for future modelling efforts for simulating particle transport in buildings. A cascade impactor uses a series of stages with circular jets machined into them. As an aerosol passes through the jets, larger particles escape the streamline causing them to impact a collection plate mounted below the jet; smaller particles continue on through the cascade impactor to the subsequent stages that are designed to capture progressively smaller particles. The size of the jets, number of jets, and the airflow rate through the impactor are what determine the size particles that are captured. This device is typically used to measure flue gas constituents, ambient air particle concentrations, and spray characteristics for medical delivery devices.

The laboratory tests were set up to measure the particle size distribution of an aerosol as it travels through a duct. Since the sealant used for the aerosol envelope sealing process is diluted with water, particles are expected to change in size as they travel down the duct. For the initial tests, WCEC sampled the aerosol approximately four meters from the point of injection. Figure 9 shows a schematic of the laboratory apparatus used for the cascade impactor testing.

**Figure 9: Cascade Impactor Test Apparatus**

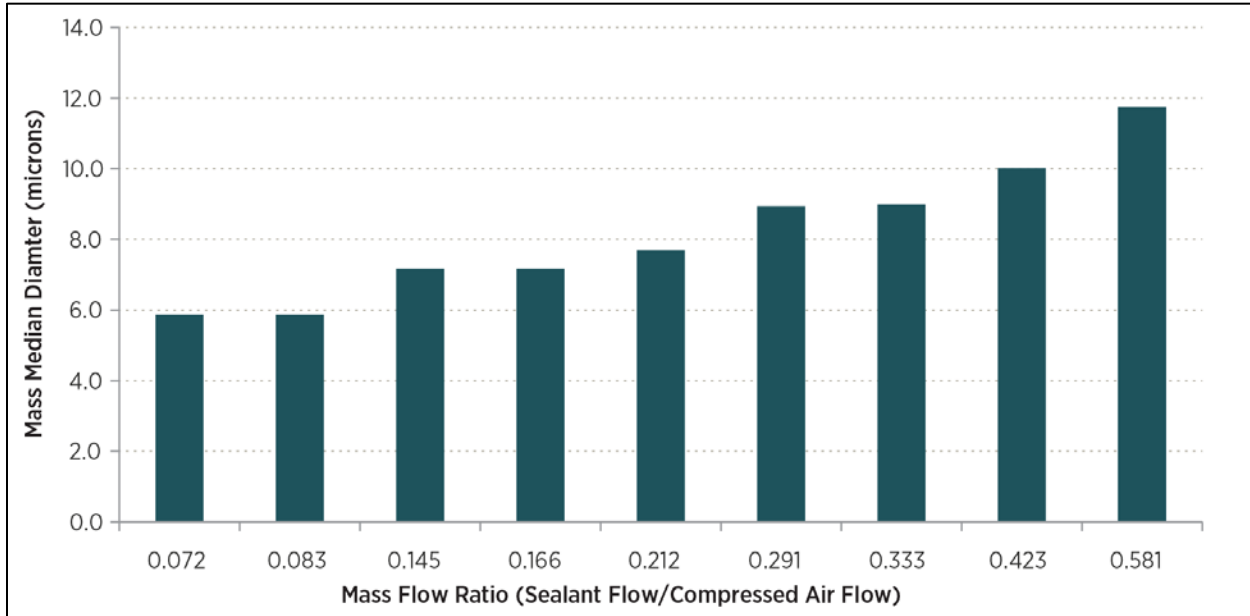


- |                             |                            |                                       |
|-----------------------------|----------------------------|---------------------------------------|
| <i>A. Flow, ambient air</i> | <i>D. Layflat Duct</i>     | <i>G. Damper for pressure control</i> |
| <i>B. T, RH ambient air</i> | <i>E. 14" Rigid Duct</i>   | <i>H. P, T compressed air</i>         |
| <i>C. Spray nozzle</i>      | <i>F. Cascade Impactor</i> | <i>I. Flow, compressed air</i>        |

A calibrated fan is used to control the airflow rate through the duct in order to match the velocity in the duct with the velocity of the air that enters the sampling tube for the cascade impactor. The temperature and humidity of the air entering the duct system is measured before going through the fan and the pressure of the duct is controlled. The flow rate of compressed air used for atomization is measured using a venturi mass flow meter, and the sealant injection rate is controlled with a peristaltic metering pump. A number of cascade impactor tests have been completed at various nozzle operating conditions. Pictures of the impaction plates show the deposition pattern of the various stages.

The particle size distribution of an air-atomization nozzle is expected to rely on the ratio of the mass flow rate of liquid to the mass flow rate of compressed air. As this mass flow ratio increases the particle size distribution is expected to increase. Figure 10 shows the mass median diameter calculated based on the results of several cascade impactor tests. The mass median diameters follow the expected trend indicating larger particle size distributions produced as the mass flow ratio of sealant to compressed air increases. Having a method established for characterizing an aerosol allows alternative sealants and nozzles to be tested and compared systematically, as well as better input assumptions for modeling aerosol transport in buildings.

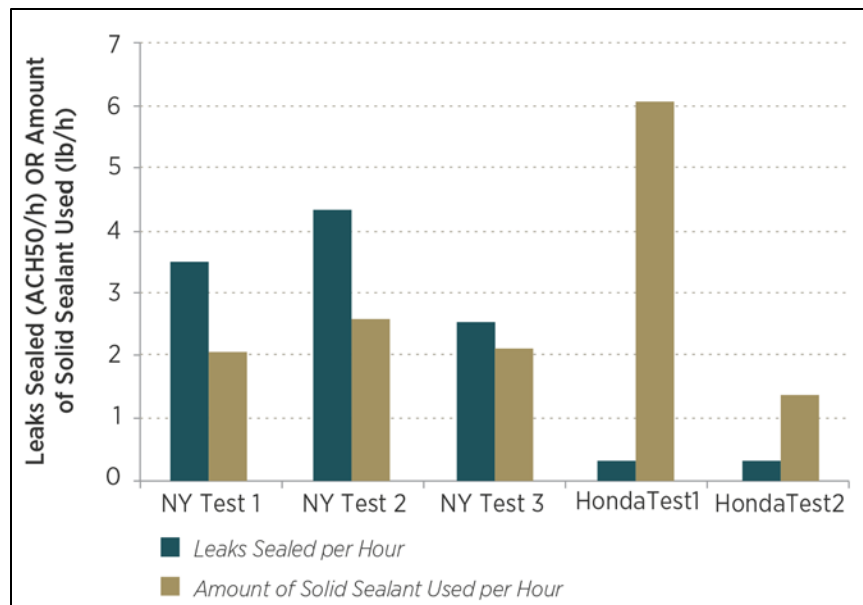
**Figure 10: Mass Median Diameter Calculated from Cascade Impactor Results at Different Operating Conditions**



### 1.3.2 Field Testing: Current Multi-Nozzle Air Based Injector System

The latest version of the technology is capable of multiple air-atomization nozzles to generate the aerosol “fog” and has achieved sealing rates more than ten-times those of applications with previous versions of the equipment as shown in Figure 11, which includes the latest field testing done in three apartments.

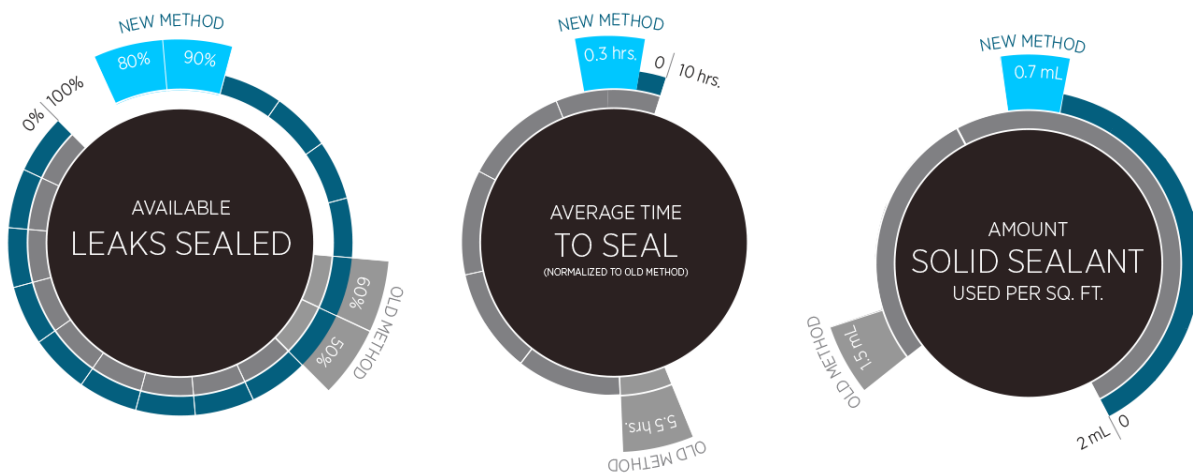
**Figure 11: Leaks Sealed vs. Amount of Sealant Used**



Following the successful application of the aerosol envelope sealing process on the Honda Smart Home, tests of a new air-atomization injection system capable of multiple injection points was conducted through funding from both the Energy Commission (for development of the injection system) and the Department of Energy’s Building America program (for the field demonstrations). The first application using the new injection system was performed on several apartments.

Figure 12 shows the sealing performance from all four sealing demonstration on the apartments. Figure 12 shows that the process was capable of sealing at least 80% of the air leaks in less than two hours. The plateau in sealing rate occurs when all smaller leaks have been sealed (<0.5” in the smallest dimension) and only large leaks that cannot be sealed by the aerosol process remain. Depending on the initial bulk-sealing level of the building this plateau will occur at different points.

**Figure 12: New Sealing Method from Field Test vs. Previous Aerosol Method Field Tests**



### 1.3.3 Field Testing: 6 Large Homes in Clovis, California

The UC Davis Western Cooling Efficiency Center completed demonstrations of the aerosol sealing process on six single-family homes in Clovis, California. The homes were sealed during the rough-in stage of construction after drywall was installed and taped, and included both one- and two-story homes ranging in size from 2,000 ft<sup>2</sup> to 3,500 ft<sup>2</sup> (Figure 13). Table 2 provides a summary of some of the building characteristics of each homes sealed.

**Figure 13: Clovis Aerosol Test Housing Development and Stage of Construction the Homes Were in Before Sealing.**



**Table 2: Characteristics of Each House Sealed**

| Test # | LOT #  | # Floors | Floor Area (ft <sup>2</sup> ) | Building Volume (ft <sup>3</sup> ) |
|--------|--------|----------|-------------------------------|------------------------------------|
| 1      | LOT 4  | 2        | 3,550                         | 33,725                             |
| 2      | LOT 13 | 1        | 2,019                         | 20,190                             |
| 3      | LOT 9  | 1        | 2,324                         | 23,240                             |
| 4      | LOT 10 | 2        | 3,550                         | 33,725                             |
| 5      | LOT 15 | 1        | 2,324                         | 23,240                             |
| 6      | LOT 12 | 1        | 2,324                         | 23,240                             |

*Description of Aerosol Sealing Setup*

The preparation of the homes before each installation was not extensive since there were no finished surfaces to protect. The crucial items that required preparation to prevent unwanted deposition were exterior doors and HVAC ducts. Since California Title 24 Building Codes require heating and cooling ducts to be blocked during construction to prevent dust from getting into the duct systems, much of this work was already completed (Figure 14).

**Figure 14: Showing Supply Ducts Covered to Prevent Dust from Entering Duct System.**



Large holes were taped off including undercuts on exterior doors, large plumbing penetrations, and network access points that were unfinished (Figure 15). The motivation for taping over large holes is to increase sealant use efficiency by preventing large aerosol plumes from escaping to the outside and onto unwanted surfaces. While there is no theoretical limit to the size of hole that can be sealed by the aerosol sealing process, there is a practical one. The time required to seal a hole with the aerosol sealing process has been shown to increase with the square of the increase in the size of the leak, measured by the leak's minimum dimension. [Carrie and Modera]. Figure 16 shows significant deposition on electrical access points that were not taped before the process. While the sealant can be easily removed in this case, the material that deposited in this location was wasted since it will not result in tightening the building envelope.

**Figure 15: Network Access Point Prepared for Aerosol Sealing Process**



**Figure 16: Untaped Network Access Points on an Interior Wall with Significant Deposition**



There is a consideration as to the time required to block a hole versus the impact it will have on the sealing process. If there is little potential that a hole, which will likely not be sealed by the aerosol process, will lead to deposition on an unwanted surface and taping would be considered too time consuming, then it can be left uncovered for the sealing process. The result is a decrease in sealant application efficiency but also a decrease in the time required for setting up the sealing process. An example of a hole that was considered too time intensive to tape is shown in Figure 17. It is expected that this air leak would be sealed by the builder at a later date, and taping over the larger hole could result in a seal that was formed on an appropriate part of the leak being damaged when the tape was removed.

**Figure 17: Hole Near Ventilation Supply Duct**



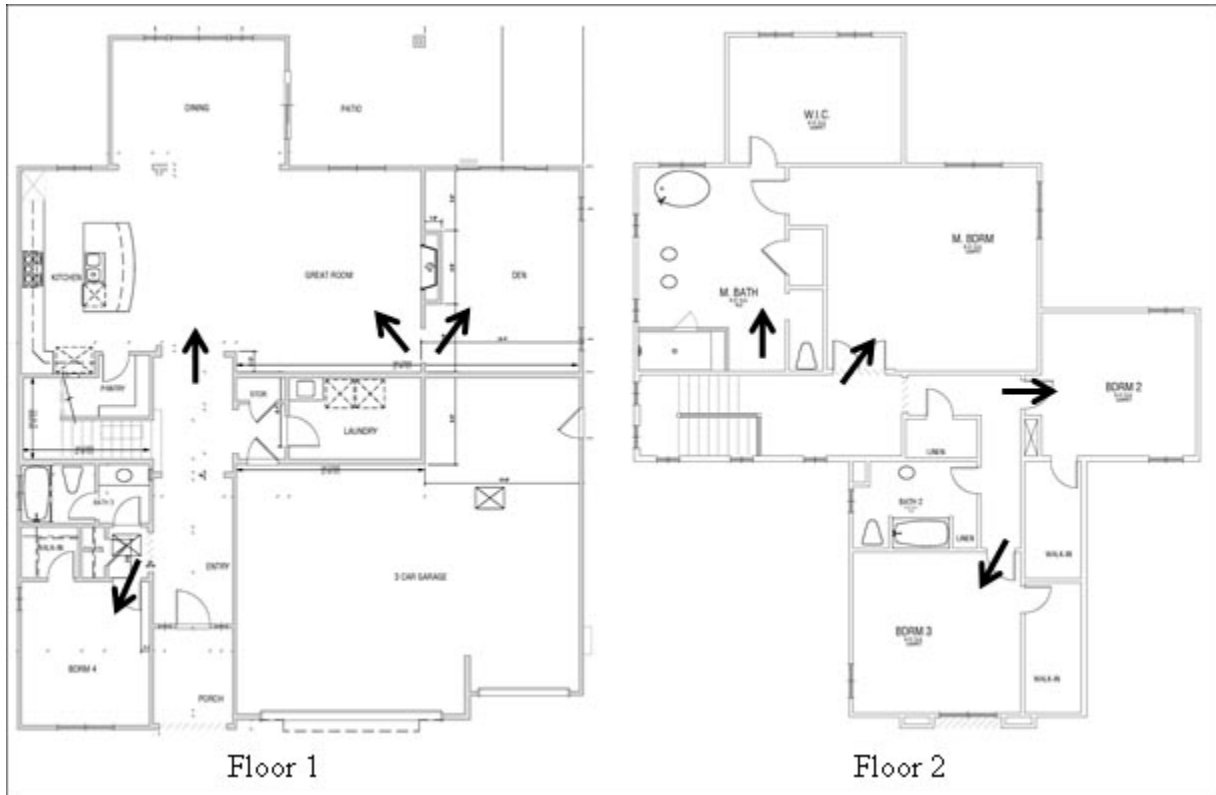
While not expected to be sealed by the aerosol process, the hole near the supply duct was left uncovered to reduce the time required for setup.

Another critical component of the preparation for aerosol sealing is to assure that the pressure imposed on the building, typically at 100 Pa during sealing, does not blow a hole open during the process. In the case of the demonstrations for this project, WCEC chose a lower pressure of 75 Pa because the covering used by the contractors to block the heating and cooling ducts were in some cases insufficient and could potentially blow open. The attic access also needed to be taped to avoid lifting the access door during the sealing process.

#### *Nozzle Placement*

When applying the aerosol envelope sealing process to a space with dividing interior walls, nozzles should be placed in each room to improve aerosol distribution and maximize the sealing efficiency. The aerosol sealing equipment used for this project was capable of delivering spray to up to eight nozzles, which in some cases did not allow for a nozzle to be placed in each room. Figure 18 shows the nozzle placement used on the home with the largest floor plan of the development (3,550 square feet [ft<sup>2</sup>]).

**Figure 18: Nozzles Placement for One of the Aerosol Envelope Sealing Installations**



A common mistake is to assume that interior walls do not contribute to the overall leakage of a building. Previous applications of the aerosol sealing process have revealed significant deposition on interior walls where leak paths are present that lead to an attic or other space that is open to outdoors. Therefore, spaces completely enclosed by interior walls should still be considered a space that needs to be treated by the aerosol sealing process.

### *Results*

Table 3 presents the results of sealing each of the test homes. The pre- and post-sealing test results are based on the single-point depressurization measurements performed before and after the sealing, as opposed to the monitored leakage data collected during pressurization of the building for the aerosol application.

**Table 3: Summary of Sealing Results - Single-Point Depressurization Tests**

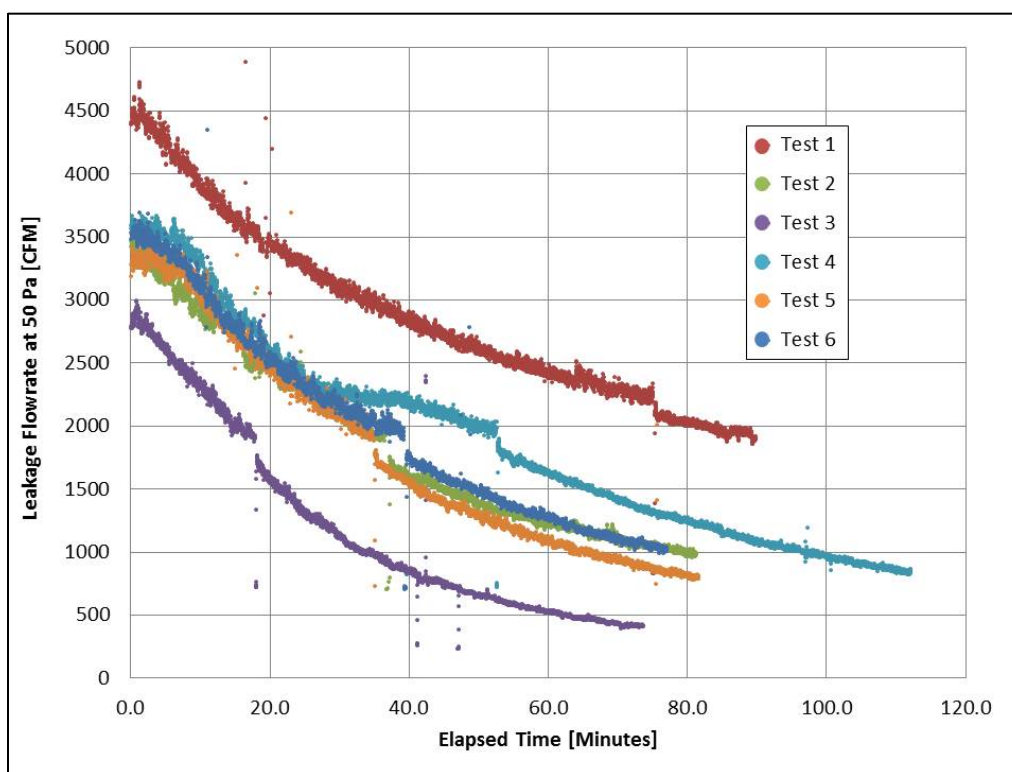
| Test # | Sealing Time (min) | Leakage Pretest (CFM50) | Leakage Post-Test (CFM50) | ACH50 Pre Leakage | ACH50 Post Leakage | Percent Reduction |
|--------|--------------------|-------------------------|---------------------------|-------------------|--------------------|-------------------|
| 1      | 90                 | 5,100                   | 1,936                     | 9.1               | 3.4                | 62%               |
| 2      | 81                 | 4,603                   | 1,690                     | 13.7              | 5.0                | 63%               |
| 3      | 74                 | 4,472                   | 676                       | 11.5              | 1.7                | 85%               |
| 4      | 112*               | 4,758                   | 1,018                     | 8.5               | 1.8                | 79%               |
| 5      | 82                 | 4,813                   | 969                       | 12.4              | 2.5                | 80%               |
| 6      | 77                 | 5,095                   | 1,226                     | 13.2              | 3.2                | 76%               |

\* air compressor ran out of fuel causing a pause in the sealing

Since the process was applied at a rough-in stage of new construction, a significant amount of leakage that existed would be expected to be sealed in later stages of construction with the exception being duct leakage. The leakage data presented in Table 3 shows the infiltration measurement performed with HVAC ducts blocked, and large holes. Test 2 indicates a significantly higher ACH50 result at the end of sealing which may have been caused by multiple HVAC ducts becoming unblocked during pressurization.

The sealing profiles for each of the sealing demonstrations are presented in Figure 19. The initial sealing rates were similar for each of the demonstrations showing about 1,000 CFM at 50 Pa sealed in the first 20 minutes of injection. This result appears to be independent of the size of the home being sealed or initial leakage level.

**Figure 19: Profiles for the Sealing Demonstrations**



There was a significant discrepancy between the pressurization leakage measurements obtained during the sealing and the depressurization measurements obtained before and after each sealing installation. There are two potential causes for this discrepancy: 1) a poorly calibrated fan which has had significant sealant deposition on it in the past requiring cleaning, and 2) the fact that the fan is ducted into the Blower Door frame which may affect the manufacturer calibration. Current methods for installing the aerosol envelope sealing process have nearly eliminated sealant deposition on the fan by using a short duct to separate the Blower Door fan from the space being sealed.

The depressurization tests were performed as intended by the manufacturer with a different fan and are assumed to be more accurate. The Blower Door manufacturer has confirmed that a special calibration could be performed to include the impact of ducting the fan into the Blower Door frame, which will be considered for future demonstrations.

Table 4 presents the data collected on the time required to complete each sealing demonstration. With three people performing the demonstrations, the average time to perform the sealing was less than four hours. The time spent sealing the house is relatively short compared to the time required for setup and cleanup. It is expected that with a more mature technology and trained installation personnel that the labor required to perform the sealing can be reduced.

**Table 4: Summary of Time Required to Complete the Sealing for Each Demonstration**

| Test # | # Floors | Floor Area (ft <sup>2</sup> ) | Time Required (person hrs.) |            |         |
|--------|----------|-------------------------------|-----------------------------|------------|---------|
|        |          |                               | 1. Setup                    | 2. Sealing | Cleanup |
| 1      | 3. 2     | 4. 3,550                      | 5. 6.3                      | 6. 1.5     | 7. 5.0  |
| 2      | 8. 1     | 9. 2,019                      | 10. 5.9                     | 11. 1.3    | 12. 3.4 |
| 3      | 13. 1    | 14. 2,324                     | 15. 6.7                     | 16. 1.2    | 17. 4.2 |
| 4      | 18. 2    | 19. 3,550                     | 20. 6.9                     | 21. 1.9    | 22. 4.0 |
| 5      | 23. 1    | 24. 2,324                     | 25. 3.5                     | 26. 1.4    | 27. 1.9 |
| 6      | 28. 1    | 29. 2,324                     | 30. 4.6                     | 31. 1.3    | 32. 3.4 |

Sealant accounted for the majority of the disposable costs for each demonstration. The sealant is a commercially available air-barrier product that can be purchased for about \$40 per gallon. The sealant is diluted with water for use in the aerosol application.

Table 5 lists the sealant cost for each demonstration site. The average cost was about \$3.60 per 100 ft<sup>2</sup> home floor area but this value ranged anywhere from \$2.75 - \$4.51. Other disposable costs including tape, fuel for the compressor and generator, and peristaltic pump tubing were estimated to cost less than \$15 for each installation.

**Table 5: Summary of Sealant Costs for Each Demonstration**

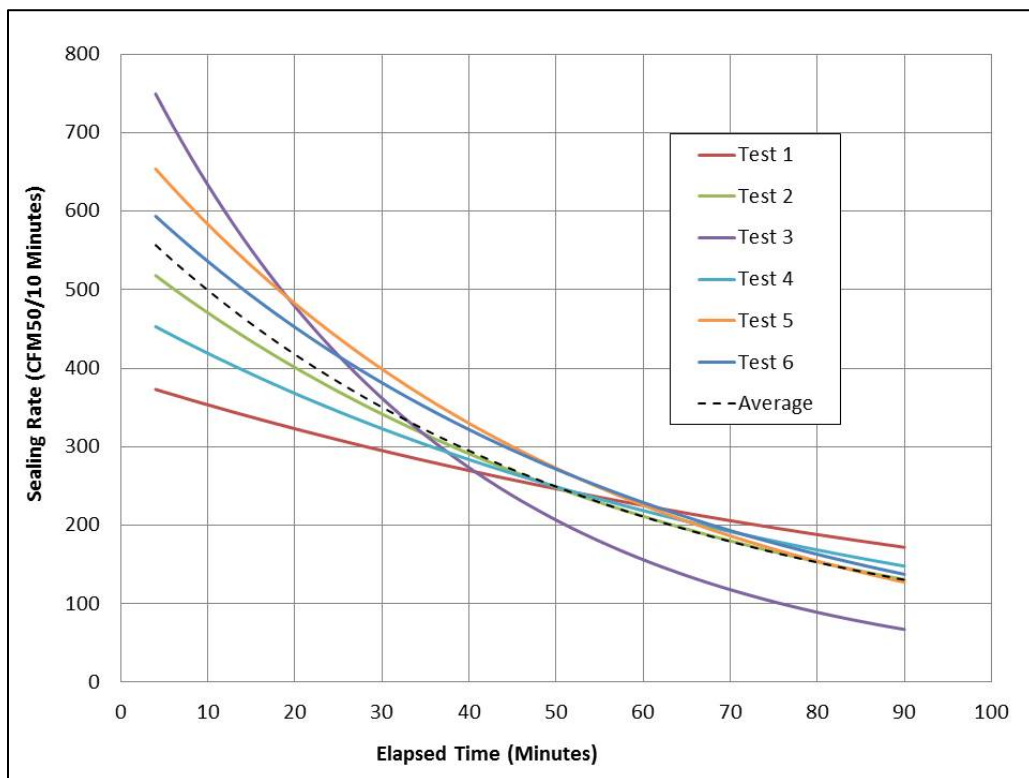
| Test # | # Floors | Floor Area (ft <sup>2</sup> ) | Diluted Sealant Used (gal.) | Sealant Cost            | Sealant Cost/100ft <sup>2</sup> |
|--------|----------|-------------------------------|-----------------------------|-------------------------|---------------------------------|
| 1      | 33. 2    | 34. 3,550                     | 35. 10.0                    | 36.<br>\$16<br>0.0<br>0 | 37. \$4.51                      |
| 2      | 38. 1    | 39. 2,019                     | 40. 5.0                     | 41.<br>\$80<br>.00      | 42. \$3.96                      |
| 3      | 43. 1    | 44. 2,324                     | 45. 5.0                     | 46.<br>\$80<br>.00      | 47. \$3.44                      |
| 4      | 48. 2    | 49. 3,550                     | 50. 7.5                     | 51.<br>\$12<br>0.0<br>0 | 52. \$3.38                      |

|   |       |           |         |                    |            |
|---|-------|-----------|---------|--------------------|------------|
| 5 | 53. 1 | 54. 2,324 | 55. 5.0 | 56.<br>\$80<br>.00 | 57. \$3.44 |
| 6 | 58. 1 | 59. 2,324 | 60. 4.0 | 61.<br>\$64<br>.00 | 62. \$2.75 |

Overall, the builder that provided the sites for the tests was extremely pleased with the result as it helped them surpass the California Title 24 minimum requirement for residential envelope air-tightness of 5 ACH50. Thus, these homes are expected to qualify for incentives from the local utility through the California Advanced Homes Program (CAHP) for exceeding the minimum requirements for air-tightness.

The leakage rates measured during the sealing process continuously fell as leaks were sealed. The average sealing rates achieved were 560 CFM50 per 10 minutes at the beginning of the tests and 130 CFM50 per 10 minutes at the end of the test. The average sealing rate achieved throughout the entire sealing process was 290 CFM50 per 10 minutes of injection. Figure 20 presents an exponential fit of the sealing rate data for each of the six tests.

**Figure 20: Sealing Rate Profile for Each Sealing Demonstrations**



When the sealing process begins smaller leaks seal much more quickly than larger leaks resulting in high initial sealing rates. As the smaller leaks begin to close off the sealing rates begin to drop as the larger leaks begin to seal. The installer can continue the sealing process until the targeted ACH50 leakage rate is achieved, or can mechanically seal leaks that are too large to seal effectively with aerosol before completing the final depressurization test. Future research could focus on procedures for attaining a particular target air tightness and when to stop the aerosol injection.

#### *Estimated Costs*

The average labor time required to complete the aerosol envelope sealing installations at the six sites was less than 11 person-hours. Only one person on the installation team had previous experience using the technology to seal homes, and the data collected on the time to complete each step of the process clearly showed that the team's speed improved during the second round of sealing demonstrations. It is expected that if the technology were commercialized the labor required to complete the sealing could be reduced significantly. The equipment used for this system is a prototype that could be made more efficient. One example of how the process could be simplified would be to employ hose reels. A substantial amount of time was spent winding and unwinding the 8 compressed air lines used to operate the nozzles, and using hose reels to manage the hoses would significantly shorten set-up and break-down time. Managing the hoses without a hose reel system required on average about two person-hours for each of the installations, or about 17% of the total time required.

It is estimated that with fully developed equipment and trained installation personnel it would require two contractors four hours each to prepare and seal a single-family home. Assuming each contractor earns \$30/hour, this would work out to be \$240 in labor for each installation. The material costs add another \$100 (\$16 per gallon) for sealant and \$15 for other disposables including tape and fuel. Thus, the complete cost for each installation would be about \$355, which would include documentation of the structure's airtightness. Depending on construction quality, this is likely to be a much lower cost than what would be required to achieve similar air tightness using strictly manual, mechanical caulking and sealing methods, which do not include airtightness documentation.

#### *How the aerosol sealing process be worked into a typical construction schedule*

It is expected that as builders become more familiar with the aerosol envelope sealing process there could be some slight modification to existing construction schedules that would reduce the preparation time needed for aerosol sealing. Through better coordination with the other trades builders and/or installers may find a more suitable time to apply the aerosol sealing to a building that would reduce the time required for all aspects of the sealing process. The demonstrations completed for this project were all performed after drywall was installed and taped. This stage of construction seems to be the most appropriate for the aerosol sealing process since most of the larger leaks have already been sealed, which allows the process to target the smaller leaks that are the most appropriate for this technology to seal.

This process is adaptable to alternative construction techniques. Current construction practices typically use the drywall to create the air barrier for a home; however, the many penetrations of drywall including electrical boxes and plumbing make it a relatively poor barrier. As building air leakage requirements become more stringent, builders may instead choose to adopt strategies that place the air barrier on the outer surface of a wall where there are significantly fewer penetrations. The aerosol process could still be used to seal the small distributed leaks on the inside of the “exterior envelope” that are not obvious to contractors at an earlier stage of construction as long as windows and doors are installed on the home.

## **1.4 Conclusion and Path Forward**

This project verified that the aerosol envelope sealing technology developed by University of California Davis can be a cost effective method for reducing air infiltration in new homes. The sealing method was capable of sealing 60-85% of the air-leakage present within 90 minutes of sealant injection. The installations were performed by University of California Davis engineers and students, only one of which had previous experience with a prototype injection system. Each installation required about four hours to setup, seal, and cleanup or about 11 person-hours. Considering the limited experience of the installation crew, this was a remarkable result. The cost estimate with commercial equipment and trained installation personnel would be \$355 to seal a large single-family home well below what standard building practices can achieve, with a far better result.

The market potential for this technology is extensive and growing as codes and standards start tightening the requirements for building envelope air leakage. While manual sealing will continue to be the most appropriate method for sealing large obvious air leaks, the aerosol sealing technology can quickly and cost-effectively address the small distributed leaks in a building allowing buildings to become extremely tight. An additional benefit of the technology is that it provides immediate feedback and certification of the building tightness which could satisfy testing requirements that may exist for a home. Deployment of this technology will likely occur through a manufacturer that would provide equipment and training to contractors such as HERS raters or HVAC contractors.

*Automated Aerosol Sealant Technology to Seal Gas Pipelines*

**Figure 21: Laboratory Sealant Test Using Black-light Sensitive Dye (left), WCEC Student Researcher Installs Aerosol Distance Measurement Apparatus (right)**



The project has sparked much research and commercial interest. The WCEC will soon commence a project funded by the Department of Defense to explore the sealing of commercial building envelopes, both in new construction and retrofit projects. Additionally, WCEC is building on lessons learned through this project to use aerosol sealing of leaks in other, novel ways. WCEC is, for example, now exploring the use of aerosols to seal low-pressure gas pipelines via funding from the Energy Commission's Energy Innovations Small Grant program. Figure 21 shows laboratory sealant test using black-light sensitive dye to be used to provide better data on where leaks exist in homes and gas pipeline sealing. The University of California Davis is in discussions with several companies interested in licensing the technology in advance of taking it into the marketplace.

## CHAPTER 2: Studies in Rainwater Collection and Storage for Evaporative Cooling

*This project received the 2014 ASCE-Sacramento "Improvement Energy Project" award by focusing on the development of carbon-neutral-alternative-energy solutions.*

Evaporative condensers are an energy efficient cooling solution for hot, arid climates. Even though evaporative systems have a large potential to reduce both the peak electricity demand and the energy use associated with cooling, water management for evaporative cooling units is essential and particular care must be taken to reduce the effects of hard water and overall water consumption of the system. Evaporative processes lead to the concentration of minerals in the cooling water reservoir, which eventually precipitate out of solution, scaling the condensing coil, pumps, piping, and other surfaces.

The goal of this research was to investigate whether the use of stored rainwater compared to tap water, as an alternative water resource, increases or decreases the risks (scaling, corrosion, and biological growth) associated with residential evaporative cooling systems. This research will also see if stored rainwater can serve as a sufficient water source to reduce or completely offset the need for municipal water in evaporative cooling.

### 2.1 Water quality in an above ground rainwater cistern

Evaporative processes lead to accumulation of mineral scale on the heat exchanger, whose performance thereby degrades over time (Figure 22). Several strategies were used to improve water-use efficiency and/or minimize scale formation in evaporative cooling systems; however, no cost effective solution has been found that enables long-term use of these systems in hard water areas.

By harvesting rainwater, this project will enable the use of evaporative cooling systems in hard water areas. Evaporative cooling systems are approximately 30% more energy efficient than air cooled systems<sup>2</sup>. For example, compared to the baseline home with an air-cooled condensing unit, a single-family residential building in the western part of the United States could achieve annual electricity savings of about 8 billion kWh (total site energy consumption) by using evaporative condenser units. This energy savings corresponds to preventing 6 million tons of carbon dioxide (CO<sub>2</sub>) emissions per year<sup>3</sup>.

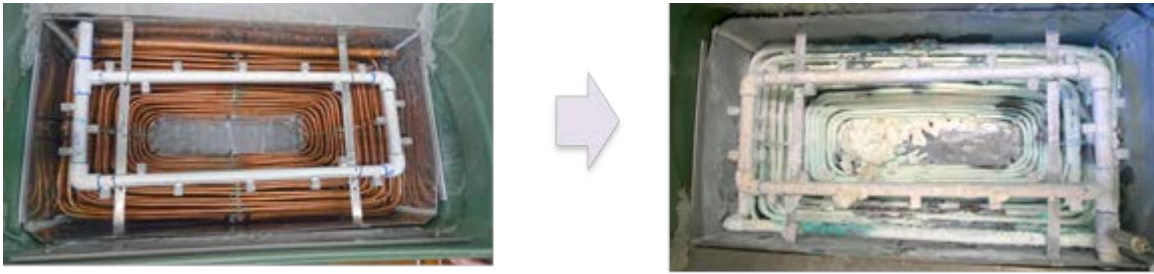
In addition, replacing potable water with rainwater in a nonpotable application reduces energy use and environmental damage and lessens the strain on drinking water supply.

---

<sup>2</sup> McKenzie, E.R., et al., An investigation of coupling evaporative cooling and decentralized graywater treatment in the residential sector. *Building and Environment*, 2013. 68(0): p. 215-224.

<sup>3</sup> Data Taken From U.S. Energy Information Administration (EIA) ; Available from: <http://www.eia.gov/consumption/residential/>

**Figure 22: Scale Formation on the Surface of the Copper Coil in an Evaporative Condensing Unit Supplied with Municipal Tap Water**



The first stage of the study investigates the chemical, physical and microbiological composition of the harvested, collected and longtime stored rainwater for the later use in evaporative cooling system. While numerous studies determined the chemical characteristics of collected rainwater, no work has been completed in an effort to model or to gain an understanding of water quality characteristics in rainwater tanks, particularly after long-term storage, for later use in applications such as an evaporative cooling system.

This project investigates the benefits and feasibility of using harvested rainwater as a strategy to reduce tap water consumption and extend equipment life for evaporative cooling systems. It is expected that the low hardness levels in rainwater compared to tap water will minimize scale formation, which increases system life and efficiency. The goal of this project was to determine feasibility of using harvested rainwater in an evaporative cooling system, based on assessment of the chemical, physical and microbiological composition of harvested rainwater immediately after collection and during a six-month storage period.

### 2.1.1 Quantifying roof runoff volume

Rainwater harvesting is practical only if the volume and frequency of rainfall and the size of the catchment surface can generate a volume of water sufficient for the intended purpose. As shown in Figure 2-2, based on the annual climate design condition, the amount of rainfall produced per dwelling from a roof on a one-story 1,800 ft<sup>2</sup> house would provide sufficient volume of water needed for an evaporative condenser in most of the major population centers in each climate zone 10 and 12 for both minimum and average design precipitation. In climate zone 13, 100 percent and about 80 percent of the evaporative cooler water demand can be fulfilled by harvesting rainwater based on average and minimum rainfall precipitation condition, respectively.

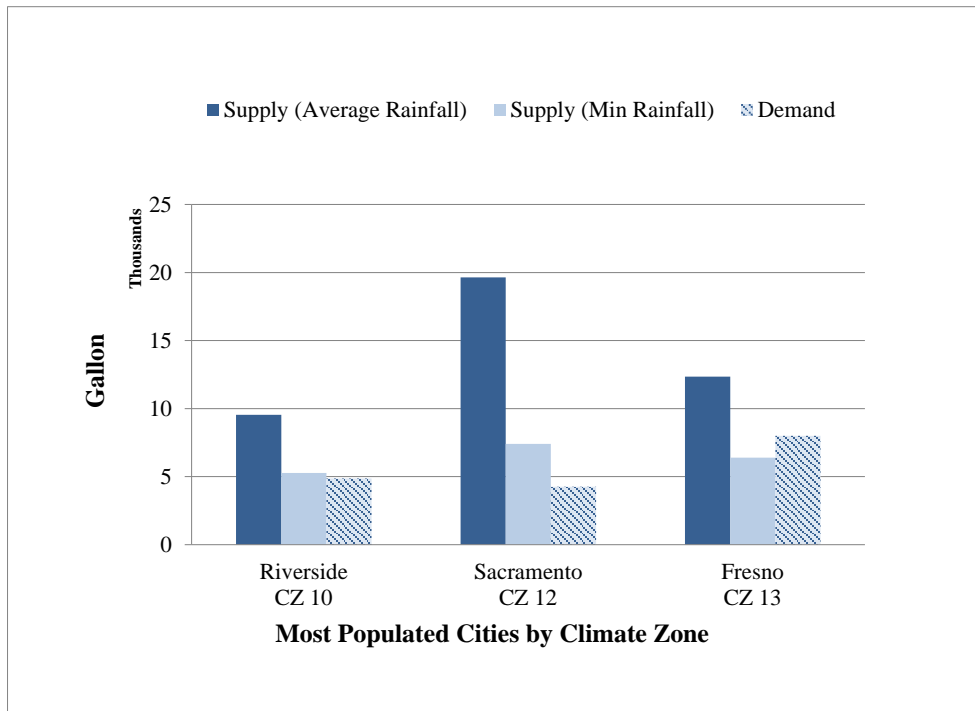
The results for a home's water burden for a residential evaporative cooling are taken from the previously published paper by McKenzie, E.R., et al.<sup>4</sup> The same roofing size of 1,800 ft<sup>2</sup> was used to be able to compare between the volume of water demand modeled in the paper and supply calculated in this report.

---

<sup>4</sup> McKenzie, E.R., et al., An investigation of coupling evaporative cooling and decentralized graywater treatment in the residential sector. *Building and Environment*, 2013. 68(0): p. 215-224

A typical 15-year old home, with 1,800 ft<sup>2</sup> roof, in climate zone 12 (e.g., Sacramento) and 10 (e.g., Riverside) consume 4,253 and 4,860 gallons of drinking water for cooling with an evaporative condensing unit, respectively. The same home in climate zone 13 (e.g., Fresno) consumes 8,000 gallons of drinking water. Knowing the size of the roof catchment area, the volume of water needed for its specific intended purpose, and using rainfall data, an appropriate cistern size can be realistically determined. According to Figure 23, for example, cisterns in the range of 5,000 (668 cubic feet) are recommended for a home this size in climate zone 10 and 12 and 8,000 gallons (1,070 cubic feet) in climate zone 13. There are commercially available many options for different over ground and underground water tanks designed for a wide volume range.

**Figure 23: Annual Average and Minimum Rainfall Supply from 1,800 ft<sup>2</sup> Roof**



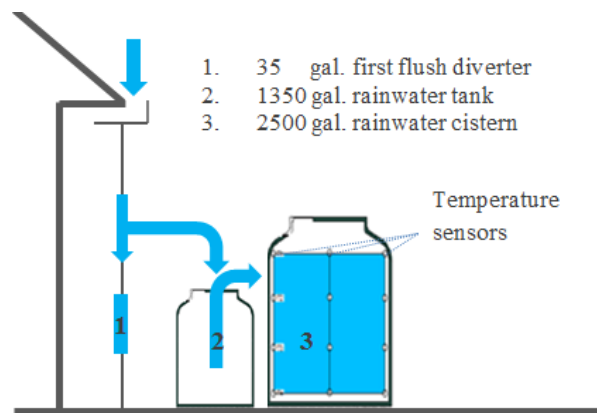
(Rainfall harvest potential and annual demand (evaporative cooling water requirements)).<sup>5</sup>

### 2.1.2 Methods, Procedures, and Facilities

For the purpose of this research study, the most common, easily installed and readily available 2,500 gallon above-ground polypropylene water tank was used to collect rainwater from a residential composite shingle roof (Figure 24). During the period of November through December 2012, the tank filled with rainwater. The rainwater was stored until summer, with its water quality examined on a weekly basis between November 2012 and June 2013.

<sup>5</sup> Committee, A.S., ASHRAE HANDBOOK: Fundamentals 2013. 2013, ASHRAE.

**Figure 24: Schematic of the Rainwater Cistern**



(1,350 gallons tank was used to test rainwater quality from each rain event before adding to the 2,500 gallons rain water cistern)

The first flush system disposes of a fixed volume of the first rainfall of the season. The paper published by Michael E. Barrett et al. 2010 for first flush volume suggested a minimum of 10 gallons for every 1,000 square feet of collection surface area. Since the characteristics and composition of rainwater vary depending on climate conditions, roof materials, and the surrounding environment, a 35-gallon first flush system was installed for a 1,500 ft<sup>2</sup> roof with over-hanged trees. The 35-gallon first flush chamber consists of a ball float, and once the chamber was full, the diverter of chamber directs the additional rain into the cistern and slowly drained out through the small drain in the bottom. The idea is redirecting the first-flush water to prevent most of the pollutants collect over the roof to enter the cistern.

The experimental design was separated into two different stages. First, a dynamic system simulated intermittently harvested rainwater for the winter season followed by a batch system to simulate the water quality for the spring and summer period. A primary goal of first phase was to evaluate the bacterial growth pattern in intermittently harvested rainwater. The aim of the second stage was to provide water quality analysis after long time storage in a batch system. Using an opaque material for the cistern eliminated the effect of sunlight. During the six month period the rainwater was monitored by measuring pH, hardness, turbidity, dissolved oxygen (DO), temperature, coliforms (criteria for water quality), dissolved organic carbon (DOC), nutrients and metals, on a regular basis. Temperature influences water chemistry and has a direct impact on the organisms living in the water. In this study, twelve water temperature sensors and one air temperature sensor were recording temperature variation for both water and air. Methods for water quality characteristics are shown in Table 6.

**Table 6: Methods for Water Quality Characteristics**

| Test                  | Symbol                           | Unit                          | Method                          |
|-----------------------|----------------------------------|-------------------------------|---------------------------------|
| <b>Conventional</b>   |                                  |                               |                                 |
| Temperature           | 63. T                            | 64. °F                        | 65. HQ30d portable meter        |
| Electric conductivity | 66. EC                           | 67. µs/cm                     | 68. HQ30d portable meter        |
| Turbidity             | 69. Turbid                       | 70. NTU                       | 71. 2100Q Portable Turbidimeter |
| pH                    | 72. pH                           | 73. pH unit                   | 74. HQ30d portable meter        |
| Hardness              | 75. Hardness                     | 76. mg/L as CaCO <sub>3</sub> | 77. Hach Method 8213            |
| Dissolved Oxygen      | 78. DO                           | 79. mg/L                      | 80. DO meter                    |
| Organic Carbon, Total | 81. DOC                          | 82. mg/L                      | 83. UV persulfate digestion     |
| <b>Organisms</b>      |                                  |                               |                                 |
| Total Coliform        | 84. TC, E.coli                   | 85. MPN/100ml                 | 86. IDEXX                       |
| E.coli                | 87. TC, E.coli                   | 88. MPN/100ml                 | 89. IDEXX                       |
| Fecal Coliform        | 90. FC                           | 91. MPN/100ml                 | 92. IDEXX                       |
| <b>Nutrients</b>      |                                  |                               |                                 |
| Ammonia               | 93. NH <sub>4</sub> <sup>+</sup> | 94. mg/L                      | 95. Hach Method 8155            |
| Nitrate               | 96. NO <sub>3</sub> <sup>-</sup> | 97. mg/L                      | 98. Flow Injection Analysis     |
| Orthophosphate        | 99. Ortho-P                      | 100. mg /L                    | 101. Flow Injection Analysis    |
| <b>Metals</b>         |                                  |                               |                                 |
| Copper                | 102. Cu                          | 103. pp b                     | 104. ICPMS                      |
| Calcium               | 105. Ca                          | 106. pp b                     | 107. ICPMS                      |
| Magnesium             | 108. Mg                          | 109. pp b                     | 110. ICPMS                      |
| Iron                  | 111. Fe                          | 112. pp b                     | 113. ICPMS                      |
| Lead                  | 114. Pb                          | 115. pp b                     | 116. ICPMS                      |
| Arsenic               | 117. As                          | 118. pp b                     | 119. ICPMS                      |
| Aluminum              | 120. Al                          | 121. pp b                     | 122. ICPMS                      |
| Selenium              | 123. Se                          | 124. pp b                     | 125. ICPMS                      |
| Barium                | 126. Ba                          | 127. pp                       | 128. ICPMS                      |

|           |      |    |         |            |
|-----------|------|----|---------|------------|
|           |      |    | b       |            |
| Manganese | 129. | M  | 130. pp | 131. ICPMS |
|           | n    |    | b       |            |
| Chromium  | 132. | Cr | 133. pp | 134. ICPMS |
|           |      |    | b       |            |
| Silver    | 135. | Ag | 136. pp | 137. ICPMS |
|           |      |    | b       |            |

<sup>a</sup> NTU = nephelometric turbidity unit (measure of water clarity)

<sup>b</sup> MPN = The most probable number method (measure of indicator bacteria)

### 2.1.3 Results and discussion

WCEC used a 2,500-gallon polypropylene tank to investigate the quality of rainwater stored over a 6-month period. As shown in Figure 25, the temperature in the tank followed the trend of the ambient air temperature but experienced significantly less fluctuation. The temperatures at different depths within the storage tank correspond to the locations indicated in Figure 2-3. During the experimental period ambient temperature ranged from 20°F to 100°F and water temperature varied from 39°F to 82°F. In addition, two different regions are observed in the temperature profile. The first region, which ends around January 30th, corresponds to the tank being filled with rain as it arrives. The second region corresponds to a storage period, during which the average water temperature increases steadily, and during which stratification of water temperatures within the tank increases and then stabilizes. The observed temperatures indicate the expected thermal stratification is developed inside the tank, with the temperature difference between the top and bottom of the tank settling to roughly 46°F.

Some chemical and physical parameters remained fairly stable during the storage period, as shown in (Figure 26). Electrical conductivity and pH were the same for top and bottom of the tank and stayed relatively unchanged during the storage period. The average electrical conductivity was about 38 microsiemens per centimeter ( $\mu\text{s}/\text{cm}$ ) during the storage period. The pH of the harvested rainwater samples from shingle roof was in the near-neutral range of 6.9-7.3. This near-neutral pH range shows that the potential corrosion risk to evaporative cooling systems decreases due to the roofing material buffering capacity. Turbidity, which is often used to measure the presence of particles in water, was low. During the experiments, the turbidity in the stored rainwater averaged  $2.5 \pm 0.8$  NTU. By the end of the experiment, the turbidity was reduced to less than 1NTU. Dissolved oxygen dropped from 11 milligrams per liter (mg/L) to 6 mg/L after storage period, where usually levels lower than 1 mg/L causes undesirable tastes and odor problems.

WCEC conducted biological contamination tests to investigate the presence of total coliforms, fecal coliforms and E. coli for samples collected from each rainwater event. Once the tank was full, the research team monitored the tank on a weekly basis. Total coliforms, E. coli and fecal coliforms were detected in the initial collected rainwater during the dynamic period but continued to decrease, with the exception of a regrowth phenomenon during weeks 20-24, to a safe level less than one MPN per 100 milliliters (MPN/100ml) for total coliforms, E. coli and fecal coliforms during the storage period (Figure 27). Several environmental factors influenced the

indicator bacteria decay. Winter's low water temperature, aging, and nitrification inside the tank are possible reasons for the bacteria's inactivation. The regrowth phenomenon could be possibly associated with the higher water temperature when the temperature of the tank approaches to the optimum temperature for bacterial growth (95°F for total coliform and E. coli and 112°F for fecal bacteria) in this period. The bacterial population decreases suddenly because the lack of nutrient sources such as nitrogen (ammonia  $[NH_3] < 0.01$  mg/L) and phosphorous (phosphate  $[PO_4^{3-}] < 0.05$  mg/L) required for proper growth. The initial source may result from dissolving the debris, plants and soil biota over the roof.

**Figure 25: Water and Ambient Air Temperature Profile in Home's Rainwater Cistern Davis, California**

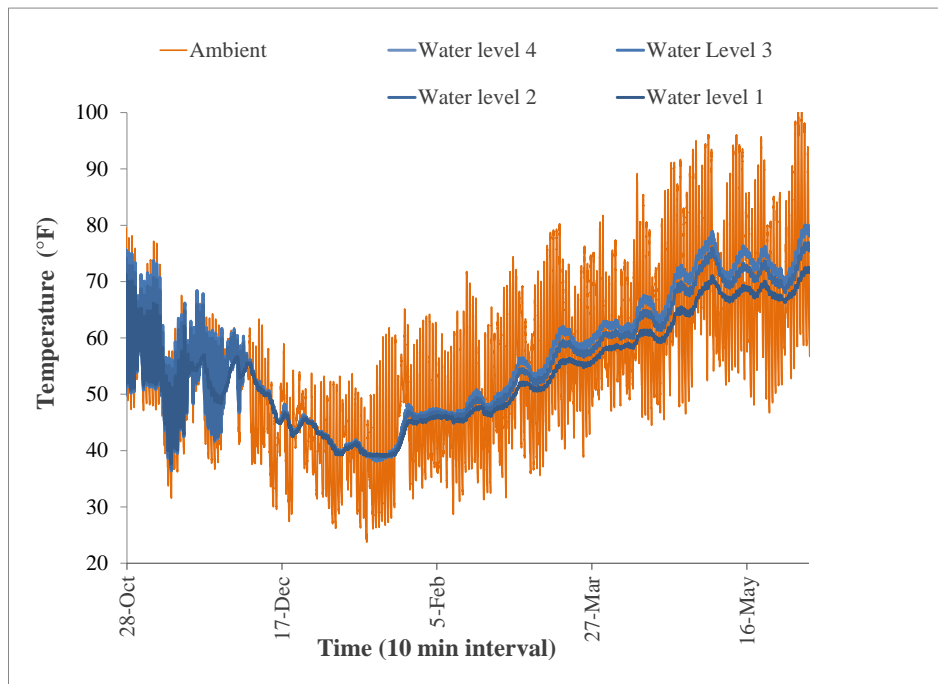
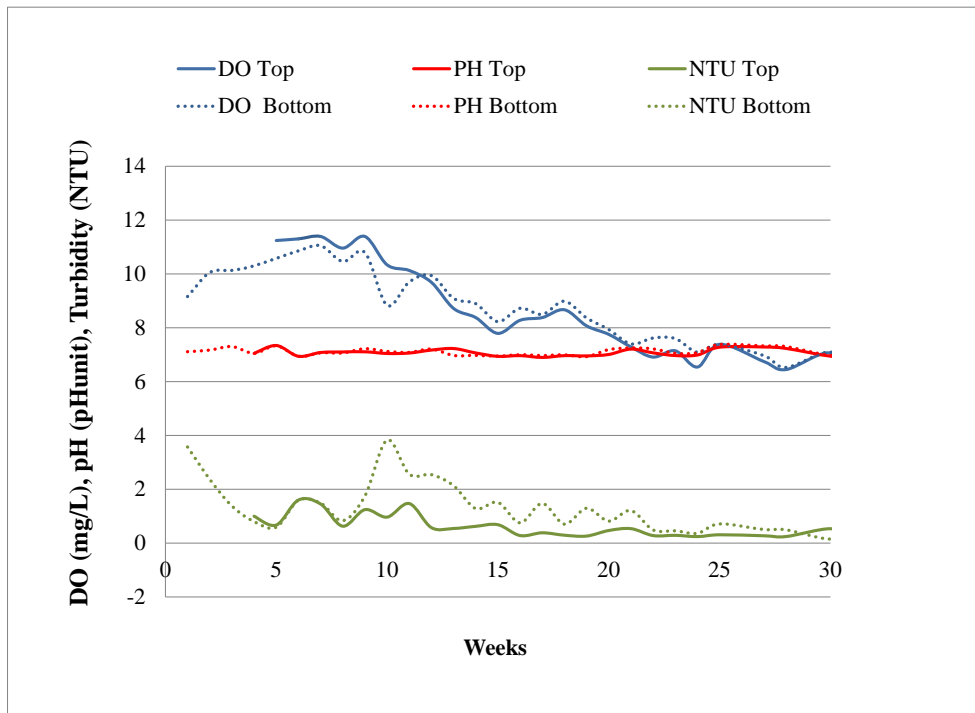
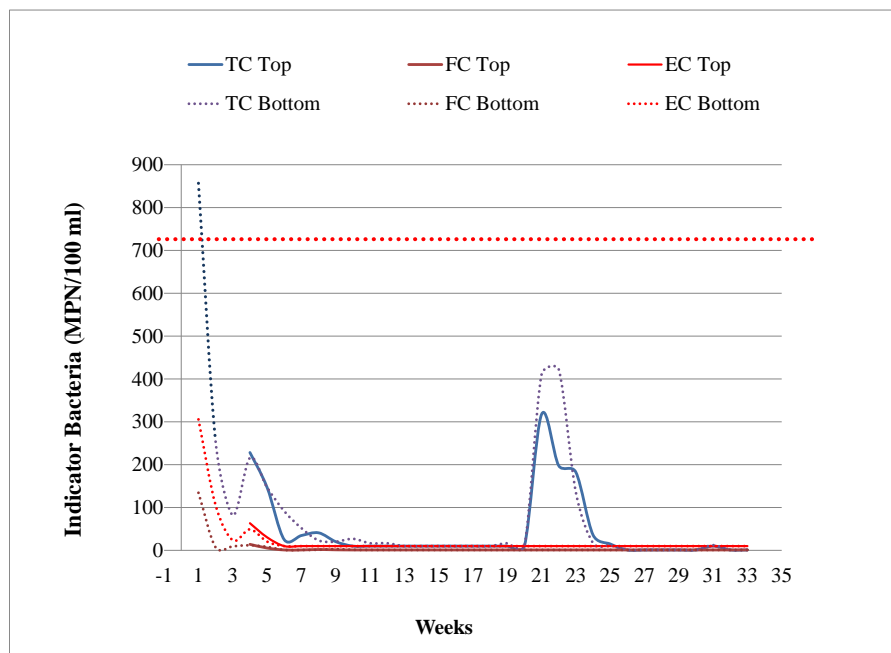


**Figure 26: Dissolved Oxygen, pH and Turbidity During Storage in the Rainwater Cistern**



**Rainwater Harvesting Policies Developed by EPA**

**Figure 27: Load and Decay Trend for Coliforms in the Rainwater Cistern**



Total coliforms (TC), fecal coliforms (FC) and E. coli (EC) in the rainwater cistern

As shown in Figure 28, stored rainwater likely loses a proportion of ammonia due to a growing microbial community that converted any ammonium to nitrate. Nitrification may cause oxygen to decrease. Both nitrification and less solubility of dissolved oxygen due to temperature increase of the tank are possible reasons for the reduction of dissolved oxygen concentration in the tank. Total dissolved organic carbon measure about 2 mg/L and remained unchanged throughout the experiment. This observation possibly indicates that the heterotrophic bacteria did not establish a large enough population to change the dissolved organic carbon.

According to Table 7, WCEC found consistent concentrations of calcium and magnesium over the course of this experiment. The average concentrations of arsenic, lead, iron, copper, barium and zinc in the rainwater harvested after the first-flush for were below the corresponding California’s primary or secondary drinking water standard of arsenic of 10 ppb, lead of 50 ppb, iron of 300 ppb, copper of 1,000 ppb, barium of 1,000 ppb and zinc of 5,000 ppb. Aluminum, selenium, chromium, silver and manganese were not detected.

**Figure 28: Dissolved Organic Carbon, Nitrate and Ammonia in the Rainwater Cistern**

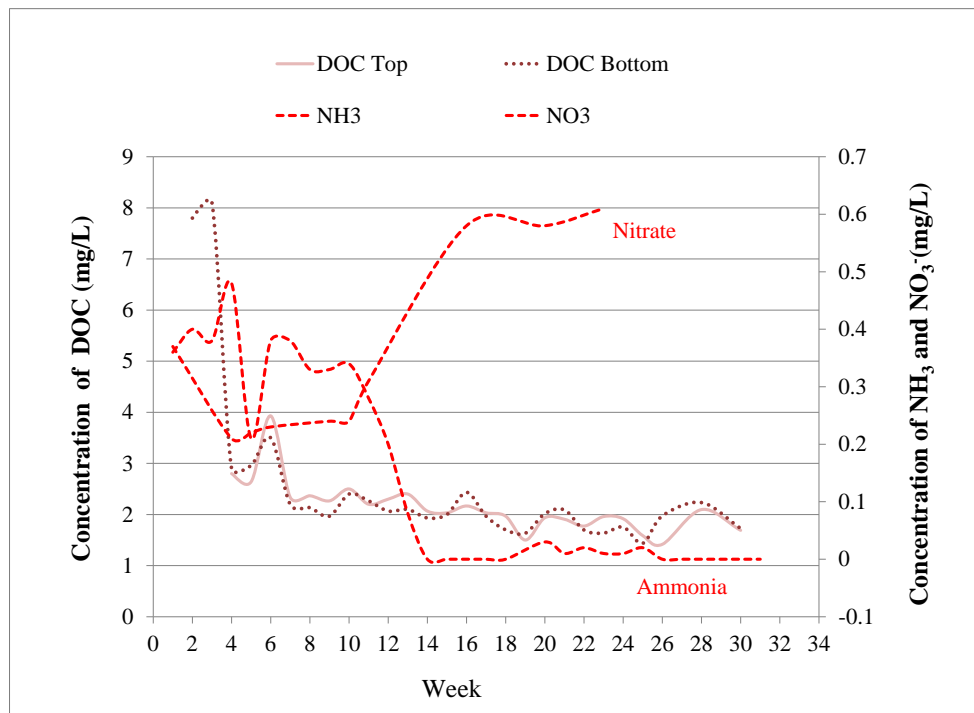


**Table 7: Metals Concentration in the Rainwater Cistern**

| Metal     | Symbol | Unit | Detected | Drinking water standard <sup>1</sup> |
|-----------|--------|------|----------|--------------------------------------|
| Sodium    | Na     | ppb  | 1191.46  | -                                    |
| Potassium | K      | ppb  | 216.46   | -                                    |
| Calcium   | Ca     | ppb  | 5173.54  | -                                    |
| Magnesium | Mg     | ppb  | 672.06   | -                                    |
| Copper    | Cu     | ppb  | 6.35     | 1000                                 |
| Iron      | Fe     | ppb  | 13.46    | 300                                  |
| Zinc      | Zn     | ppb  | 129.27   | 5000                                 |
| Arsenic   | As     | ppb  | 0.11     | 10                                   |
| Lead      | Pb     | ppb  | 0.85     | 15                                   |
| Barium    | Ba     | ppb  | 3.95     | 1000                                 |

<sup>1</sup> Environmental protection agency (EPA) primary or secondary drinking water standard

\*Aluminum, selenium, chromium, silver and manganese were not detected.

\*\*The Average hardness for the rainwater collected from the roof measured 15 mg/L as CaCO<sub>3</sub>. Hardness for hard water areas varies between 150-500 mg/L as CaCO<sub>3</sub>.

#### 2.1.4 Conclusion

Experiments were conducted to evaluate the presence of indicator bacteria for a six month storage period in an over ground rainwater cistern. The research team detected total coliforms, E. coli and fecal coliforms in the initial collected rainwater but continued to decrease to less than 1.0 MPN/100ml for total coliforms, E. coli and fecal coliforms by the end of the storage period. Initial visual comparison in Figure 29 shows there is no major visual difference between tap water and the collected rainwater after storage for six months. Based on this field experiment, stratification and nitrification occurred during the storage period, and the concentration of the indicator bacteria decreased to 1.0 MPN/ml over six months of storage. WCEC attributes the decrease to death and decay mostly due to a lack of nutrients. The results suggest that stored rainwater is a good potential water source with a simple treatment device such as chlorination, ozonation, and UV light. Further research is needed to verify the most cost effective and efficient method.

Assuming one colony forming units (CFU) equals one MPN <sup>6</sup>, the results of the conducted field experiment, stored rainwater would not need any complex treatment to meet the minimum nonpotable water quality guidelines developed by the EPA. The guidelines indicate that the acceptable level of total coliforms should be less than 500 CFU/100 ml, and fecal coliforms levels should be less than 100 CFU/100 ml for nonpotable water usage<sup>7</sup>.

<sup>6</sup> [http://www.epa.gov/waters/tmdl/docs/33596\\_drafttmdl\[1\].pdf](http://www.epa.gov/waters/tmdl/docs/33596_drafttmdl[1].pdf)

<sup>7</sup> Managing Wet Weather with Green Infrastructure Municipal Handbook: Green Infrastructure Retrofit Policies. US Environmental Protection Agency, 2008

This study suggests that the disinfection of stored rainwater before usage, as a relatively simple method, would result in a safe and reliable approach for use in an evaporative cooling system while protecting against uncertainties in both initial microbial contamination load and microbial growth during operation.

**Figure 29: Tap and Collected Water and Six Month Stored Rainwater**



Tap Water (left) and Collected and 6 month stored rainwater from a nine years shingle roofing material with over hanged branches over roof (right).

## **2.2 Experimental results of different water quality in evaporatively cooled condenser with a copper coil**

A laboratory test with a small-scale evaporative condensing unit, with copper coil, investigated both tap water and rainwater effects in cooling systems. Various water sources for use in a residential evaporative condenser, representing tap water characteristics typical to California, were tested. The potential sources included groundwater-derived municipal water, surface-water-derived municipal water, and harvested rainwater. The project evaluated the interplay between water quality, evaporative-condenser fouling and performance, and water burden for each water source.

### **2.2.1 California Water Quality Analysis by Water District and Climate zone**

WCEC obtained water quality information for the State of California from the California Department of Public Health, and contained measurements of pH, conductance, total hardness, calcium and magnesium, hydroxide alkalinity and carbonate alkalinity for each water district in the state.

The research team removed outliers and filtered the data set to contain only districts that serve 30,000 people or more and had 30 or more observations for each of water quality parameter. The data was used to calculate summary statistics for water quality variables for each water district. Water districts were categorized by 1) drinking water source of either groundwater or surface water from a source assessment map and 2) climate zone location in California<sup>8</sup>.

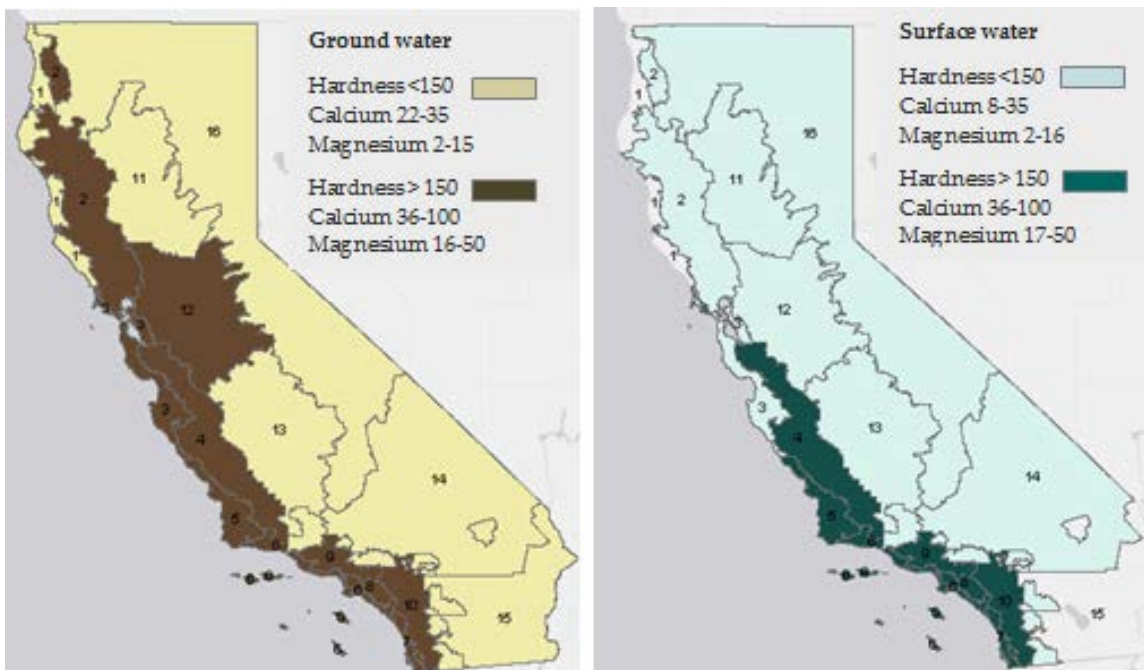
---

<sup>8</sup> Health, C.D.o.P.; Available from: <http://www.cdph.ca.gov>

Figure 30 represents the range of calcium and magnesium in California's water, discriminated by climate zone, for both groundwater and surface water sources. This research study categorized water sources based on their mineral content as very hard water and moderately hard water areas. Hardness is often defined as the sum of polyvalent cations (e.g.,  $Mg^{++}$ ,  $Ca^{++}$ ) and is expressed in units of  $CaCO_3$ . More than 150 mg/L as  $CaCO_3$  was categorized as very hard water and less than 150 mg/L as  $CaCO_3$  was categorized as moderately hard water<sup>9</sup>.

Using the water quality data analysis produced in this research study, the water quality characteristics for California municipal tap waters were replicated to create artificial water for the experiment.

**Figure 30: The Range Concentration of Total Calcium (mg/L) and Magnesium (mg/L) in California's Tap Water by Climate Zone**



Calcium ion concentration for municipal average calcium concentrations for moderately hard water and very hard water areas were evaluated 25 mg/L (SD=10.3) and 72.2 mg/L (SD=34.1) consequently, while average magnesium concentrations were 8.2 (SD=5) and 23.7 (SD=17.3) in moderately hard water and very hard water areas, respectively (Table 8).

<sup>9</sup> Engineering, H., Handbook of Public Water Systems. 2002: Wiley.

**Table 8: Water Quality Parameters**

|                                | Hardness (mg/L) as CaCO <sub>3</sub> |   | Magnesium (mg/L) |   | Calcium (mg/L) |             |   |             |   |             |
|--------------------------------|--------------------------------------|---|------------------|---|----------------|-------------|---|-------------|---|-------------|
| <b>Hardness</b>                | 138.<br>H                            | L | 139.<br>H        | H | 140.<br>H      | 141.<br>H   | H | 142.<br>H   | L | 143.<br>H   |
| <b>Average</b>                 | 144.<br>5                            | 9 | 145.<br>80       | 2 | 146.<br>.2     | 147.<br>3.7 | 2 | 148.<br>5.0 | 2 | 149.<br>2.2 |
| <b>Standard deviation (SD)</b> | 154.<br>2.4                          | 3 | 155.<br>26.9     | 1 | 156.<br>.0     | 157.<br>7.3 | 1 | 158.<br>0.3 | 1 | 159.<br>4.1 |

\* The areas with hardness less and higher than 150 mg/L as CaCO<sub>3</sub> were called Low Hardness (LH) and High Hardness (HH).

### 2.2.2 Systematic testing of influential water quality parameters

The following investigation assessed the effects of various water quality parameters to determine their influence on scale formation. The water quality parameters evaluated include two water quality scenarios to represent the breadth of water quality conditions in California to capture the range of water conditions in California’s drinking water supply as shown in Table 2-3. This experiment examined four setups in parallel with low (about 7%) bleed rate systems with two different tap water qualities. Table 9 presents each individual setup. Bleeding of a system is the rejection of a portion of the cooling water in the system either continuously or at regular intervals during operation. Tap water replaced the volume removed.

The small-scale apparatus ran up to four tests simultaneously to reduce the variability in test conditions. The strategy applied was to compare low and high hardness water-source systems in a small scale of aqua chill. By using a newly made copper coil and an old copper coil (previously coated with solids from the previous experiment), the research team looked to understand the effect and presence of previously precipitated solids in the system. The four small-scale units ran in parallel for 15 days.

**Table 9: Make Up Water Characteristics**

| Parameter  | Unit                      | A                 | B                  | C                 | D                  |
|------------|---------------------------|-------------------|--------------------|-------------------|--------------------|
|            |                           | Low Hardness (LH) | High Hardness (HH) | Low Hardness (LH) | High Hardness (HH) |
|            |                           | New Copper Coil   |                    | Old Copper Coil   |                    |
| pH         | pH unit                   | 7.5               | 7.5                | 7.5               | 7.5                |
| Calcium    | mg/L                      | 14                | 83                 | 14                | 83                 |
| Magnesium  | mg/L                      | 4                 | 31                 | 4                 | 31                 |
| Alkalinity | mg/L as CaCO <sub>3</sub> | 75                | 75                 | 75                | 75                 |
| Hardness   | mg/L as CaCO <sub>3</sub> | 51                | 335                | 51                | 335                |

\* Water quality parameter in the feed water with hardness more and less than 150mg/L based on Figure 2-9.

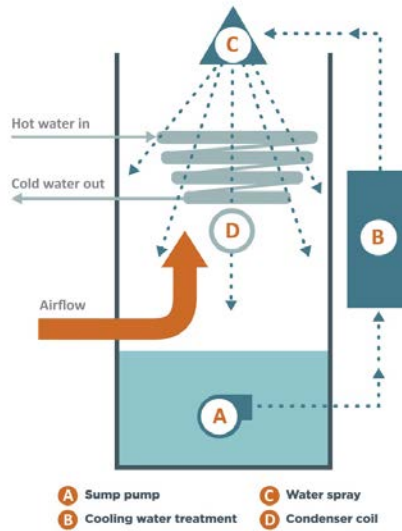
### 2.2.3 Experimental Setup

Each parallel system consisted of a copper coil supplied with hot water from a water heater to simulate a hot condenser coil (Figure 31 and Figure 32). A pump sprayed the coil with water from a sump in the bottom of the chamber. A fan upstream and a constant airflow damper controlled the supply airflow. A peristaltic metering pump controlled by a float switch replaced the evaporated water.

**Figure 31: Water Treatment Parallel Testing Experimental Setup**



**Figure 32: System Schematic of Single Small-Scale Test Chamber**



### *Airflow*

An analog dial on the side of the fan housing set regulated the fan speed. Air leaving the fan passed through four 1.4 kilowatt (kW) heaters to bring the temperature up to 95°F as controlled by the data acquisition system. When ambient conditions prevented proper conditioning of the air, the experiment was paused until the air reached 95°F.

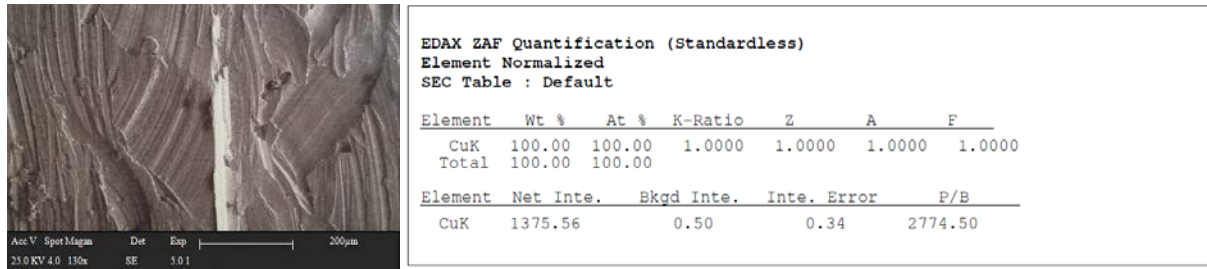
Once conditioned, the warmed air entered a 10-inch round by 54-inch long manifold where the flow was then separated into four 6-inch flexible round ducts, one for each test chamber. Sensors monitored the pressure at the entrance to each of the four ducts while the temperature and humidity were measured at the center of the manifold, 42 inches from the inlet. The airflow was then routed through a 6-inch flexible duct where it entered the chamber, passed over the coil and carried heat and water vapor out the exhaust.

### *Hot water flow*

To simulate hot refrigerant coils, a constant speed pump circulated hot water through the small-scale coils constructed of 0.25-inch outer diameter copper tube with 0.03-inch wall. The flow exiting the water heater passed through a 50-micron filter before entering a thermostatic mixing valve used to blend incoming hot water with cooler water returned from the coils. The valve manually varied the mix to supply a constant temperature (122°F) output stream. Resistive temperature devices (RTDs) measured water temperature before splitting into four streams, one for each test chamber, and after leaving each coil. An Omega FTB2001 paddle wheel flow sensor measured the flow rate before the inlet of each copper coil.

Scanning electron microscopy was used to obtain qualitative information for elemental composition of the copper coil. As shown in Figure 33, the analysis showed the purity of copper coil was 100% by weight of the elements found in the substance.

**Figure 33: Elemental Composition of Copper Coil using Scanning Electron Microscopy**



### *Cooling water flow*

The cooling water was recirculated from sumps under the test chambers. Each test chamber had an individual spray nozzle and sump reservoir, which held the cooling water and contained a sump pump used to supply cooling water to the respective spray nozzle. To ensure consistency among the four chambers, the initial performance of each pump and nozzle system was measured and found to have a flow rate of  $0.58 \pm 0.02$  gallons per minute (gpm). The nozzles provided a wide aperture with a hollow cone spray pattern. They produced large droplets, which minimized drift loss into the airstream. The water leaving the spray nozzle wetted the heat exchange coil where approximately 1% evaporated and the remainder fell back into the sump reservoir.

The sump level control used a float switch that actuated an individual peristaltic pump, model Mightyflex 907, for each test chamber. Each pump was individually calibrated on-site by measuring the amount of water mass pumped in one minute. The calibration was checked every two days to assure consistency. During the experiment, the data acquisition system recorded each pump’s runtime to calculate the water replacement rate.

### 2.2.4 Water chemistry analysis

The system ran for total of 15 days in 1 hour on and 30 minutes off cycles. Samples from each small-scale sump were collected for total 15 days and the last 5 days data set was used to perform a mass balance analysis assuming steady state condition based on known influent and effluent composition. The samples were taken every day from the bleed during the same time and were analyzed for pH, conductance, temperature, alkalinity and metals, including calcium and magnesium hardness. WCEC analyzed pH with a Hach HQ40d meter and a Hach IntelliCAL PHC301 probe (0.01 pH unit resolution). All meters and probes were calibrated daily before use per manufacturer’s instruction using standard solutions. Alkalinity was measured by sulfuric acid titration to the phenolphthalein endpoint (Hach Method 8203). Metals were measured for both total and “dissolved” metals, where the latter was operationally defined as the hardness of the water passing through a 0.2 µm polyvinylidene difluoride (PVDF) filter. All data discussed in this report are based on the dissolved concentrations. Metals analysis was completed using an inductively coupled plasma mass spectrometer (ICP-MS; Agilent 7500i, Ar

plasma at 1,350 W) on dilute acid extracted samples according to EPA method 602010. This instrument is sensitive for concentrations across seven orders of magnitude. The limit of detection for calcium and magnesium was  $<0.1$  mg/L, which is far less than the concentrations observed in any of the samples.

### 2.2.5 Initial results

The water deliberately was removed from the system as blowdown or bleed in this experiment at regular intervals during operation and was replaced by the tap water source based on lowest bleed rate recommended by the manufacturer for soft water areas. Bleed rate was defined as a portion of water removed from the system divided by the portion of cooling water evaporates.

Figure 34 shows a reasonable consistency among desired bleed rates of low 6% to 7% in this series of experiment.

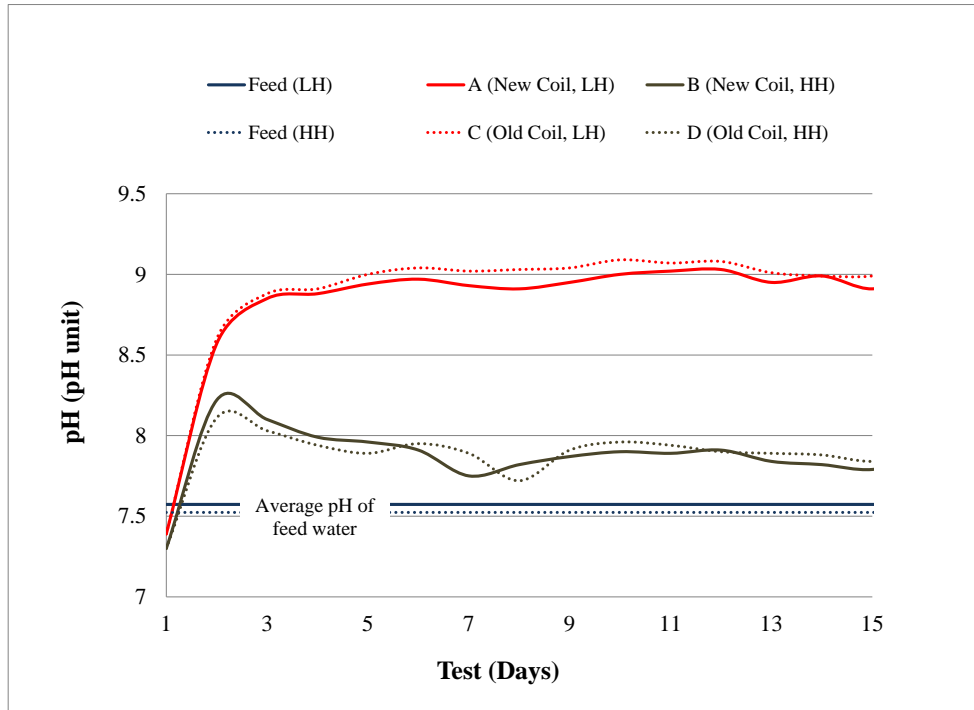
**Figure 34: Bleed Rates for Each Test**



There are many factors in evaporative condensers that contribute to favorable conditions for precipitation reactions. Calcium carbonate is the most common scale-forming compound in many different water systems. When water evaporates it not only concentrates the minerals, it also concentrates the carbonate species, which creates a carbonate-system super-saturated solution. As  $\text{CO}_2$  (aqueous) concentrations are reduced by releasing  $\text{CO}_2$  (gas) into the atmosphere, concentrations of bicarbonates and carbonates increase and the pH increases. This

result increased the solution pH, which corresponds to an increase in  $\text{CO}_3^{2-}$ . As shown in Figure 35, pH increased in all cases; however, pH increased more in A and C (Low Hardness feed, LH). The final pH values average of 9.2 for A and C (Low Hardness feed, LH) and 7.87 for B and D (High Hardness feed, HH). The elevated pH in all systems, compared to influent, demonstrates the effects of evaporation and off gassing of  $\text{CO}_2$ . As the pH increases, more total carbonates are present in the system and the speciation (division among the three forms) shifts toward the scale forming species ( $\text{CO}_3^{2-}$ ).

**Figure 35: Coil pH Values**

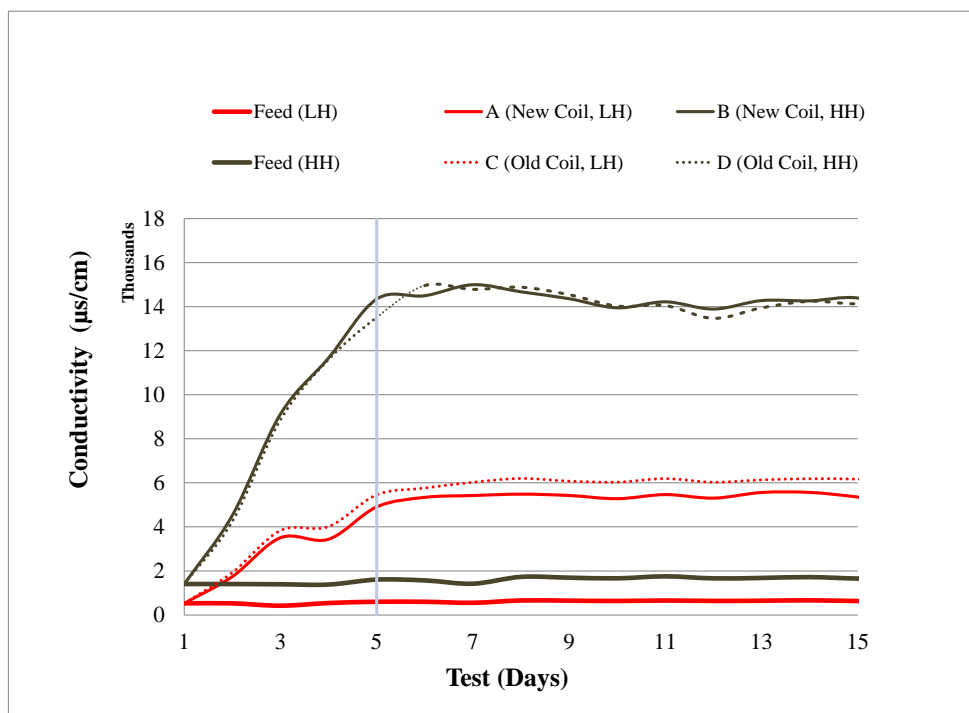


A (New coil, LH feed), B (New coil, HH feed), C (Old coil, LH feed), D (Old coil, HH feed)

Evaporation removes only water; therefore, the soluble minerals concentration increases. As expected, sump water conductivity was always higher than feed in all cases and higher in B and D (High Hardness feed, HH) than in A and C (Low Hardness feed, LH).

Conductivity measurement indicates that all systems needed at least five days to achieve the steady state condition in terms of mineral concentration. Calcium and magnesium concentration also showed the same trend as conductivity and the sump concentration reached the steady state after five days of operation. As shown in Figure 36, the electrical conductivity of a sump increased from 530  $\mu\text{S}/\text{cm}$  to 5,500  $\mu\text{S}/\text{cm}$  for A and C (Low Hardness feed, LH) and from 1,400  $\mu\text{S}/\text{cm}$  to 13,900  $\mu\text{S}/\text{cm}$  for B and D (High Hardness feed, HH).

**Figure 36: The Experimentally Measured Conductivity Values**



A (New coil, LH feed), B (New coil, HH feed), C (Old coil, LH feed), D (Old coil, HH feed) until steady state condition prevails. Conductivity measurement indicates that the system needs at least five days to achieve the steady state condition in terms of minerals.

It is assumed that the sump ion concentration is the same as effluent or bleed water. Declining sump dissolved calcium and magnesium concentrations were observed at higher pH values in A and C (Low Hardness feed, LH) due to pH dependency of calcium and magnesium solubility. Similar trends were observed with total calcium and magnesium concentrations.

As shown in Figure 37, in A and C (Low Hardness feed, LH), sump calcium concentration showed a reduction compared to the feed water, while in B and D (High Hardness feed, HH), showed higher calcium concentration compared to the feed water (Figure 38).

Magnesium concentration showed an increase compared to the feed water for both low hardness and high hardness feed systems (Figure 39 and Figure 40).

Figure 37: Average Dissolved Calcium Ion Concentration at Steady State for A (New coil, LH feed) and C (Old coil, LH feed)

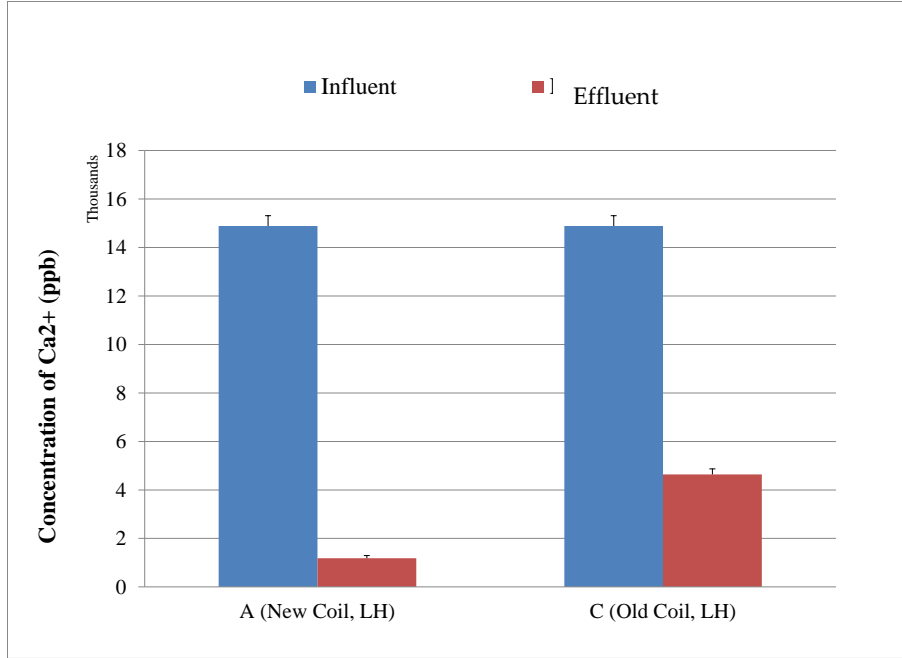


Figure 38: Average Dissolve Calcium Ion Concentration at Steady State for B (New coil, HH feed), and D (Old coil, HH feed).

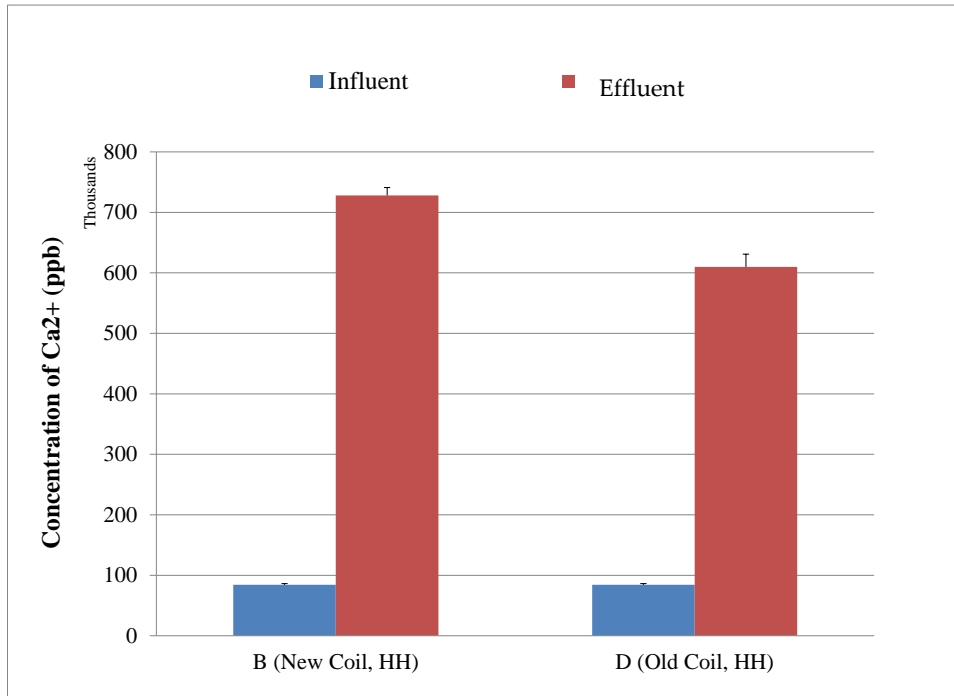


Figure 39: Average dissolved magnesium ion concentration at steady state for A (New coil, LH feed), and C (Old coil, LH feed)

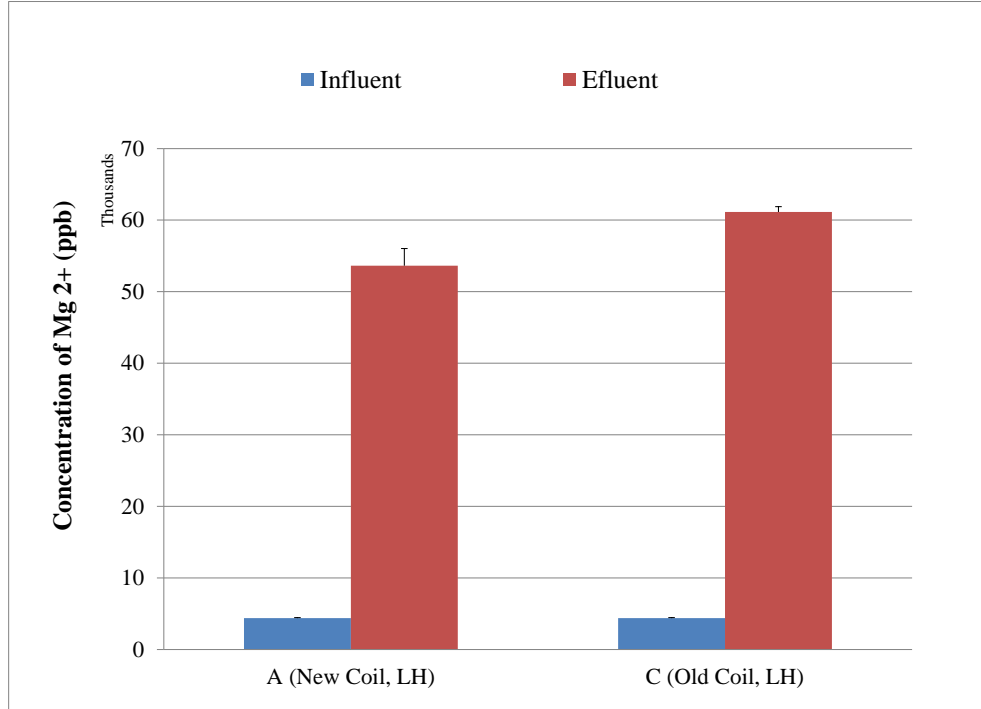
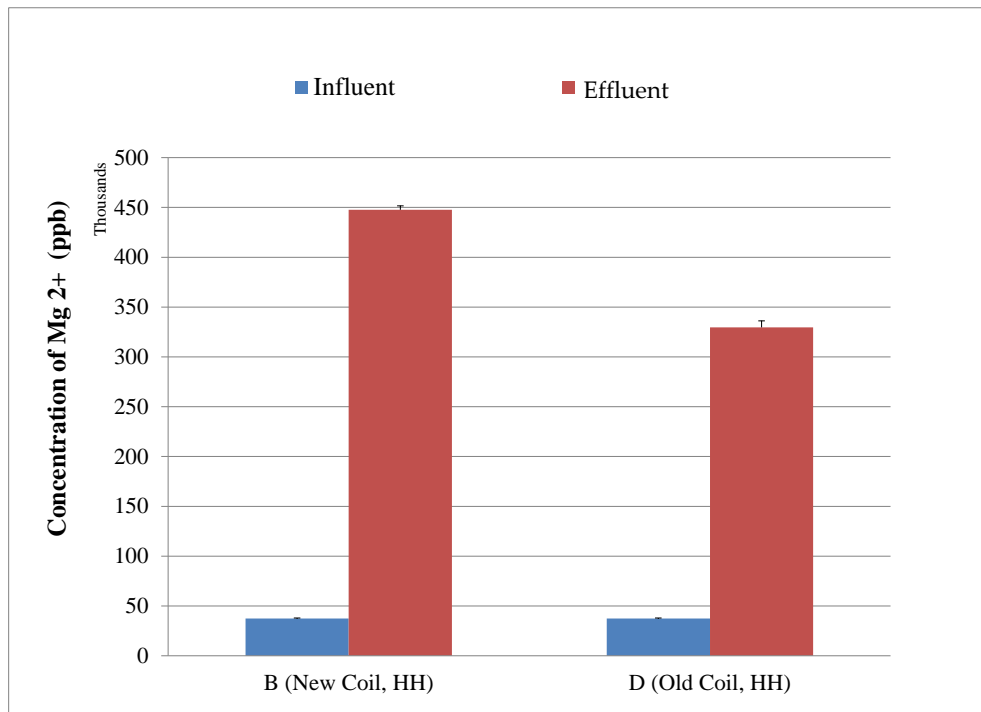


Figure 40: Average Dissolve Magnesium Ion Concentration at Steady State for B (New coil, HH feed), and D (Old coil, HH feed)



Increased evaporation of water, which increases the concentration of minerals, supersaturates the sump over a sufficient time. Vaporization of water over the copper coil leads to direct deposition on the surface of the coil. Table 10 shows the summary results of solution mineral analysis for the experiment. The amount of precipitation for each test was calculated based on the measured influent and effluent concentrations.

**Table 10: Summary of Aqueous Chemistry Results**

| System |                   | Bleed (%) | pH <sub>f</sub> | pH <sub>ss</sub> | Calcium                |                        |                     |                  | Magnesium              |                        |                     |                  |
|--------|-------------------|-----------|-----------------|------------------|------------------------|------------------------|---------------------|------------------|------------------------|------------------------|---------------------|------------------|
|        |                   |           |                 |                  | Feed (mM) <sup>a</sup> | Sump (mM) <sup>a</sup> | Deposition          |                  | Feed (mM) <sup>a</sup> | Sump (mM) <sup>a</sup> | Deposition          |                  |
|        |                   |           |                 |                  |                        |                        | (mols) <sub>b</sub> | (%) <sup>c</sup> |                        |                        | (mols) <sub>b</sub> | (%) <sup>c</sup> |
| A      | New coil, LH feed | 7         | 7.6             | 9.0              | 0.37                   | 0.03                   | 0.36                | 91               | 0.18                   | 0.02                   | 0.03                | 9                |
| B      | New coil, HH feed | 7         | 7.6             | 7.9              | 2.10                   | 18.17                  | 0.57                | 25               | 1.54                   | 0.05                   | 0.33                | 3                |
| C      | Old coil, LH feed | 6         | 7.6             | 9.0              | 0.37                   | 0.12                   | 0.36                | 91               | 0.18                   | 0.03                   | 0.04                | 13               |
| D      | Old coil, HH feed | 7         | 7.6             | 7.9              | 2.10                   | 15.22                  | 0.50                | 22               | 1.54                   | 0.20                   | 0.70                | 12               |

<sup>a</sup> Average steady state sump concentration (mM=milimolar)

<sup>b</sup> Calculated based on a mass balance approach for steady state conditions for 1L evaporated water (mols is similar to a unit of mass)

<sup>c</sup> Calculated based on a mass balance approach for steady state conditions; unprecipitated component is in sump

Calcium was observed to be largely precipitated (about 90% precipitation) in A and C (Low Hardness, LH) and the sump concentrations of calcium were actually lower than that of influent. The calcium concentration in sump was 0.03 mM for new coil test and 0.12 mM for the old coil test.

Calcium precipitated in B and D (High Hardness, HH) about 25% for new coil and 22% for the old coil.

Magnesium scale (probably magnesium carbonate) formed in all cases. Magnesium was observed to be precipitated (about 9% precipitation) in A and C (Low Hardness, LH).

Magnesium concentration in sump was 0.02 mM for new coil test and 0.03 mM for the old coil test. Magnesium precipitated in B and D (High Hardness, HH) systems about 3% for new coil and 12% for the old coil. In the HH system thus high concentration condition for new coil, magnesium contributed higher to mineral scale formation compared to the LH system the amount of precipitation almost was increased when the system was old (400% increase).

Indicating that previously precipitated solid on the coil can lead to excessive precipitation and therefore reduces solution concentration especially when the influent concentration is high such as D. The presence of nucleation sites on the copper coil may encourage the scale formation on the surface. This effect was lower (45% increase) when the effluent had a low concentration as was observed in low hardness systems (LH) such as A and C.

## 2.2.6 Recommendations for Follow-up Experiments

### *The systematic testing of influential water quality parameters in high bleed case*

Recent work at the WCEC indicated that the two principal elements contributing to water hardness – calcium (Ca) and magnesium (Mg) – behave very differently in an evaporative condenser in the low bleed rate scenario. In this investigation, the effects of the examined water quality parameters will be assessed to determine their influence on scale formation in the high bleed scenario (25%). An analytical model will be developed to determine optimized bleed rates based on the defined tap water quality. The results of this study will be used to develop bleed recommendations for evaporative condensing equipment operating in different climate zone in California, with the objective of optimizing water use while minimizing scale formation.

### *Rainwater storage water quality assessment on cooling system*

Recent work at the WCEC assessed the implications and feasibility of long-term (e.g., 6 months) rainwater storage. To be able to determine the appropriate and ideal disinfection device it is necessary to understand the operating pH for the system by using rainwater. Since pH plays a critical role both in the extent of scale formation and disinfection efficiency, if any disinfection is added for rainwater source. To be able to recommend the most cost effective disinfection device such as chlorination (liquid bleach, sodium hypochlorite), ozonation or UV, the artificial rainwater will be recirculated in the small-scale aqua chill. The operating pH will be monitored because the pH of the disinfectant solution affects the reaction kinetics. If the final pH is low (pH<8), for example, either chlorination or copper-silver ionization will be recommended due to the high disinfection efficiency of free chlorine and copper-silver ionization at lower pH values (around 7.5).<sup>11</sup> If the final pH is high (pH>9) ozonation will be tested instead. Different ozone dosages are required for different pH values.<sup>12</sup>

In this experiment, the dissolved copper ion concentration (leached from copper condenser coil using rainwater) will be also monitored in recirculation water since, the concentration of copper ion in some extend in water will limit the bacterial grow significantly.

---

<sup>11</sup> Yu-sen E. Lin, R.D.V., Janet E. Stout, and Victor L. Yu, Negative Effect of High pH on Biocidal Efficacy of Copper and Silver Ions in Controlling Legionella pneumophila. 2002.

<sup>12</sup> Drinking Water Treatability Database: Ozone, EPA.

# CHAPTER 3: New Techniques for Ground Source Heat Pumps (GSHP)

## 3.1 Problem Statement

Traditional geo-thermal techniques require expensive drilling rigs that can bore vertically 200 feet into the earth. Large Diameter Earth Bore (LDEB) and Directional Bore installations aim to reduce these costs by reducing the drilling depth while maintaining an adequate amount of heat exchange with the earth. The LDEB's innovative system utilizes a 24 inch diameter, 20 foot deep helical coil constructed of ½ inch diameter high density polyethylene (HDPE) tubing placed into the borehole and backfilled with dirt from the drilling, sand, rock, or other fill. Drilling for these shallow bore heat exchangers is quick, and far less expensive than conventional techniques. Each bore may take less than an hour to drill, allowing around eight to be completed in a typical workday. A day of work may yield around 150 linear feet of heat exchange depth; however, on a per foot basis, each LDEB exchanger has approximately 250 feet due to the effective increase in surface area. The Directional Bore system drills many shallow lanes across a plot of land creating a large amount of heat-exchange surface area in a short amount of time and at a reduced cost compared to more conventional GSHP.

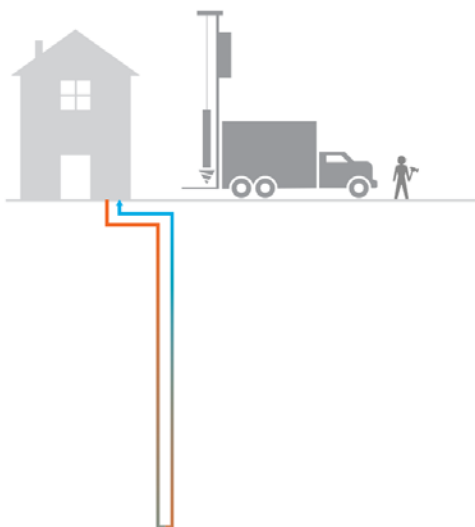
In collaboration with the Energy Commission, Sacramento Municipal Utility District, and American Honda Company, WCEC was able to expand the scope of this project to include an even greater number of field tests. This research will lead to a more comprehensive

understanding of the benefits and shortfalls of a more diverse GSHP strategies.

**Figure 41: Conventional GSHP Install**

### EARTH EXCHANGER

- » 150+ foot drill hole
- » Large, expensive drilling rig



## 3.2 GSHP Technologies

### *Conventional Vertical Bore Earth Exchanger*

Conventional vertical boring drills deep vertical boreholes typically 60 – 200 feet in depth and 4 to 6 inches in diameter. Installers then bury and grout a u-tube heat exchanger into each bore. Fluid fills each heat exchanger pipe to transfer heat with the ground.

Approximately 270 to 350 feet of piping can provide 12,000 Btu/hr of heat pump capacity, but this estimate is subject to pipe surface area and length, temperature difference between the ground, load profile, and other factors.

Closed loop ground source heat pump systems have heating COP ratings between 3.1 and 4.9, while cooling EER ratings range from 13.4 to 25.8. Air source heat

pumps, on the other hand, typically have COP ratings between 3 to 3.5 and rapidly lose efficiency at temperatures below freezing and in high temperature regions.

**Figure 42: Directional Bore Earth Exchanger Install**

**DIRECTIONAL BORE EARTH EXCHANGER**

- » 20 foot deep borehole, 150-feet across
- » Compact, less expensive, drill rig
- » Simultaneous drilling and pipe installation

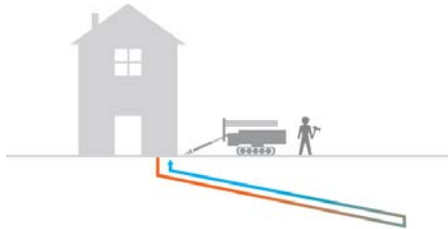
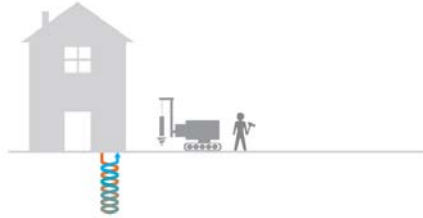


**Figure 43: Large Diameter Bore Earth Exchanger Install**

**EXCHANGER**

- » 20 foot deep borehole
- » Compact, less expensive, remote-controlled drill rig
- » Borehole drilled in less than 1 hour



The costs of ground source heat pump equipment is marginally higher than the air cooled equivalent, but this is mostly due to low volume of ground source equipment as GSHP make up only a small fraction of the total market. In actuality, ground source equipment has the potential to be less expensive than air source equipment, as ground source systems use smaller condenser heat exchangers and pumping motors. The majority of the cost associated with ground source heat pump is the typical cost of creating vertical deep wells, which is mostly dictated by field installation expenses. The HDPE tubing and couples costs may only be \$1 - \$2 per foot; however, the installation costs may drive expenses to \$25 - \$40 per foot.

*Directional Bore Earth Exchanger*

Horizontal boring, used largely as an alternative to trenching when laying pipe or running underground conduit, can also be used for the installation of geexchange fields. The technique takes advantage of the wide availability of the relatively inexpensive and easily transported horizontal boring equipment. Unlike vertical drilling, where a new setup is required for each bore, a directional bore field takes advantage of being able to originate all bores from a single central location. This method eliminates multiple setups and simplifies the connection and manifolding required connecting the earth

exchange field to the mechanical equipment. The technique also allows ground source technology to be considered on too-small parcels for conventional vertical boring machinery and techniques by allowing a smaller drill rig and the ability to drill the bores under housing structures, landscaping, and other obstacles.

*Large Diameter Earth Bore Exchanger*

Traditional geothermal techniques require expensive drilling rigs that can bore vertically deep into the earth. LDEB installations aim to reduce these costs by reducing the drilling depth while maintaining an adequate amount of heat exchange with the earth. This innovative concept utilizes a 24 inch diameter 20 foot deep helical coil constructed of ½ inch diameter HDPE tubing placed into the bore hole and backfilled with dirt from the drilling, sand, rock, or other fill. Drilling for these shallow bore heat exchangers is quick, and far less expensive than conventional techniques. As stated above, each bore may take less than an hour to drill,

allowing around eight bores to be completed in a typical workday. A day of work may yield around 150 linear feet of heat exchange depth; however, on a per foot basis the LDEB exchanger has more capacity due to the effective increase in surface area.

### 3.3 Demonstration: Directional Earth Bore Exchanger at Rio Mondego

Figure 44: Demonstration Home (left) horizontal GSHP pipes (right)



The project at Rio Mondego (1988 3-bedroom single-family home with central heating and air) demonstrated a ground source heat pump system using directional boring technology, as shown in Figure 44. The construction of the heat exchanger utilized five directionally bored holes of approximately 130 feet in length emanating from a single point manifold. Into these bores a conventional u-tube heat exchanger was placed and the bore was filled with grout.

The performance of the earth heat exchanger was adequate during summer cooling months without any failures; however, inspection of the peak entering water temperatures (as referenced to the heat pump) and ambient temperatures showed that these temperatures are nearly the same. Compared to other GSHP systems, the daily range of water temperatures entering the heat pump appears to be higher than what would be expected of a standard GSHP system. This may be an indication that the field was undersized for the load that it is experiencing.

The system proved it was capable of fairly high efficiencies, ranging from 10 – 20 EER in the summer and 3.5 to 6 COP in the winter. The efficiencies over the complete season for this system were found to be EER of 10.9 for cooling and COP of 3.9 for heating if the extra energy recovery from the desuperheater is ignored. If this energy is credited, the efficiency numbers are 12 EER and 4.6 COP. The low overall efficiency is most likely the consequence of an undersized or underperforming geo-exchange loop. If the unit was able to operate around 10 °F above or below earth temperature, the system could achieve EERs in the range of 17-18 and COP of around 4.7.

### 3.3.1 Thermal Analysis

The system was installed in the middle of summer and started collecting data just after an extended period of high temperatures. Figure 45 shows the daily high and low temperatures for outside air as solid lines. Dashed lines indicate the ground loop temperatures, with markers. Areas in which markers are absent indicate days when the heat pump system did not operate at all. The maximum and minimum ground loop temperatures are recorded. The maximums and minimum ground loop temperature is can be from either the GEO\_EWT or the GEO\_LWT sensor, so during cooling season the minimum will be from the GEO\_EWT sensor, but during the heating season the GEO\_LWT will record the minimum temperature. The average ground loop temperature is the average of the GEO\_EWT and GEO\_LWT temperature over the entire 1-minute date points taken throughout the day.

**Figure 45: Ground loop temperatures as a function of outside air temperature**

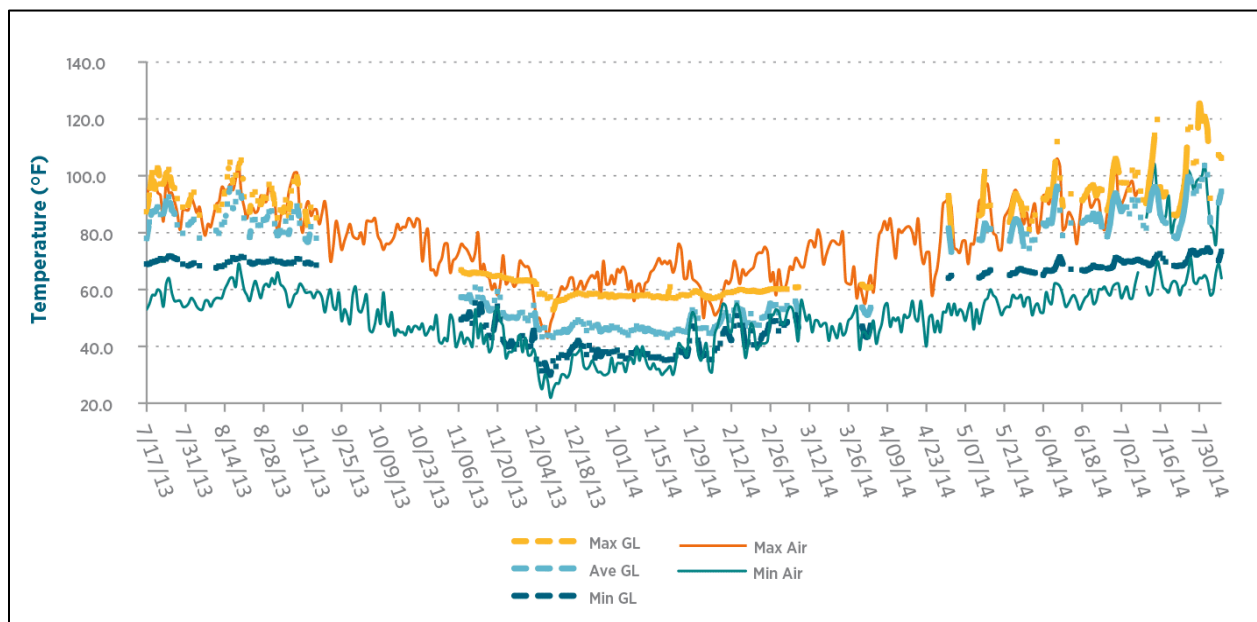
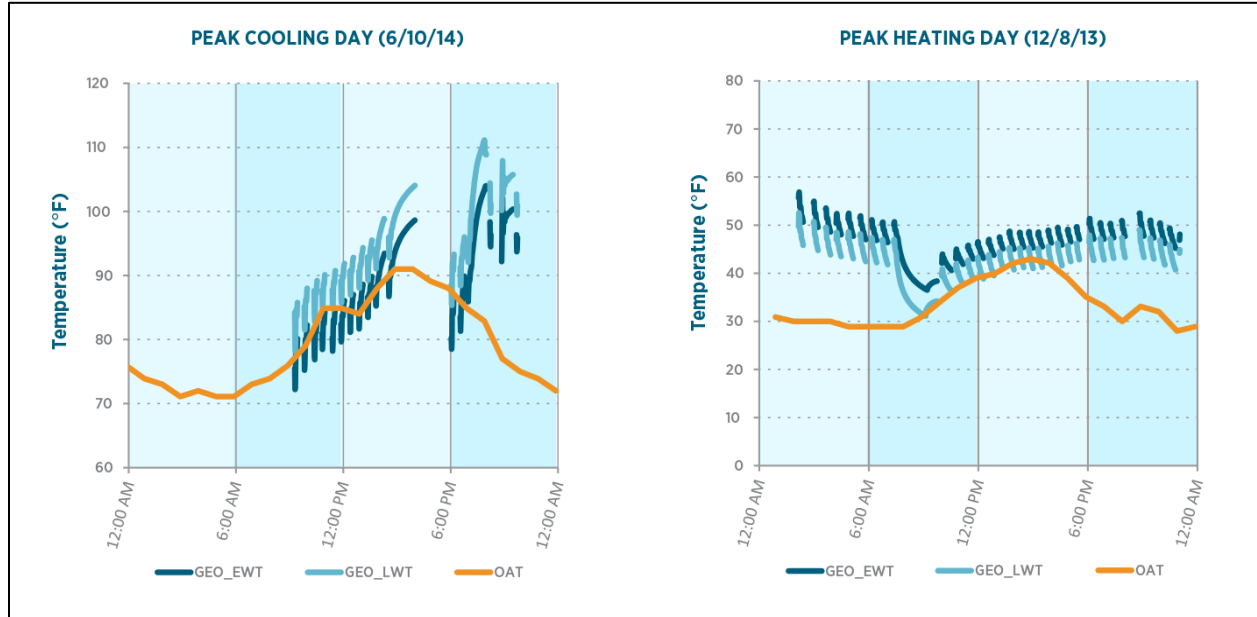


Figure 46 shows the entering water temperature (EWT) and leaving water temperature (LWT) as referenced from the GSHP for the peak cooling and peak heating day of the year. It is of interest to note that each cycle of the GSHP changed the EWT by approximately 5 degrees F, but over a complete day the change in EWT might be greater because of multiple cycles each starting at an EWT successively higher (when cooling) or lower (when heating). During the heating period on December 12, 2013, it was noted that the GSHP reached a lower temperature limit with LWT from the GSHP approaching freezing. During the peak-cooling day in the summer, the EWT rose significantly over the course of the day. These results are both indications that the geexchange field did not match to the load well.

This figure illustrates that it may be possible that during certain hours of the day, and in certain conditions, it will not always be better to use a GSHP. At least during the peak-cooling day,

there are times in the late afternoon when air temperature has fallen below the ground temperature.

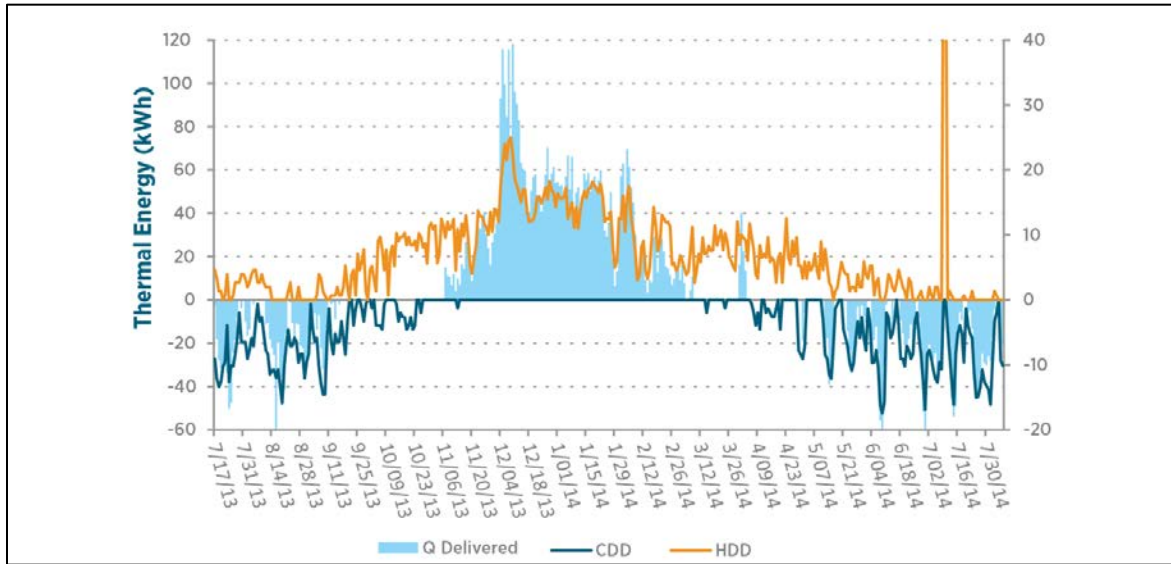
**Figure 46: Entering Water Temperature and Leaving Water Temperature During the Peak Cooling and Peak Heating Day of the Year**



Calculations were made for the thermal energy delivered to the home, as well as a metric for heating degree days (HDD) and cooling degree days (CDD). HDD and CDD were calculated using the sine wave approximation method. The base temperature was adjusted so that good correlation could be made between the xDD calculation and  $Q_{del}$  to the building and may not match other sources for tabulations of HDD and CDD.

A visualization for the amount of heat delivered to the space and the calculated degree days was produced in Figure 47. It was found that a fairly good correlation could be obtained if the thermal energy was plotted against the quantity [HDD – CDD].

**Figure 47: Amount of Heat Delivered in kWh**

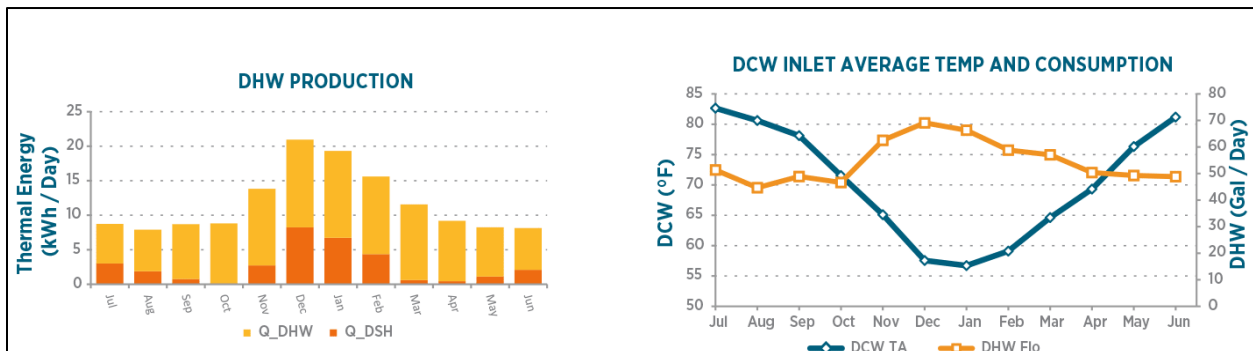


Measuring the fraction of domestic hot water heated by the natural gas heater versus the fraction heated by the heat pump was one of the most challenging calculations to make. The system installed utilized a hot water preheat tank that was heated by the desuperheater. The preheated water from this tank was drawn into the natural gas hot water heater and then heated to the final supply temperature.

Figure 48 shows a distinct increase in total heating energy for hot water during the winter season. Upon analysis it was found that two factors contributed to this increase. The occupants used more water during the winter months and the entering water temperature was much lower in winter months, thus requiring more heat to bring the domestic hot water (DHW) up to its final delivery temperature. The low entering water temperature required more DHW to mix with domestic cold water (DCW) to reach the desired usage temperature.

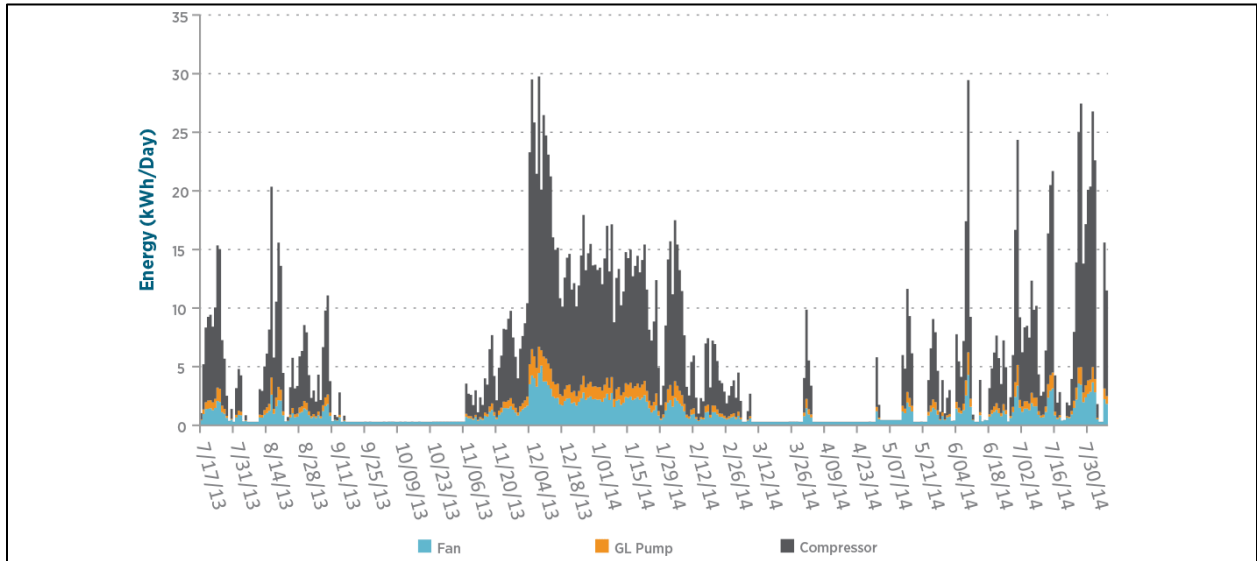
Over the course of the year, the GSHP desuperheater supplied 36% of the DHW demand while the natural-gas fueled hot water heater provided the remaining 64% DHW demand.

**Figure 48: Domestic Hot Water Production, Inlet Average Temperature and Consumption**



Heat pump input energy was evaluated in two different ways. Figure 49 shows a plot with input energy split out by component for Fan, Ground Loop Pump, and Compressor.

**Figure 49: Heat Pump Input Energy by Component**



The heat pump energy was also split out by operating mode. Figure 50 shows the same energy split out of the total by mode and condenser and air handling unit (AHU). The condenser unit represents the energy used by the compressors and water pump, while fan power is the power consumed by the indoor AHU.

**Figure 50: Heat Pump Input Energy by Mode**

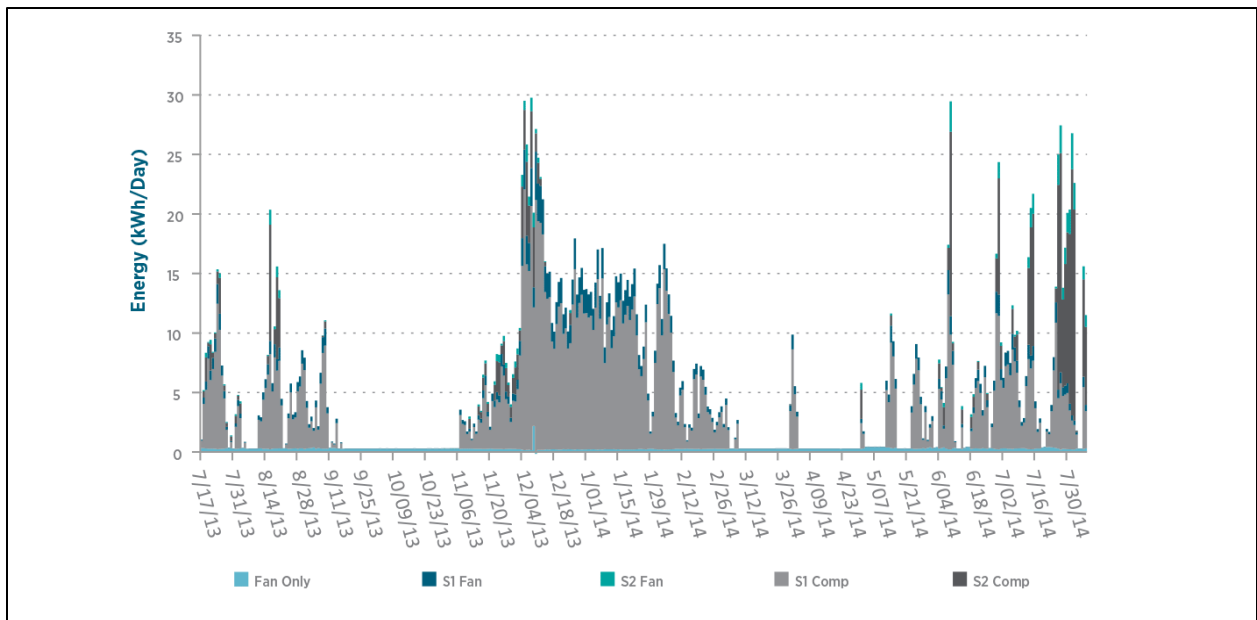


Figure 51 shows the split of input power over the complete season and that the ground loop pump uses less than half of the energy as the indoor supply fan. The compressor uses the majority of the energy.

**Figure 51: Input Energy by Mode**

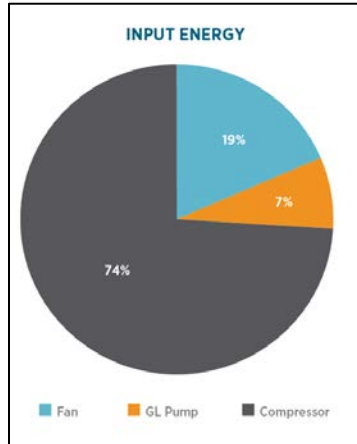


Figure 52 shows the amount of heating or cooling delivered to the home over the period of observation. Heating accounts for 68 percent of the thermal energy delivered to the home.

**Figure 52: GSHP Total Heating and Cooling Delivered**

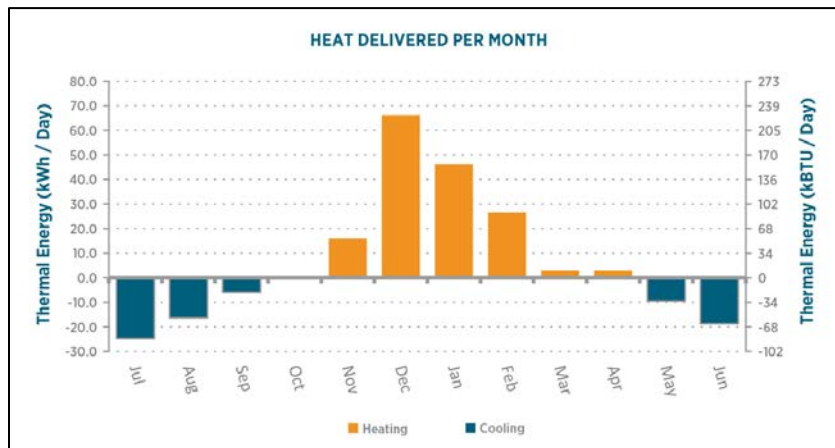


Figure 53 shows the efficiency of the system plotted against the average condenser temperature. As expected, the efficiency of Stage 1 operation is generally higher than the corresponding Stage 2 operation. Efficiency also improves as the average condenser temperature approaches the ground temperature, which the data would suggest as being around 66 °F.

**Figure 53: Efficiency of Installed System**

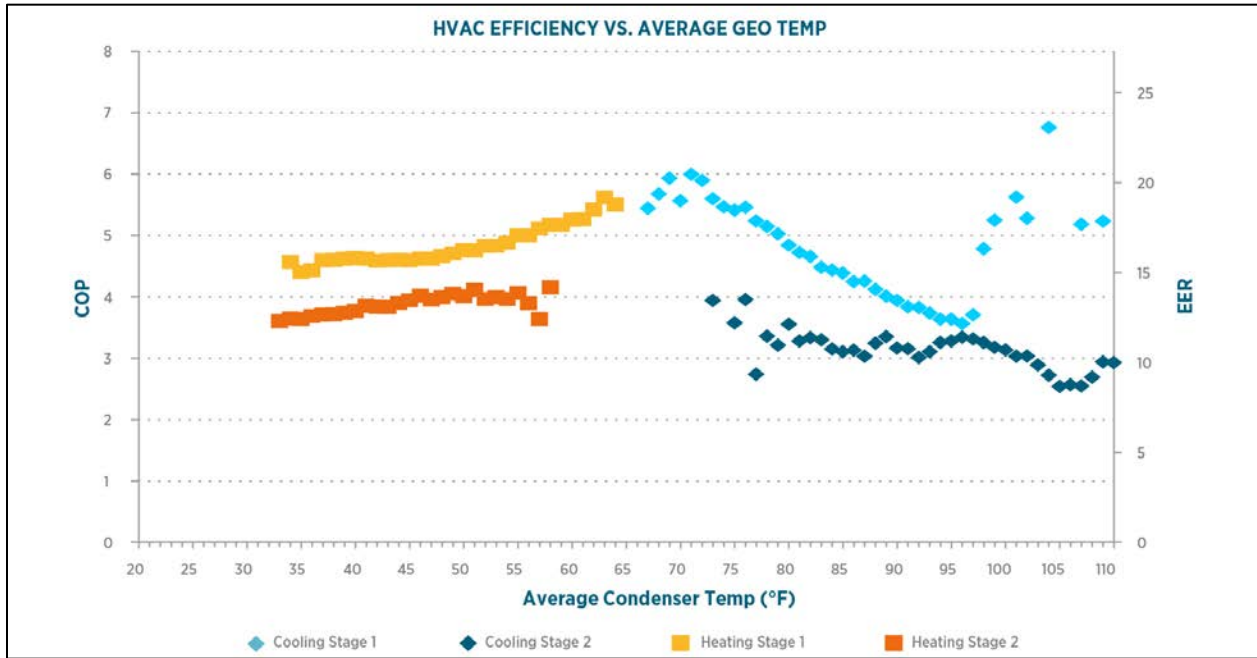
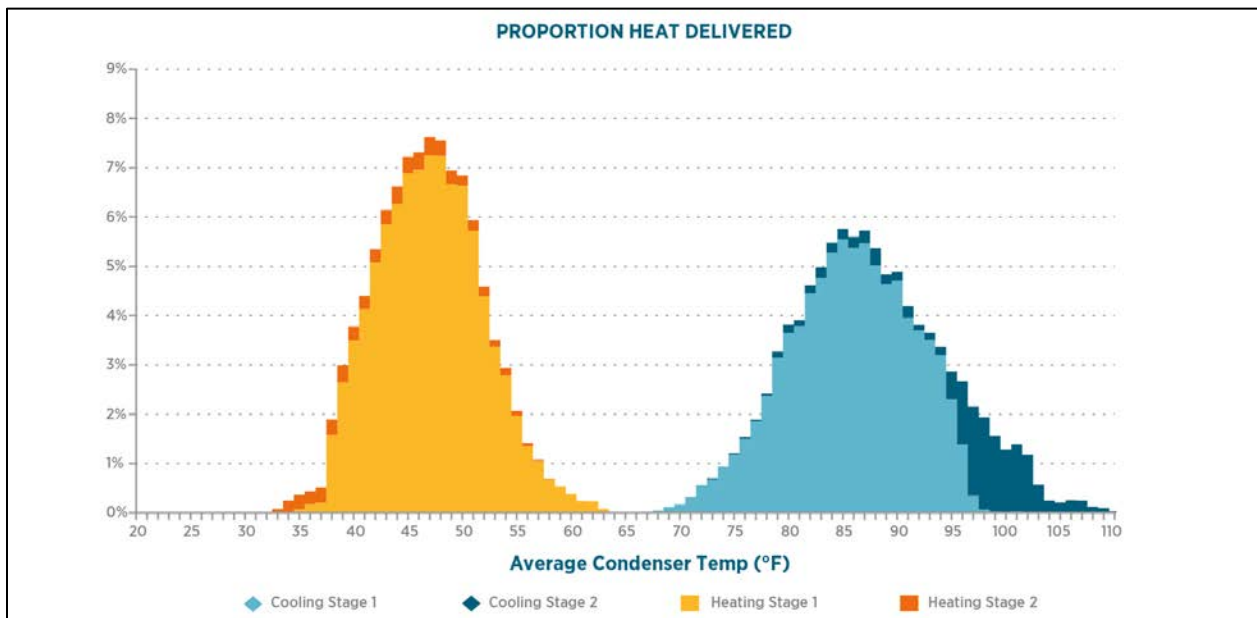


Figure 54 is a histogram showing how much time the unit spent in each mode binned for different temperatures. This plot shows that the mean temperature of operation was around 46F in heating, and around 86 °F in cooling.

**Figure 54: Proportion of Time Unit Spent in Each Mode**



The installation at Rio Modego showed that a horizontal drilling technique can be employed to install ground loops on small parcels of land with minimal disruption to surface features. Based on performance of the system, it is possible that this geo exchange loop was undersized, or under-performing as demonstrated by the temperature lockout experienced during the peak heating day of the year. Greater efficiency can be expected if the EWT temperature excursions can be minimized during the day. But clearly, more demonstrations of this method of installation need to be analyzed to understand its true potential.

### 3.4 Demonstration: Large Diameter Earth Bore Exchanger Demonstration: Honda Smart Home

A LDEB technique for building geo-exchange fields has been installed at the Honda Smart Home at University of California Davis' West Village Zero Net Energy (ZNE) community, as shown in Figure 55. The installation is testing two different field configurations using earth bores 24 inches in diameter and 20 feet in depth. In both of these configurations a coil of ½ inch polymer tubing just slightly smaller than the hole is inserted into the hole to exchange heat with the earth. One configuration is testing a dry borehole construction backfilled with dirt from the original hole. The other configuration utilizes a construction which places a large polymer pipe liner in the hole with the coil heat exchanger inside. The pipe is filled with cobble and grey water from the house and is allowed to percolate from the bottom of the bore to the top. This design allows for geo-exchange with the earth but also heat recovery from greywater produced in the house.

Tenants have only recently moved into this building in September 2014. In order to gain an accurate picture of energy usage/savings, WCEC will not release the preliminary energy data until they acquire more comprehensive and sufficient seasonal data.

**Figure 55: Installation of the LDEB system at the Honda Smart Home in West Village, Davis and the completed home.**



### 3.5 Demonstration: Large Diameter Earth Bore Exchanger at Capay, California

This project proposes a system utilizing uninsulated storage vessels buried underground to store water to be cooled during favorable conditions at night to later be used during the day when building cooling loads are the highest, as shown in Figure 56. In this way full advantage can be taken of California's large diurnal swings in ambient temperature by storing a complete day of cooling load heat energy in the water reservoir storage system and then rejecting this heat at night when conditions are most favorable. The complete system will integrate thermal energy storage, a modified residential split system compressor unit, and an appropriately sized evaporative fluid cooler to reject the heat at night time.

**Figure 56: Installation of the LDEB system at a home in Capay, California**



The implementation of this system as a retrofit would require only minor changes to the existing system. The system could use any water storage reservoir that already exists, such as naturally occurring stream or underground water storage tanks. To take advantage of thermal storage the existing split system air conditioner could be retrofitted with a water-to-refrigerant heat exchanger, a pump and a controller. As a result, the required space for this system is

minimal, aside from the water reservoir, and could be integrated into existing construction. Should the storage system be undersized, or a night of adverse weather conditions prevent the thermal energy from being completely rejected from the water storage – the air conditioner still would function as originally designed without adversely affecting customer comfort.

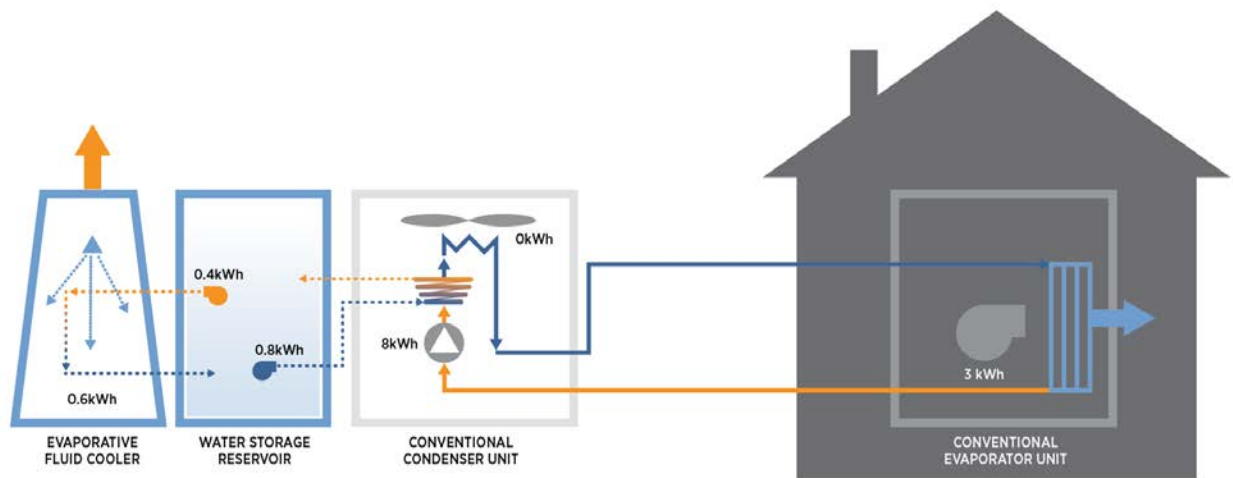
In order to determine both the technical and economic feasibility of this system, the project consisted of a modeling study of the expected system performance, laboratory testing, and a field installation of the proposed system. The thermal reservoir allowed the condensing section of the vapor compression system to operate at lower, and consequently more efficient, temperatures. Fan energy necessary to move air through the air-cooled condenser was replaced with the much more efficient process of pumping a small amount of water through the water to refrigerant heat exchanger. Additionally, the cooling load shifted from the day to the night resulting in a peak load reduction on the power grid.

### 3.5.1 System Design and Construction

#### *Water Heat Exchanger*

This retrofit of an air conditioning condenser unit was an important part of the project to prove out the concept that the system might be installed as a retrofit to currently installed systems used widely throughout California. In order to accomplish this task a conventional split system condenser, the type that is typically used in residential construction, was retrofit with a coaxial water-cooled heat exchanger, as shown in Figure 57.

**Figure 57: System design diagram for the large diameter earth bore exchanger at Capay, California**



#### *Indoor Evaporator Unit*

For this project the indoor evaporator unit did not require any modification. This demonstrates one of the advantages of this retrofit, namely that all modification and construction can take place outside of the house without affecting any of the interior systems.

### *Conventional Condenser Unit*

The outside condenser was replaced with a new unit. This replacement was performed to facilitate testing and so that service would be interrupted for the least amount of time for the test site volunteer. The water heat exchanger was integrated with the condenser unit where the liquid line and suction line would normally interface with the house. For this installation, the suction line from the house entered the unit at the same point, only the liquid line was diverted to run through the water-cooled heat exchanger before entering the house.

Modifications to the controller and electronics were also minimal. The only internal change made to the condenser unit was to intercept the condenser fan power with a normal closed relay. When the controller signaled that the unit should operate in water-cooled mode, the fan power was interrupted, and the water pump was enabled.

### *Thermal Storage Geo Heat Exchanger*

Many designs were contemplated for the construction of the hybrid heat exchanger and thermal storage component. The design that was ultimately chosen was constructed of HDPE culvert pipes, which were capped with HDPE plates. Internal to these pipes, before sealing, a polymer HDPE pipe heat exchanger consisting of four parallel  $\frac{3}{4}$  inch braided pipes was inserted. One of the major design advantages was that the thermal storage heat exchanger was manufactured offsite. This construction technique has the potential to lower costs by leveraging manufacturing economy of scale advantages.

As a final step, a second external HDPE heat exchanger consisting of four parallel pipes each measuring 39 feet, was wrapped around the pipe in order to allow testing of both internal and external arrangements.

### *Boring and Installation*

Large bore auger equipment typically used for piling drilling was used to drill 3 foot diameter holes 23 feet into the earth. After drilling, 6 inches of concrete was poured into the bottom of the holes, the pipes were placed, and then each heat exchanger was cased in concrete in a two-step process. In the first step, a small amount of concrete (about 6 inches) was cased around the bottom of the heat exchanger. The concrete needed to set before encasing the remaining length of the pipe in concrete. Allowing the concrete to set was necessary to prevent buoyant forces from forcing the tank out of the hole. The installation was finished by connecting the heat exchangers to the rest of the system via HDPE pipe and back filling the hole with sand and native soil.

### *Heat Exchanger Flow Center*

The pump for the heat exchanger loop was a GSHP nonpressurized type that did not require the typical flushing, sealing and pressurization that is typical of these systems. This results in quicker installation and ultimately costs less than traditional GSHP units.

### *Cooling Tower and Pump*

The cooling tower chosen was an open system fiberglass model nominally rated at 8 tons of cooling capacity. These types of cooling towers are inexpensive, quiet and easy to ship and install. The pump for the cooling tower was a high efficiency variable frequency drive type for maximum efficiency. The pump was installed at the lowest point in the system, in the valve box with the water-cooled heat exchanger. This installation method ensured that the pump would always be primed and work properly. It also protected the unit from freezing.

### 3.5.2 Thermal Analysis

Figure 58 shows the internal house temperature and the thermostat set point that the air conditioner unit was set to maintain. The system was able to maintain internal house temperature to within +/- 3 degrees of the set point (set at 73 °F). A more thorough set of system tests will take place in the next heating season under an existing GSHP contract and this work will be integrated into a larger study capable of funding a much more thorough development and analysis of this technology.

**Figure 58: Measured Indoor Air Temperature (10/6/14)**

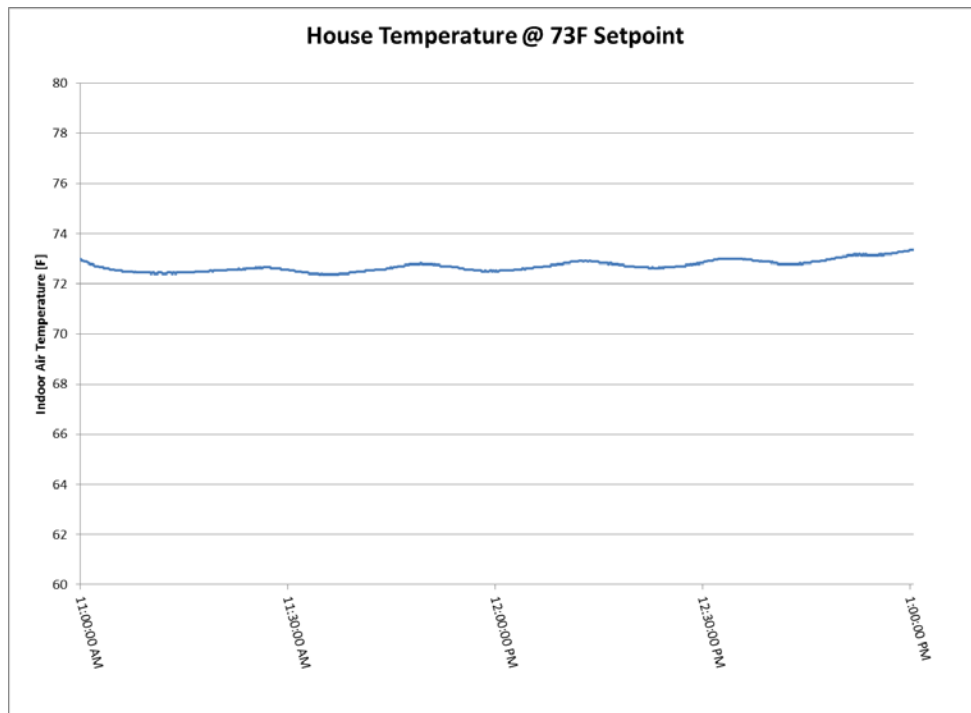


Figure 59 shows the operating characteristics of the system during the hottest day of the year in climate zone 12. The condenser inlet and outlet temperatures show characteristics of fast temperature rise from an initial point on the order of a couple minutes then transitioning to a steady state temperature rise on the long time scales. The initial temperature rise is due to the low volume of fluid within the heat exchanger loop coming up to temperature, the slower temperature rise thereafter is due to the bulk temperature rise of the storage thermal fluid mass. After each cycle, the fluid temperature within the loop comes into equilibrium with the bulk

fluid temperature within the tanks, and upon the start of the next cycle, starts at the bulk fluid temperature of the tanks.

**Figure 59: [CZ 12] System Temperatures (Peak Cooling Day)**

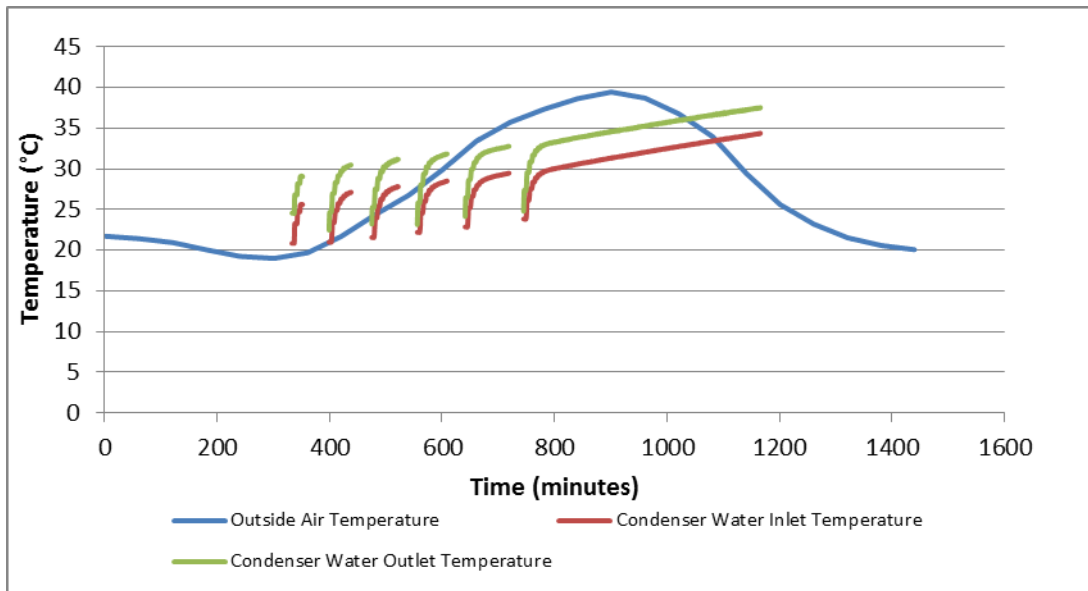
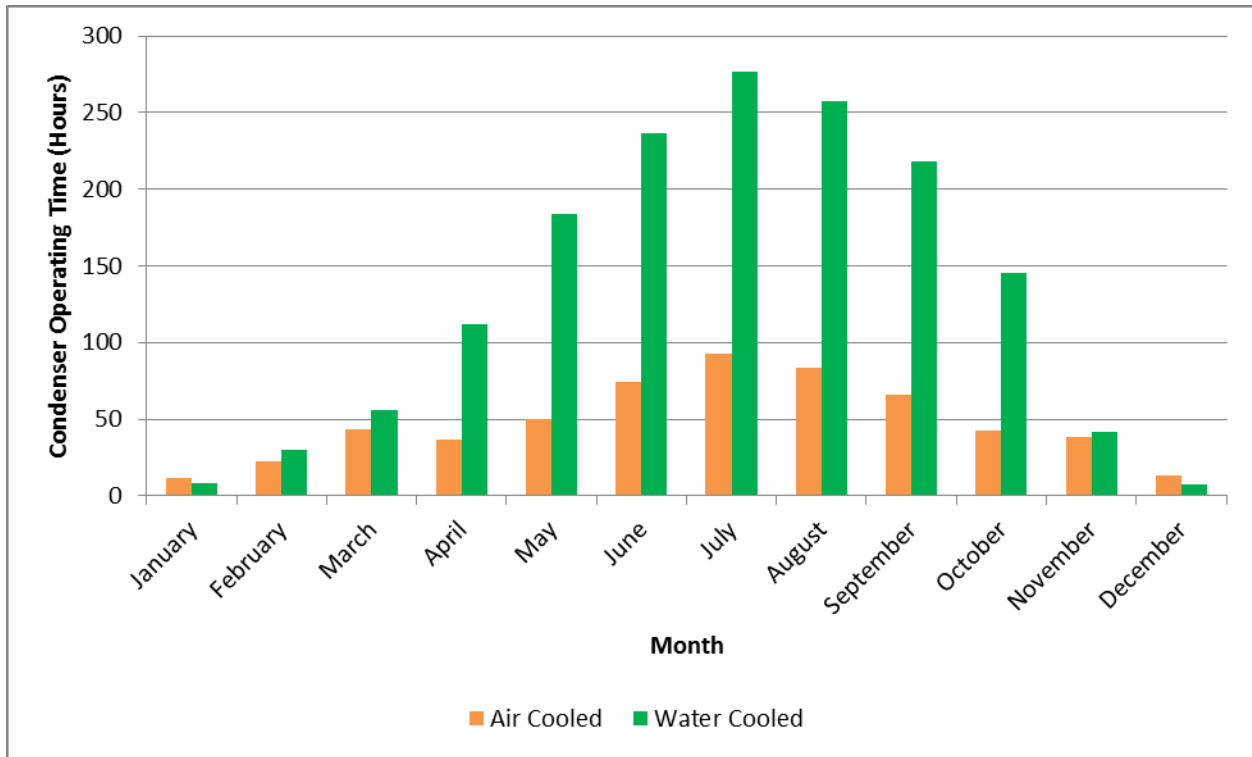


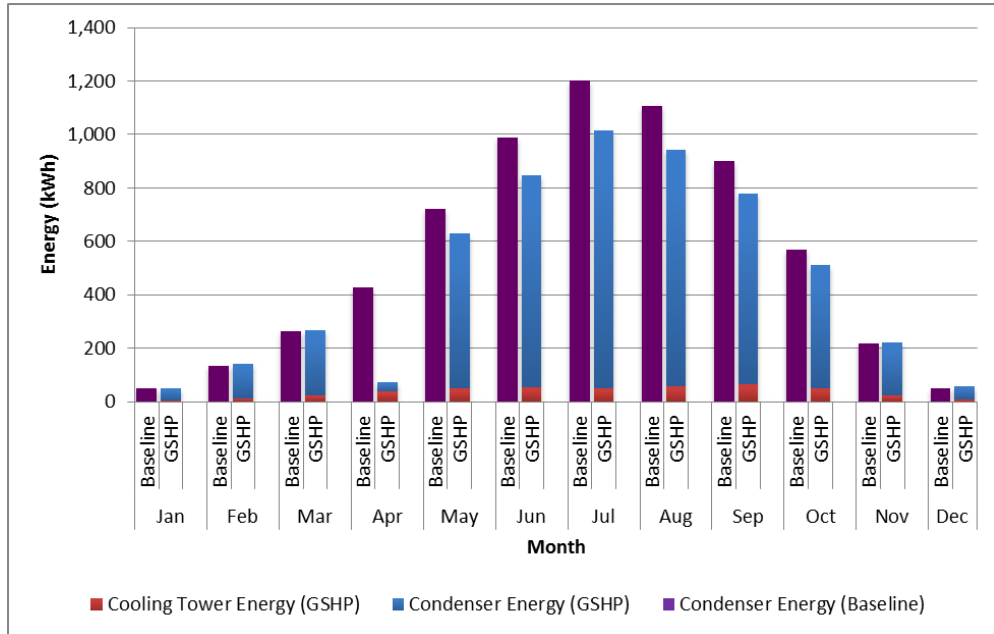
Figure 60 shows the total number of the hours that the system operates with the air-cooled condenser and the water-cooled condenser. Operation during the cool winter months is likely an artifact of the standard model used and is probably not indicative of actual operation. The system as designed shows that the water-cooled condenser tends to run most often in nearly all months of operation.

Figure 60: [CZ 12] Condenser Operating Hours



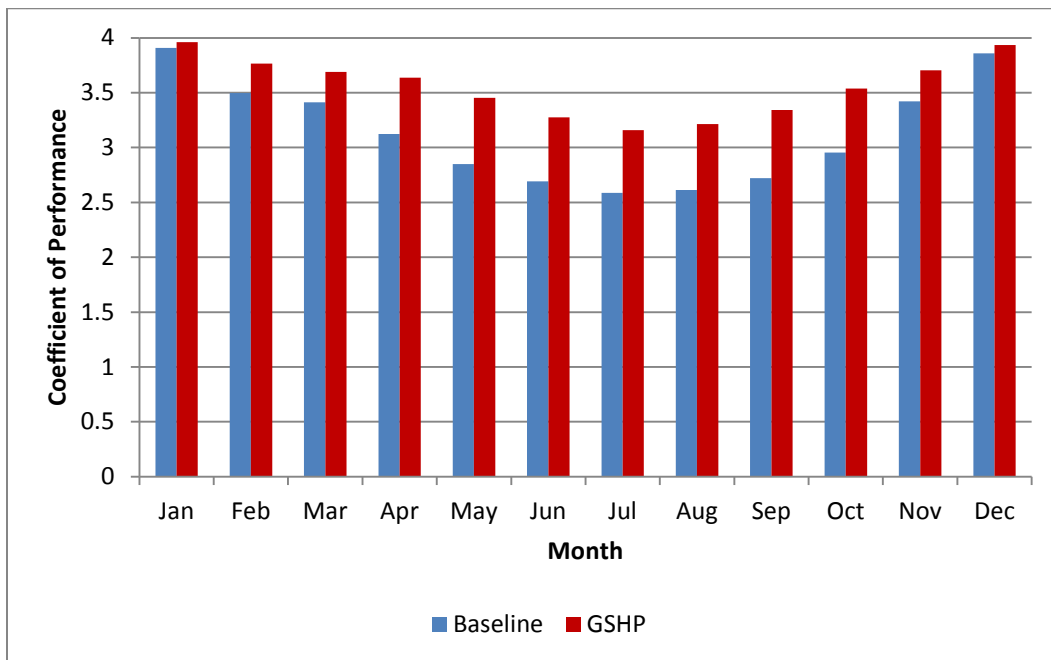
Energy usage breakdown, in Figure 61, reveals that the energy used in the operation of the cooling tower is small compared to the total energy consumption of the heat pump. The water-cooled condenser and chilled water reservoirs usage allows the proposed system to operate with a significantly reduced energy consumption in nearly all months of operation when compared to the baseline system which used a conventional air cooled condenser.

**Figure 61: [CZ 12] Total Monthly Energy Use**



The efficiency advantage of the proposed system over the baseline system is most apparent in the summertime, as shown in Figure 62. This advantage is expected due to the high daytime temperatures encountered and the ability of the proposed system to utilize lower temperature water in the condenser.

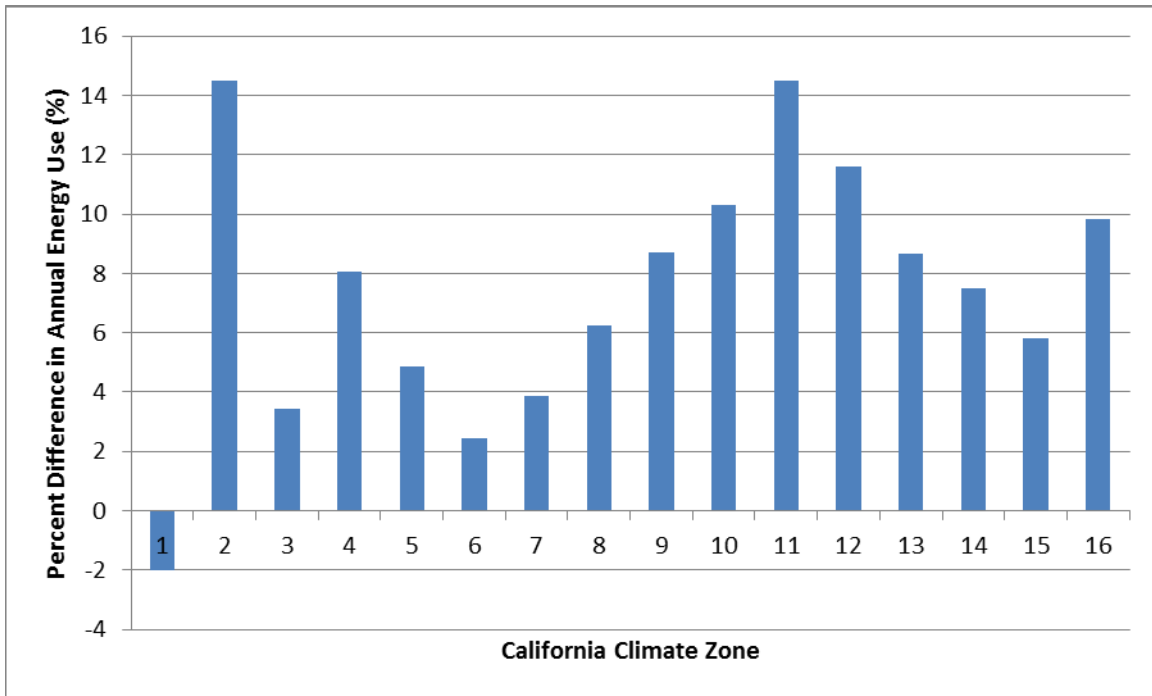
**Figure 62: [CZ 12] Average Monthly COP**



### 3.5.3 GSHP Performance Results in Various California Climate Zones

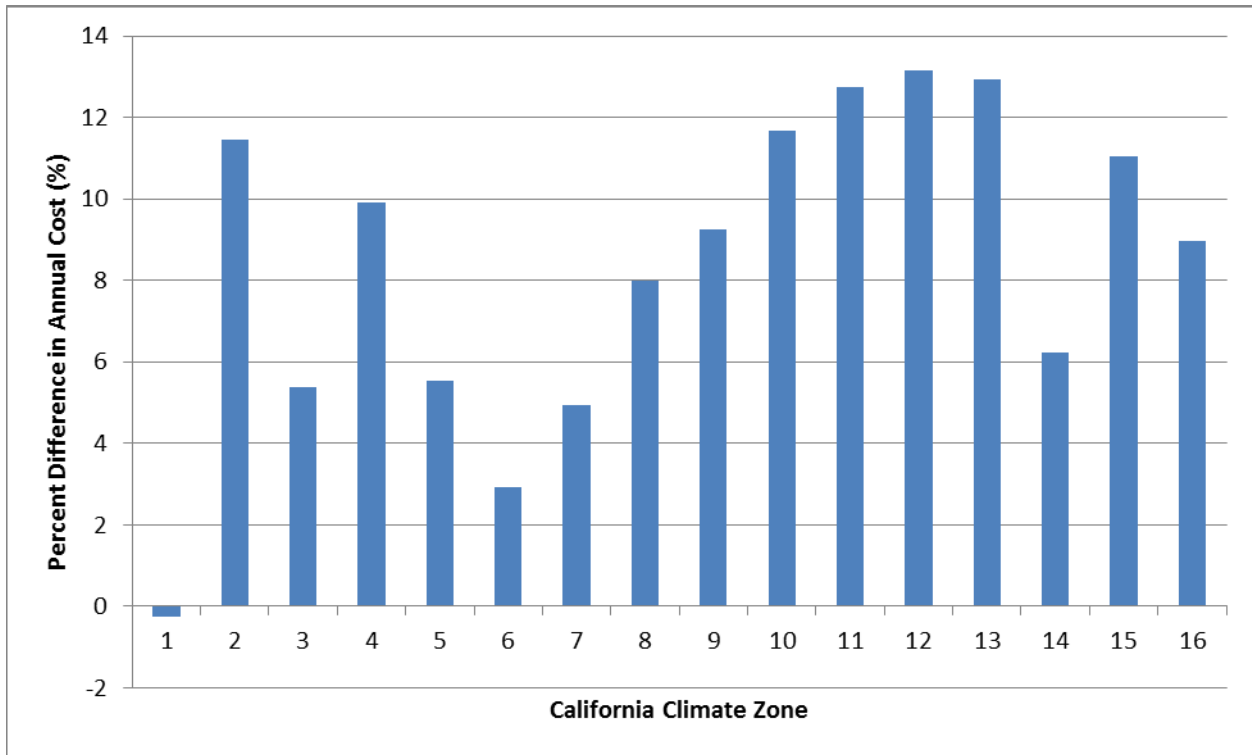
The savings for the GSHP is roughly up to 14% across all climate zones, as shown in Figure 63. Climate Zone 1, which represents the north coast from just north of San Francisco to the top of the state, actually shows negative savings over the baseline system. This negative savings indicates that the control strategy has not been completely optimized because the proposed system is able to operate in the same manner as the baseline; therefore, should never do worse than the baseline system.

**Figure 63: Baseline to GSHP Energy Use Comparison**



The research team performed an operational cost savings analysis using a time-of-use (TOU) pricing structure. The TOU pricing for the PG&E's Residential E-6 rate structure (Figure 64) was used and it was assumed that the total residential usage did not exceed the first tier of consumption.

Figure 64: [CZ 12] Baseline to GSHP Energy Cost Comparison

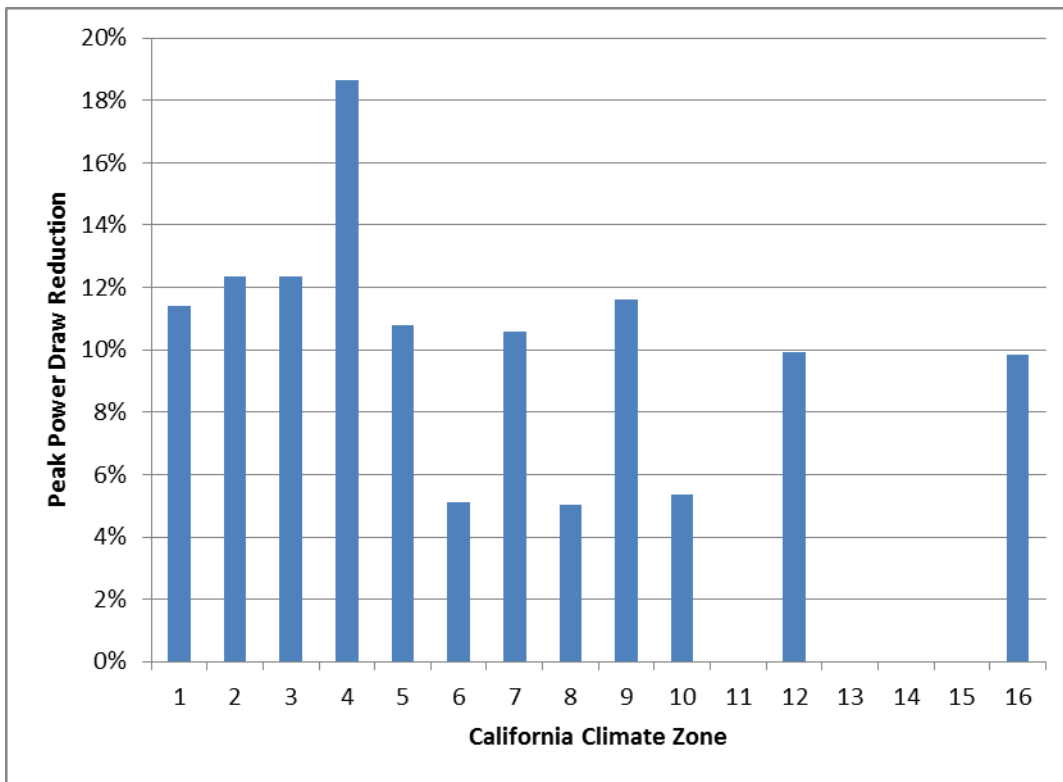


The savings over the baseline system are up to approximately 13%. This system has the ability to reduce peak loads by rejecting heat to the array and shift part of the demand to off peak hours. Further optimization of the control strategy that more properly accounts for incoming water temperatures could also improve energy savings.

#### *Peak Load Reduction*

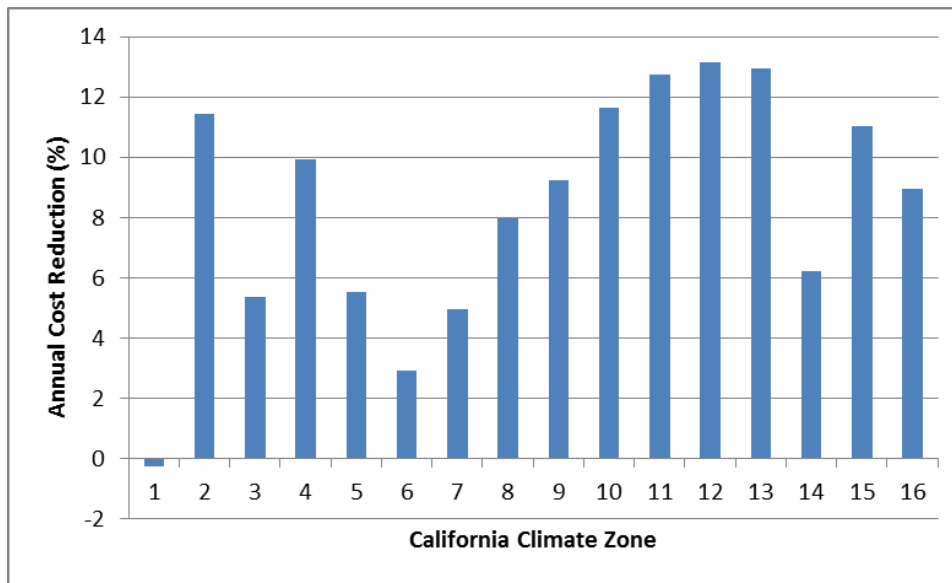
By using the water-thermal storage to reduce the peak temperature that the condenser experiences, the peak load will also be reduced. During peak summer months, air temperatures may be in excess of 100 °F in many hotter climate zones. By using cooler water to operate the system during these periods, load reductions were achievable. Figure 65 shows the amount of peak reduction power for the proposed system. Many climate zones see peak savings in excess of 10%, with some savings as high as 18%.

**Figure 65: Peak Reduction**



The proposed system offers the opportunity to shift loads associated with cooling the thermal storage reservoir to off peak and nighttime periods without system performance degradation. This system allows for a large amount of control to optimally respond to TOU energy pricing structures. Figure 66 shows the energy cost savings that can be achieved in a TOU pricing structure.

**Figure 66: Annual Energy Cost Reduction**



### 3.5.4 Conclusions and Recommendations

This project explored the use of underground thermal storage reservoirs, a cooling tower, and a modified air conditioner condenser unit to reduce energy use and peak power in residential applications.

The model constructed for the system shows that the proposed system can save energy, reduce peak power, and reduce costs when operated in a typical TOU pricing structure. As might be expected, not all climate zones are predicted to result in the same level of savings. Because the scope of the project was to look solely at the air conditioning savings, cooler coastal climate zones such as 1, 3, 5, 6, and 7 are expected to have only modest savings for cooling, between 0% and 6% annually. In all climate zones other than the coastal zones, estimated cooling savings ranged between 6% and 13%.

Ground heat exchangers (GHEs) were constructed with large HDPE culvert pipes and HDPE pipe. The construction techniques used for manufacturing these GHEs worked well and are well suited to factory production techniques. In large-scale deployments, the GHEs can be constructed offsite, and transported to the site. A single-man crew with auger equipment can quickly accomplish the pipe installation. The process has the potential to be cost effective for residential installations such as the one at Capay.

Condenser modification for the water heat exchanger presents some challenges in a retrofit situation; however, these modifications could be readily integrated into new designs with modest costs and then be integrated into residential constructions that include GHEs, swimming pools, or other methods of thermal storage.

## *Recommendations*

This research has shown that utilizing lower cost ground heat exchanger concepts can achieve energy savings. It has also demonstrated the ability for even greater percent savings in operating costs when operated within a TOU pricing structure. Challenges remain though and further research in some key areas would help eliminate remaining questions.

This concept would benefit from further research in the following key areas:

- Expanding the modeling and the installation to also perform space heating by using a heat pump, and adding other components that would aid in operation in cool ambient temperatures.

The scope of this project was limited to looking at reducing energy due to cooling loads; however, there are many California climate zones that experience greater heating loads than cooling loads. To maximize the utilization of the unique components involved in the construction of this system, a heat pump should address both cooling loads and heating loads. Further research focusing on satisfying heating loads and integrating this with cooling loads would be a logical next step.

- Exploring cost reductions and improved installation techniques for the large diameter shallow bore ground heat exchangers that this project utilized.

The GHE developed during this research represents a unique design that has not been well characterized. There remain many opportunities for improvement within this design for cost reductions, improved methods of installation, and in understanding expected performance of the design in various installations.

- Further development of the proposed system, including component optimization and system control algorithm changes to improve performance and reduce costs.

Further research into the design and construction of heat pump systems capable of utilizing air or water source heat exchangers, and controlling them for optimal efficiency or demand reduction would also be beneficial. Cost reductions could be made by delivering this feature from the manufacturer rather than by installing as a retrofit.

# CHAPTER 4: Improving Energy Efficiency in the Hospitality Sector (PCMs)

## 4.1 Problem Statement

This project is investigating the feasibility of adding microencapsulated phase change materials (mPCMs) into hydronic cooling and heating systems to reduce the energy needed to circulate the fluid in the system. The capacity of a hydronic system is primarily a function of the fluid (water) flow rate, the heat capacity, and the temperature differential across the heat exchanger. Adding mPCMs to the water will increase the effective heat capacity, allowing for a reduction in water flow rate while providing the same amount of heat transfer. Since the pumping power is roughly proportional to the cube of the flow rate, reducing the flow rate leads to significant power savings.

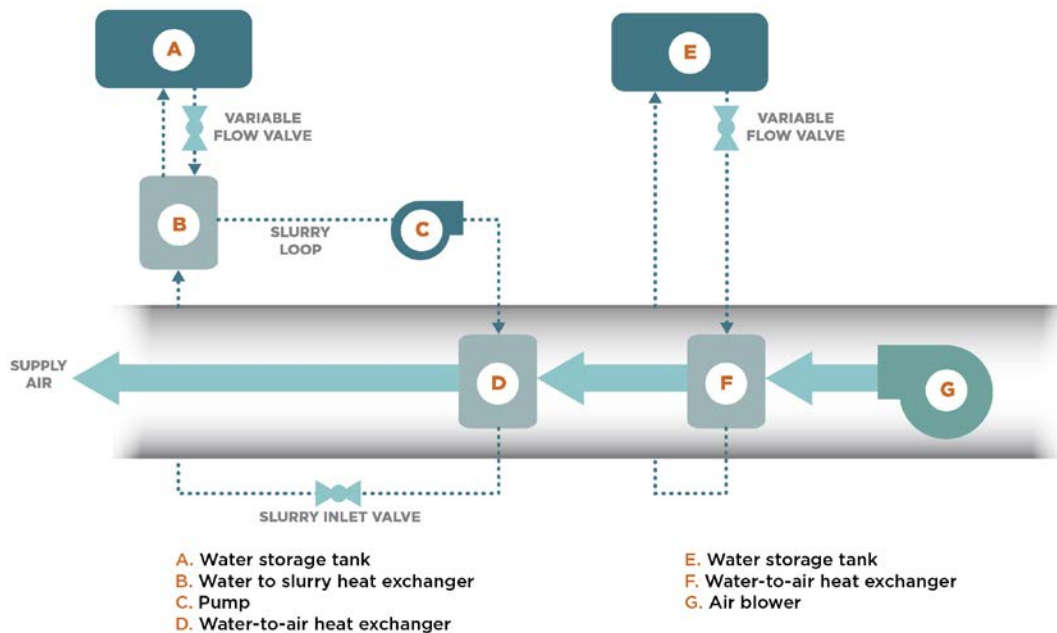
There has long been interest in using PCMs for thermal storage with the current primary focus being on pump power reduction. While the only widely available commercial system uses ice as the phase change material, this work has resulted in a significant body of literature on the properties of bulk (or macroencapsulated) PCMs, much of which is relevant to the work here.

PCMs fall into two categories: organic and inorganic. The inorganic PCMs are typically salt hydrates and organic PCMs are typically paraffins and fatty acids.

Based on the properties of the candidate materials, WCEC have been using commercially available PCMs made from paraffin waxes in the tests. The wide melting point ranges for the different chain length paraffins make them suitable for use over a wide range of temperatures covering both heating and cooling in hydronic systems.

The specific heat of water of 4.2 kilojoules per kilogram per degree Centigrade ( $\text{kJ/kg}^{\circ}\text{C}$ ) is low compared to the latent heat of fusion for commercialized PCM beads (up to 180  $\text{kJ/kg}$ ). As an example, a heat exchanger in a fan coil unit providing cooling with a water temperature differential of  $5^{\circ}\text{C}$  at a water flow rate of 5 kilograms per minute ( $\text{kg/min}$ ), the cooling capacity is 1.8 kW. Replacing just 10% of the water volume with mPCMs would deliver the same capacity at a flow rate of only 3  $\text{kg/min}$ . This reduction in flow rate of 20% equates to nearly an 80% reduction in pumping power. For the same example heat exchanger in heating mode using water only, the capacity of the system is approximately 3 times greater than for cooling because of the larger temperature differential between the entering water and entering air temperature. Replacing 10% of the water volume with mPCMs would allow a flow rate reduction of 10% and a pumping power reduction of 27%. Commercially available PCM beads have selectable phase change temperatures that would potentially allow this concept to succeed in both cooling and heating applications.

Figure 67: PCM Laboratory Test Schematic



## 4.2 Previous Research: Laboratory Apparatus, Thermal Cycling and Mechanical Cycling Tests

The selected mPCMs need to possess thermal and mechanical stability. The mPCMs must be capable of experiencing multiple cycling through a pump with a minimal amount of capsules rupturing. In addition, they should be able to experience multiple thermal cycling without rupturing and without degradation in the thermal properties; specifically the phase change temperature, the degree of super-cooling, and the latent heat. In order to separate thermal effects from mechanical effects, WCEC performed two separate tests: Thermal Cycling

Using a freezer and electrical heating tape, WCEC thermally heated eight ounces of 20%-concentration mPCM slurry with a nominal melting temperature of 6°C (Figure 68). Prior to any thermal cycling these mPCMs showed super-cooling of approximately 3°C. After hundreds of cycles, there was no sign of a shift in the melting point, or in the degree of super-cooling. Microscopy showed no sign of ruptured particles after 100 cycles.

### 4.2.1 Mechanical Cycling Tests

WCEC created a testing apparatus for mechanical cycling (Figure 69). In the three mechanical cycling tests performed, mPCMs were recirculated through a pump in an accelerated laboratory test and examined for rupture (Figures 70 and 71). WCEC used a laser *in situ* scattering and transmissometry (LISST) instrument manufactured by Sequoia, which measured the size distribution of the beads. In the first test, nominal 20-micron mPCMs were circulated by a 1-horsepower centrifugal pump manufactured by Taco for HVAC applications. The test lasted approximately several days and resulted in 372,000 cycles through the pump. The findings

indicated that beads greater than 30 microns in diameter experienced high rates of rupturing which were presumed to be due to high sheering generated at the pump's impeller (Figure 72). Smaller diameter beads appeared to hold up better during the test, leading the team to conclude that mPCMs under 10 microns in diameter were likely to experience little or no rupturing in a centrifugal pump.

**Figure 68 (left): Microscope image of mPCMs after 100 thermal cycles shows no evidence of broken capsules**

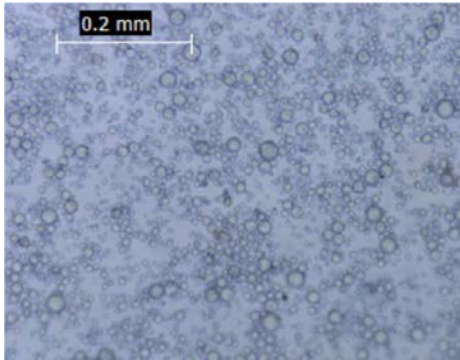


**Figure 69 (right): Completed PCM Test Apparatus**

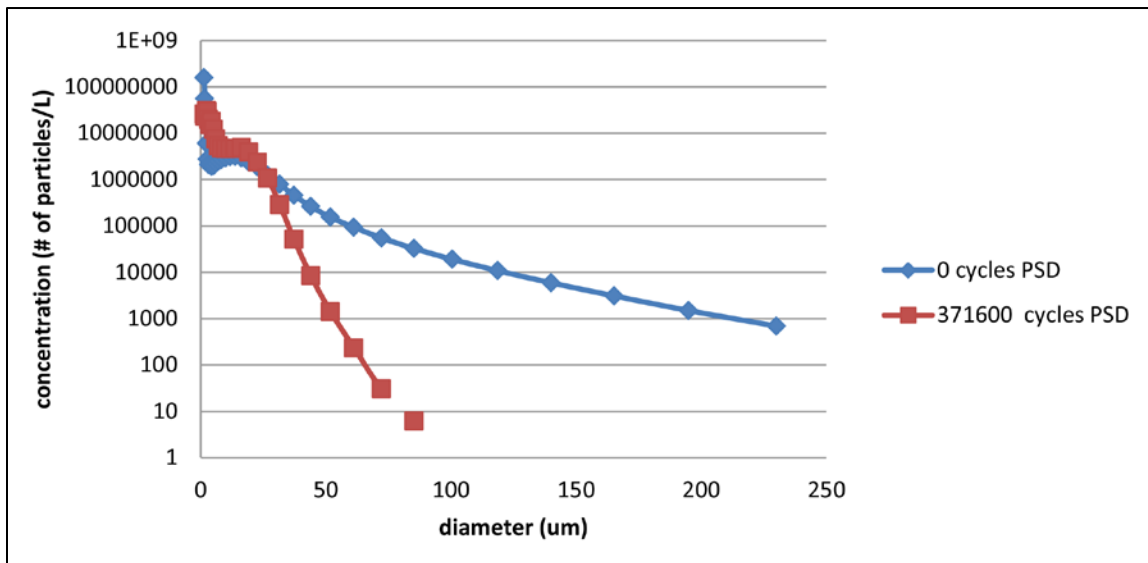


Figure 70 (left): Pump Impeller with Wax from Broken mPCMs

Figure 71 (right): mPCMs in Powder Form Shown Before Mechanical Cycling (left) and the Clumps Found After Pumping (right)



Figure 72: Relative Concentration vs Diameter of Nominal 20 micron mPCMs.

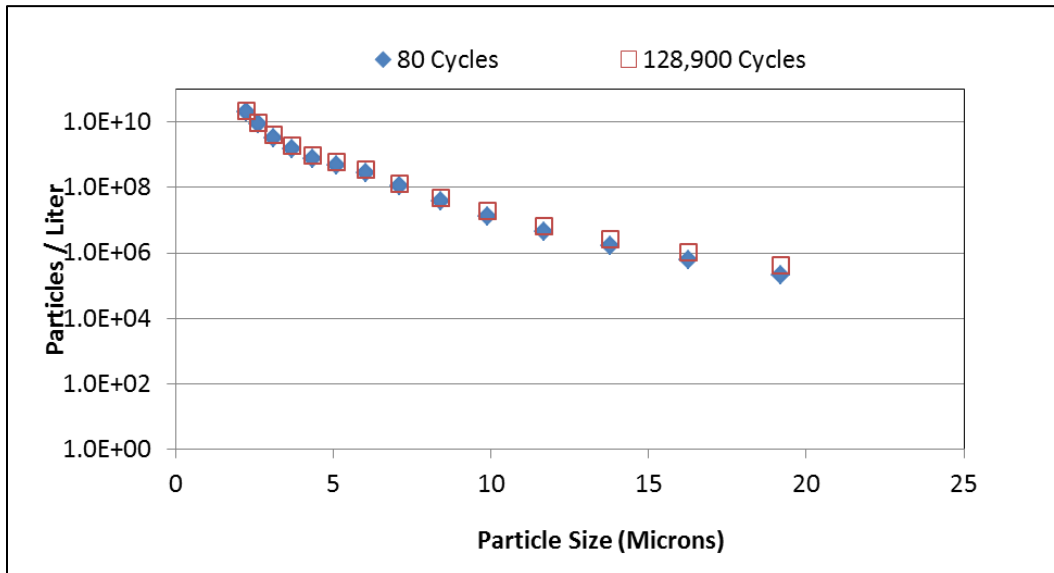


Concentration at the beginning and end of a mechanical cycling test using a centrifugal pump.

A second mechanical cycling test used a slurry of mPCMs with a nominal diameters of approximately 5 microns, or roughly 25% of the diameter of the mPCMs used in the first mechanical cycling test. A Taco centrifugal pump was again used. Cycling ran continuously for approximately 87 hours, corresponding to 130,000 cycles through the pump, with multiple samples extracted throughout the run. Figure 73 shows LISST measurements of size

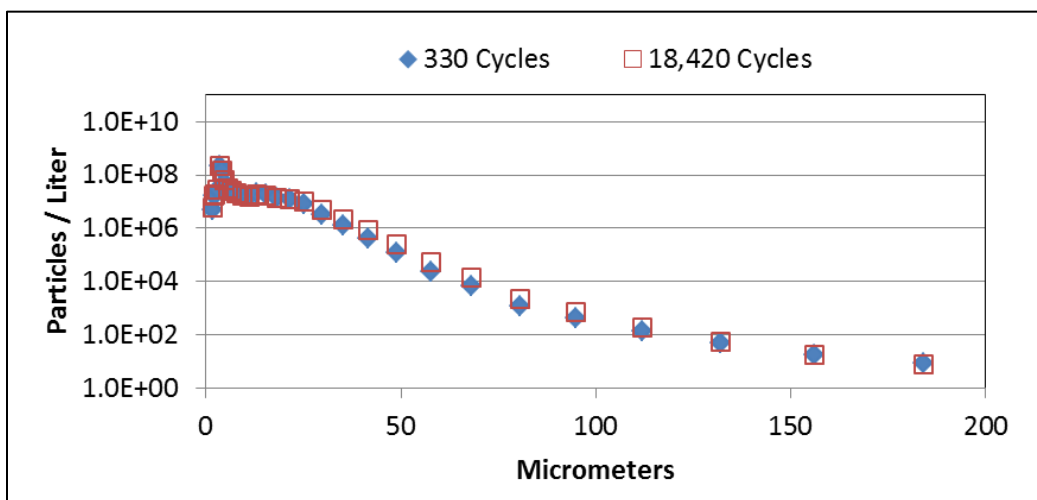
distributions of the mPCMs at 80 cycles and at 128,900 cycles. The results show that concentrations remain nearly identical out to 20 microns over the test period.

**Figure 73: Relative Concentrations of Nominal 5 Micron mPCMs After 80 and 128,900 Cycles.**



In the third mechanical cycling test, a double diaphragm pump manufactured by All-Flo mechanically cycled the large diameter mPCMs found to break in the centrifugal pump. A diaphragm pump is a positive displacement pump advertised as producing low shear and being capable of pumping slurries with solids up to 1/8 inch' in diameter. The pump was relatively inexpensive and expected to reduce or eliminate particle rupturing. The nominal 20-micron mPCMs were cycled for approximately 40 hours at flow rates between 6 and 7 gallons gpm, resulting in a total of 18,400 cycles. Figure 74 shows relative particle size concentrations and suggests little change occurs over the cycling period.

**Figure 74: Relative Concentrations mPCMs at 330 and 18,420 Cycles**



## *Conclusion*

Analysis of the mechanical cycling data suggests low rupturing rates for small diameter mPCMs in the centrifugal pump and suggests that large diameter mPCMs withstand cycling in the diaphragm pump. In particular, no dramatic “fall off” in diameter concentration is observed in either test after many thousands of cycles. Whether rupturing is eliminated in either case has not been determined. The number of cycles used with the diaphragm pump was only around 6% of the number tested in the centrifugal pump due to lower flow rates associated with this pump, which necessitated long run times to accumulate a large number of cycles.

### 4.2.2 Thermal Performance Tests - Laboratory

Full-scale hydronic performance testing, in which the mPCMs were pumped through a water-to-air heat exchanger, was conducted to determine the change in thermal performance as a result of mPCMs. WCEC used mPCMs tailored to melt nominally at 64°F, 82°F, 126°F, and 133°F were all tested in the full scale system. Most of the mPCMs were nominally 20 microns in diameter, with the exception of the 82°F mPCMs, which were nominally 5 microns in diameter. Both the variable speed centrifugal pump and the diaphragm pump were used in testing. A large portion of testing focused on the 5 micron 82°F mPCMs due to concerns over rupturing and clogging associated with the larger mPCMs. It was discovered that the 82°F mPCMs decreased, rather than increased, thermal transfer within the heat exchanger, and a significant effort was made to investigate this finding.

Extensive calorimeter experiments were performed primarily on the 82°F mPCMs in order to more accurately gauge their thermal properties and determine the cause of the poor performance observed with these particles. The experiments revealed that actual melting temperatures for all mPCMs are within +/- 5°F of the manufacturer-provided numbers and can vary from batch to batch of the same nominal mPCM. Additionally, the mPCMs appear to melt over a span of temperatures 2-5°F wide rather than at a specific temperature. This finding is consistent with past findings by other researchers (Griffiths and Eames, 2007) and is consistent with manufacturer claims.

When hydronic testing of the nominal 20-micron mPCMs began, the diaphragm pump was initially used to avoid rupturing the particles. Thermal transfer improvements of between at least 2% at approximately 16% mass concentration were observed for the 126°F mPCMs while using this pump. The diaphragm pump proved less practical than the centrifugal pump for hydronic testing purposes due to its reduced ability to maintain consistent flow rates, a tendency for its air exhaust port to ice up at high flow rates, and the need to run an air compressor continuously during the pump’s operation. More extensive testing of the 64°F mPCMs was performed using the centrifugal pump, and led to no noticeable negative effects on the system despite potential for rupture of the nominal 20 micron mPCMs.

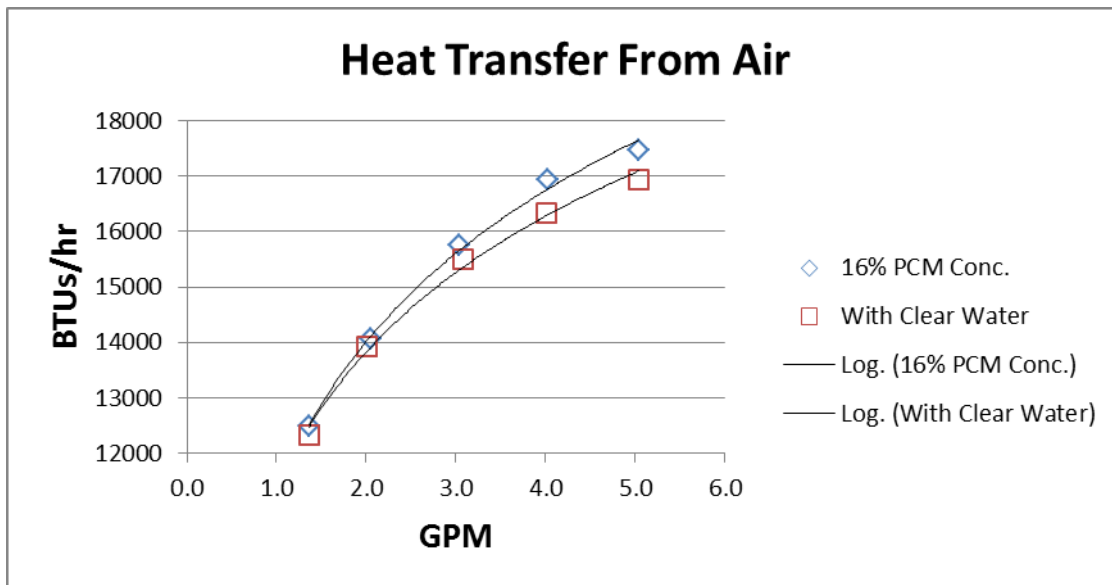
#### *Thermal Results of Large Diameter 64°F mPCMs*

Figure 4-9 shows the results using a ~16% concentration by mass of 64°F mPCMs plotted next to the results of a run using clear water at identical flow rates. This test used a variable speed centrifugal pump whose energy consumption could be directly monitored with a PowerScout

true power meter. For all tests, water/slurry supply temperature is 56°F. Inflow air temperature is 110°F, and airflow is approximately 500 CFM, or ~30 lbs/min. Heat transfer rates are estimated from the air temperature differential measured between the entry and exit points of the heat exchanger.

From the plot, two important observations are made. Firstly, thermal transfer rates for the mPCM slurry are consistently higher than those for clear water. Secondly, the relative difference in thermal transfer between water and slurry widens with increasing flow rate, suggesting that more advantage is gained from mPCMs at higher flow rates. The trend lines applied to the plot are logarithmic. It can be seen from the trend lines in Figure 75 that although the increases in thermal transfer associated with the slurry are modest at the flow rates tested, they correspond to significant flow rate differences between clear water and slurry. For example, a heat transfer rate of 17,000 BTUs/hr requires a clear water flow rate of 5 gpm, whereas the same transfer rate can be obtained with the mPCM slurry at just over 4 gpm: a 20% reduction in flow rate.

**Figure 75: Comparative Heat Transfer Rates for Clear Water and a 16% Mass.**

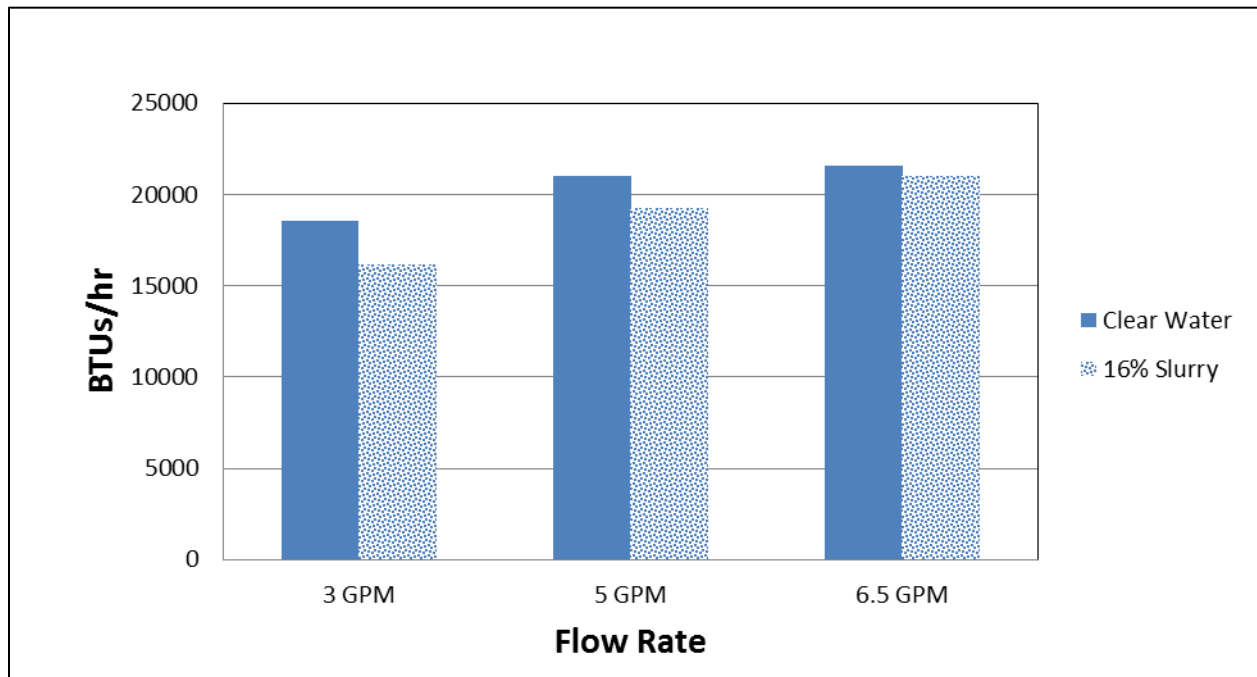


The 16% concentration of 20um mPCMs had a measured melting temperature of 60°F. For all measurements, liquid inflow temperature is 56°F and air inflow temperature is 110°F.

*Thermal Results of Small Diameter mPCMs*

No improvement in heat transfer was conclusively observed with the small diameter mPCMs. Figure 76 shows results from a typical run. This run used a 14% mass concentration. These mPCMs had a nominal melting temperature of 82°F and a measured melting temperature of ~76°F. Liquid supply temperature used for the runs shown was 74°F, which insured exit temperatures at the upper end of the melting range for most flow rates tested. The plot shows consistently higher heat transfer rates for clear water than for mPCM slurries, although the difference decreases somewhat at higher flow rates.

**Figure 76: Heat Transfer Rates Within the Melting Range of the 82°F mPCMs.**



Fluid supply temperature is 74 °F, and air inflow temperature is 120 °F at ~700 CFM

A series of calorimeter experiments was developed to isolate and possibly correct the cause of the low transfer rates. These entailed heating slurries at various concentrations in an insulated beaker and measuring the rate of temperature rise and then cooling the slurries in an ice bath and measuring the rate of temperature drop. It was found that a large fraction of the mPCMs exhibited significant supercooling, a phenomenon whereby a liquid cools down to many degrees beneath its melting temperature without freezing. This resulted in a ~50% reduction in latent heat absorption following the first heating cycle unless the slurry was recooled to ~20°F below its melting point. The calorimeter experiments also provided a way to approximate mPCM melting rates in the full-scale tests, and led to the finding that only between 30% and 50% of the mPCM material was undergoing melting during cycles through the heat exchanger. This finding is consistent with what would be expected if half the mPCMs flowing through the system supercooled. It was also found that either the latent heat of fusion of the material or the total material concentration per mPCM particle was ~16% less than the numbers reported by the manufacturer.

Notwithstanding the above findings, latent heat absorption for the 20-micron mPCMs in full-scale runs has been found to be comparable to that of the 5-micron mPCMs despite the better performance of the 20-micron mPCMs. The extent to which supercooling is exhibited by the 20-micron mPCMs has not yet been determined. It currently cannot be concluded that either supercooling or low melting rates in general are the cause of the low transfer rates observed with the 5-micron slurries. Other contributing factors may include differences in the viscosity of the small and large diameter slurries and differences in the microconvective properties of the

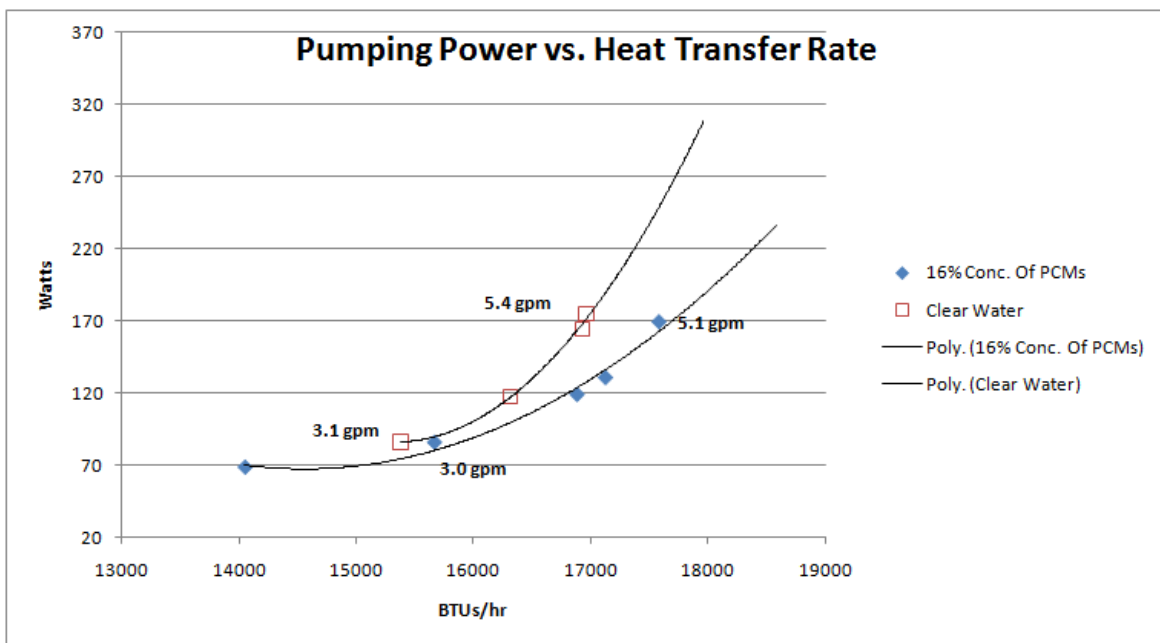
mPCM beads. It was found that, in general, thermal transfer rates for the 5 micron slurries improved when airflow was lowered and when liquid flow was sped up, suggesting that a sufficiently high ratio of slurry flow to airflow might lead to favorable results.

### Energy Savings

Preliminary studies on energy savings have been conducted in the lab using the results from the tests of the 64°F, 20-micron mPCMs. It was found that slightly greater pump speeds were required to pump mPCM slurries at the same flow rates as clear water due presumably to the increased slurry viscosity. Thermal transfer improvements due to mPCMs must therefore be above a threshold corresponding to a slightly higher RPM and flow rate for clear water before the mPCMs provide an energy benefit. Since improvements in thermal transfer appear to increase with increasing flow rate, this suggests that a threshold flow rate or heat transfer rate exists below which energy savings cannot be realized.

Figure 77 shows data from a run in which a 16% concentration of 62°F mPCMs was pumped through the heat exchanger at several flow rates. The heat transfer rates associated with the mPCMs were then matched to clear water runs. The plot shows that greater energy savings occurred at higher heat transfer rates, with savings as high as 30% at the highest flow rates tested. Energy savings appear to disappear below 15,800 BTU/hr, corresponding to flow rates of ~3 gpm.

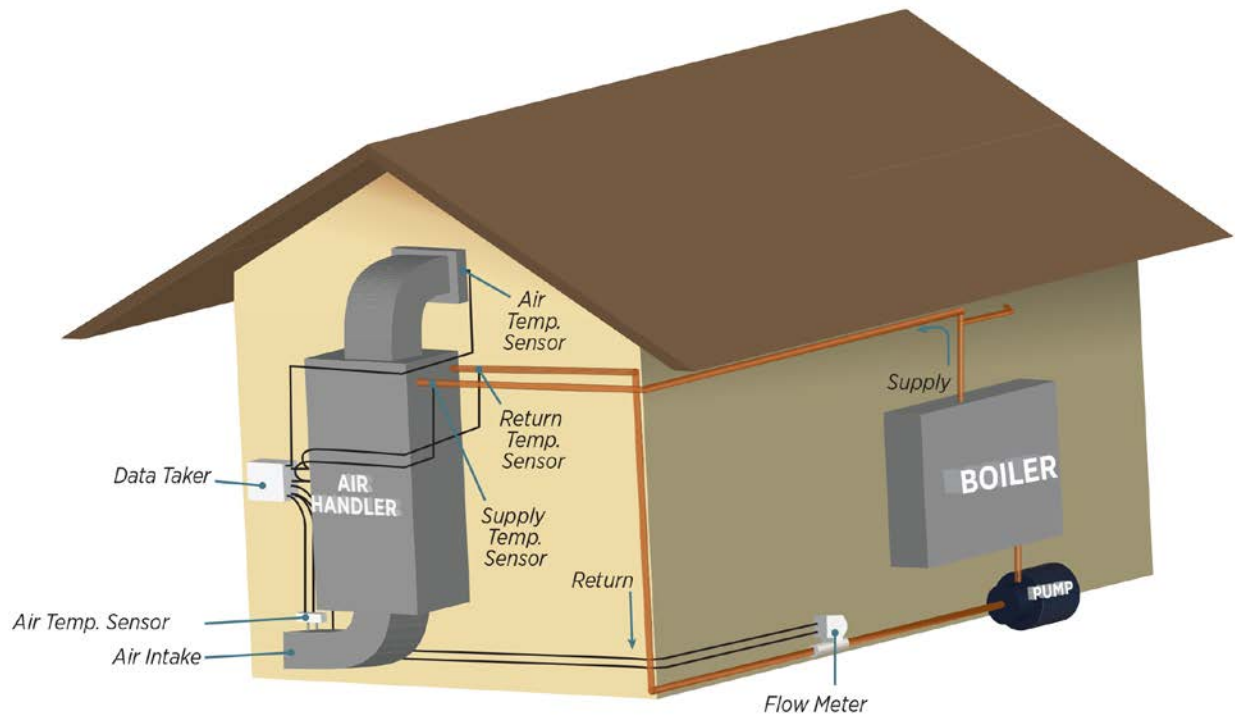
**Figure 77: Pumping Power versus Heat Transfer Rate for 62°F mPCM Slurry and Clear Water.**



Slurry entry temperature is 56°F and air entry temperature is 110°F.

## 4.3 Current Research: Thermal Performance Tests – Field

Figure 78: Diagram for the PCM demonstration building



A thermal performance test at an unoccupied demonstration building (Figure 78) was conducted to determine the performance of the mPCMs in a field test. The building is located south of the University of California Davis campus. It is approximately 200 ft<sup>2</sup> with an average ceiling height of 10.5 feet. The walls are concrete ~5 inches' thick. Its air handling unit consists of a single coil and fan which draws outside air without recirculation. The air coil was originally linked via copper pipe to a 3-ton chiller.

Experimental retrofitting began in late December. Winter conditions led to the decision to rebuild the system as a heating system rather than testing the mPCMs in the original cooling system. For the purpose, a tankless Argo "AT" series electric boiler rated at 34,120 BTUs/hr (10 kW) was selected and purchased.

### 4.3.1 Setup & Instrumentation

The boiler was mounted on an outdoor wall in order to avoid boring holes through the building's 5 inch thick concrete walls for piping and wiring. The system's original copper piping was cut at the entry and exit points to the air-handling unit and flow was rerouted to the boiler using 1inch PEX piping and Sharkbite fittings. Fittings for valves, gauges, and spigots were of galvanized steel. The piping was insulated with fiberglass pipe wrap insulation, which had a nominal R-value of 3.3.

A single horsepower Taco centrifugal pump mated to a 3-phase motor was installed to circulate the water/slurry. The pump's motor was connected to a single-phase-to-three-phase variable frequency drive (VFD) manufactured by Eaton. A relay was installed across the boiler's pump terminals to provide on/off control of the pump through the VFD, allowing the boiler to automatically shut down and start up the pump in response to a heating demand.

The building's air-handling coil and fan were left unmodified. No manufacturer data could be found on either unit. Powerscout readings over multihour runs showed the fan's speed to be nonvarying. Rough air coil-performance measurements showed that its heat transfer coefficient was higher than the laboratory coil for similar air and water flow rates. In order to safeguard against unexpected startup/shutdown of the fan, the fan's original thermostat control was disabled and control rerouted to the boiler pump relay. A resistance heating element, which originally provided heating for the building, was also disabled. Ducting and an air damper were added to the entry point of the air handling unit in order to allow control air flow into the unit.

#### *Instrumentation*

Table 11 summarizes the instrumentation used. Vasaila combination temperature and humidity sensors were mounted within the air handling unit's entry ducting and in the register box leading into the building. To monitor liquid supply and return temperatures, adhesive fast-response RTD units were mounted to the copper piping at the air handling unit's entry and exit points. Heavy insulation was wrapped around the piping out to ~5 inches on either side of the RTD sensors, and a layer of reflective metallic tape was wrapped around the outside of the insulation. Building interior and exterior temperatures were estimated from two more RTDs suspended respectively from an interior wall near the boiler's thermostat and an exterior wall near the duct entry point. Liquid flow rate was measured with an FMG-3000 series Municipal-Industrial magnetic flow meter.

Three DENT Powerscout 3 units were installed in the building's breaker panel for monitoring the power consumption of the fan, pump, and boiler. Data monitoring and recording was accomplished with a dataTaker DT85 data logging unit.

**Table 11: Field Instrumentation**

| Make                  | Model                  | Type of Measurement           | Location                           | Accuracy @ 77°F      |
|-----------------------|------------------------|-------------------------------|------------------------------------|----------------------|
| Vaisala               | 164. HMD50 Y           | 165. Air Temperature/Humidity | 166. Air outflow register          | 167. 0.54°F          |
| 168. Vaisala          | 169. HMD60 Y           | 170. Air Temperature/Humidity | 171. Air intake duct               | 172. 0.54°F          |
| 173. Omega            | 174. RTD-806           | 175. Air temperature          | 176. Interior/Exterior of Building | 177. 0.2°F           |
| 178. Omega            | 179. SA1-RTD           | 180. Surface Temperature      | 181. Coil fluid entry/exit points  | 182. 0.36°F          |
| 183. Omega            | 184. FMG-3000 Magmeter | 185. Liquid Flow              | 186. return piping to boiler/pump  | 187. 3 2μA (.046gpm) |
| 188. Dent Instruments | 189. Powerscout 3      | 190. Power, Voltage, Current  | 191. Breaker Panel                 | 192. 0.2%            |

*Choice of mPCMs & Pump*

Currently the highest temperature mPCMs available from Microtek have a melting point of 110°F and have a 20-micron nominal diameter. WCEC purchased 15 pounds of this specific mPCM in January for the building. Lab experiments on the 62°F mPCMs suggest that clogging is not a significant problem even for 20-micron mPCMs circulated by a centrifugal pump. Thermal transfer properties for these mPCMs seem moreover to remain stable for multihour runs. The 20-micron mPCMs were deemed suitable for the building experiment and the choice of a centrifugal pump was made due to the ease with which it can be controlled and monitored.

**4.3.2 Experimental Approach & Progress to Date**

The site experiments continue at present. All-night runs began on February 17<sup>th</sup>, and necessary adjustments were made to instrumentation and the apparatus based on data collected from early tests. Runs up to 40 hours in length have since been conducted, including a run in which a 14% concentration of mPCMs was used. These experiments have shown the need to improve boiler control of water/slurry supply temperature in order to obtain conclusive results.

*Experimental Approach*

The approach currently being used involves initially running the system for up to 24 consecutive hours using clear water at a constant flow rate. Boiler set-point temperature for the liquid is maintained at 2°F-5°F above the measured melting temperature of the mPCMs (~110°F). Keeping airflow rate, liquid flow rate, and boiler set-point temperature constant, the clear water is then replaced with an mPCM slurry and run for another 20-24 hours. These time lengths

insure coverage of the full range of outside temperature variation over the course of a single day.

The difference in air intake temperature and air exit temperature was compared relative to intake temperature. The rise between intake and exit temperature reflects the thermal transfer rate between the coil and the air. Thermal transfer rates are proportional to the intake temperature for a constant liquid supply temperature into the coil. The resulting approximately linear plots thus show the relationship between heat transfer rate and the outside air temperature at a fixed flow rate and liquid supply temperature. For a PCM slurry, higher heat transfer rates are expected to appear as a higher y-intercept and possibly a different slope relative to clear water plots.

*Preliminary findings*

Figure 79 and Figure 80 are plotted from data obtained respectively for a clear water baseline run and the run in which a 14% concentration of mPCM slurry was used. The clear water run was made on the day prior to the slurry run. All parameters including liquid supply temperature set-point, liquid flow rate, and damper valve angle were kept constant between the two runs. Pumping speed was adjusted on the slurry run in order to maintain the same flow rate as the clear water run. The parameters used were a fluid supply temperature of 112°F, a 5 gpm water/slurry flow rate, and a 45° damper valve angle. Each test ran for roughly 20 hours, covering both nighttime lows and day time highs. The thermostat terminals in the boiler were linked together with a jumper wire in order to produce a continuous heating demand and insure that the boiler and pump would not shut off. The Datataker recorded all temperatures and liquid flow rates every 5 seconds.

**Figure 79: Temperature Rise of Air Between Intake and Outflow.**

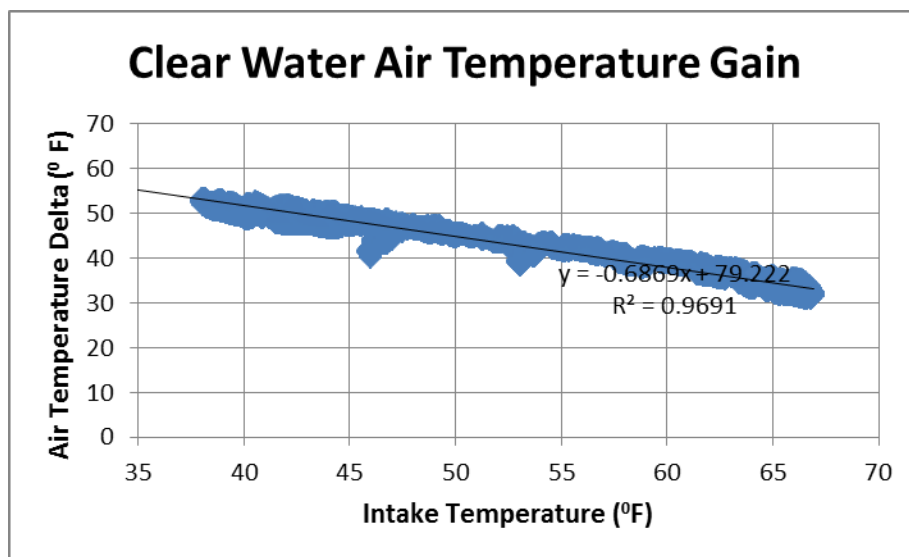
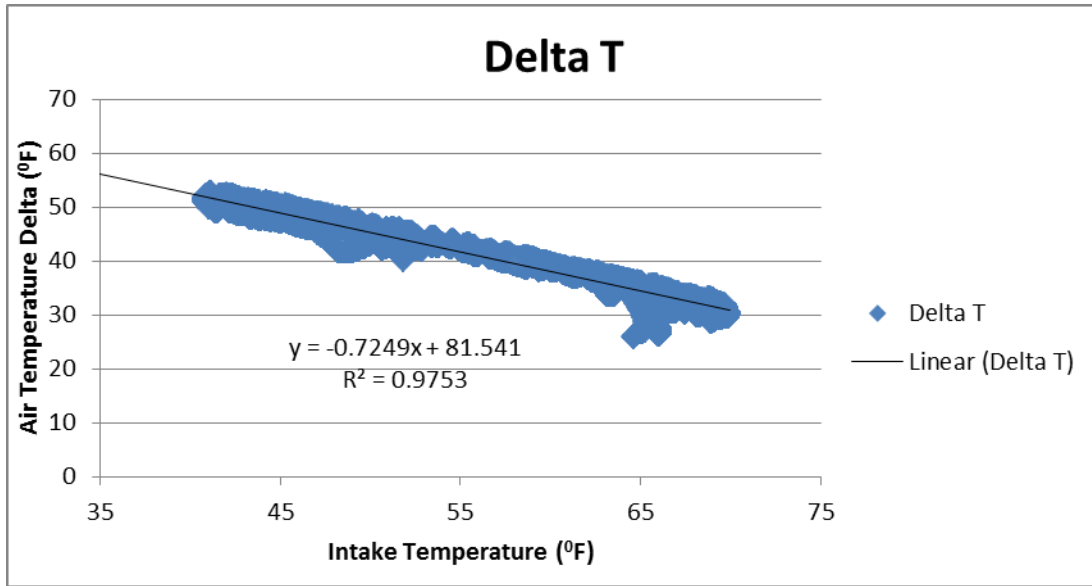


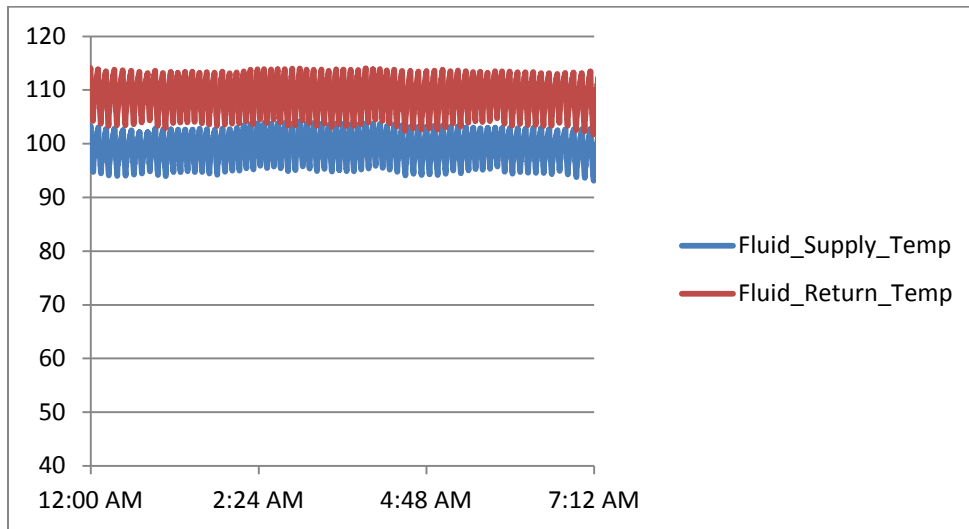
Figure 80: Air Temperature Rise Against Intake Temperature for a 14% Concentration of mPCMs



When the trend lines for the resulting plots are plotted against each other over the range of intake temperatures observed, discrepancy between the trend lines is on the order of  $0.1^{\circ}\text{F}$ , suggesting that virtually no change in air flow has occurred.

In Figure 81, supply and return temperatures have been plotted over the course of a single night for an early test in which a fixed speed pump was used to circulate water at  $\sim 5$  gpm. The heavy oscillations of both the supply and return temperatures are immediately apparent and have amplitude variance greater than or equal to  $8^{\circ}\text{F}$ . This amplitude range is roughly 4-5 times as wide as the bulk melting range for the  $110^{\circ}\text{F}$  mPCMs. Laboratory testing has shown that effectiveness of the mPCMs is highly dependent on the slurry supply temperature. This temperature must remain close to the upper or lower end of the mPCMs' melting range, with tolerances of only  $1^{\circ}\text{F} - 2^{\circ}\text{F}$ , or else the ratio of latent to sensible heat absorption rapidly falls off. It is imperative to develop a method for "tightening" boiler control of the water/slurry temperature.

**Figure 81: Fluid Supply and Return Temperatures for Clear Water.**



Boiler set-point temperature is 114 oF and flow rate is 5gpm.

*Path Forward*

Upcoming work will focus on improving boiler control of fluid temperature set-points. It is expected that once a temperature setpoint can be maintained to within a 1-2°F tolerance, observable effects from the mPCMs will be realized. Once these effects have been demonstrated, subsequent runs with clear water will be made in an attempt to match thermal transfer rates observed with the mPCMs. Once the clear water flow rate is found at which thermal transfer rate matches that observed with the mPCMs, it will be possible to gauge energy savings from comparisons of pump, boiler, and fan power consumption between the slurry and clear water runs.

# CHAPTER 5:

## Previously Completed Research Projects

*Project Status: The Energy Commission portion of this research is completed; based on its success, the project has been sustained by funding from Southern California Edison.*

### 5.1 Evaporative Cooler Precooling

#### 5.1.1 Problem Statement

Evaporative precoolers are available to retrofit air-cooled air conditioning systems often used in residential and light commercial sectors. These systems operate by evaporating water into the condenser air stream, cooling the incoming condenser air. This precooling of the condenser air stream allows the air-cooled system to perform more efficiently. Evaporative condenser-air precoolers are of special interest in dry arid climates such as those in the western United States.

While there are well-established test standards for rating the performance of air-cooled systems, a test standard to objectively compare the performance of condenser-air evaporative precoolers is not available. Establishing a specific protocol for the measurement of evaporative precooler performance allows end-users and utilities to make objective comparisons between products. Without such a standard, each developer will evaluate their product differently, and in a way that puts their product in a better light. Since this technology is growing in the market, and utilities are interested in a methodology to determine values for rebates and deemed savings, it is imperative that a standard protocol be put in place.

#### 5.1.2 Research Findings & Results

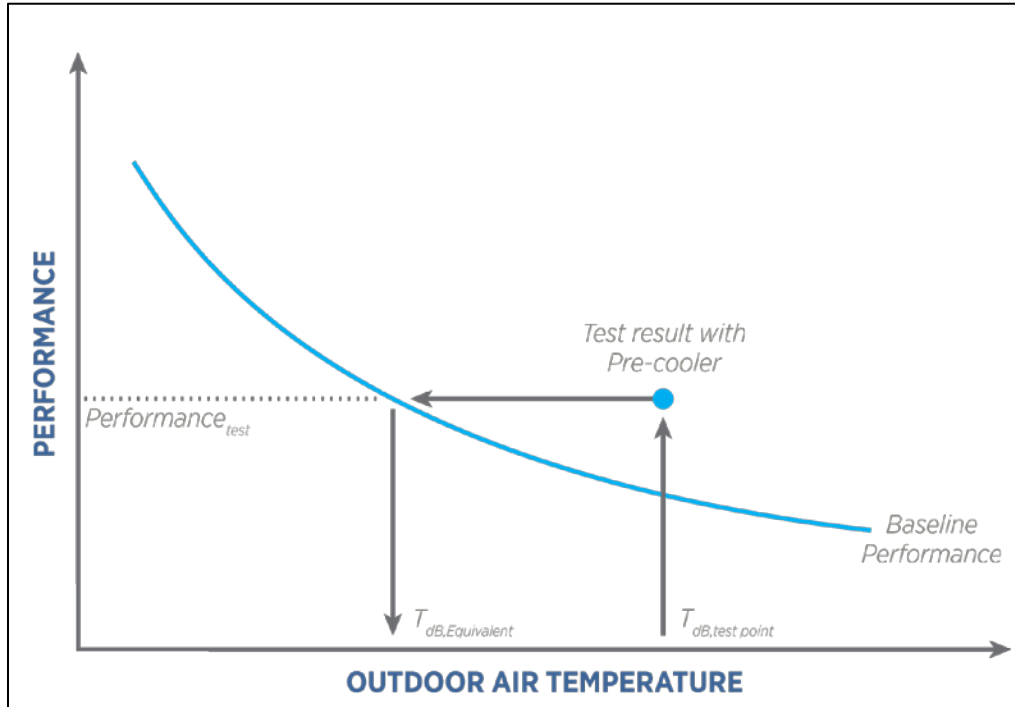
In the effort to create a performance evaluation standard, WCEC, in partnership with the ASHRAE, developed a laboratory testing protocol. An equivalent performance method was developed in order to determine the temperature drop in the air entering the air-conditioner. Temperature drop is a very difficult metric to measure because of the water vapor in the air as a result of the precooling process; when water vapor lands on a temperature sensor, it may evaporate and therefore cool the sensor, which causes it to report an artificially low dry bulb temperature. In addition, the air is not well mixed, making it difficult to pick a location for the temperature measurement. The equivalent performance method assumes that the air-conditioning unit performs comparably for the two following scenarios:

- The outside air temperature is 86°F and there is no evaporative precooler installed, or
- The outside air temperature is 104°F, the installed evaporative precooler cools the air to an average of 86°C, and supplies this air to the condenser coil

Using this assumption, it is possible to back out the temperature of the air after leaving the precooler apparatus but before entering the condenser coil as shown in Figure 82. In this figure, the baseline performance represents the performance of the unit before the precooler apparatus was installed. The test result with precooler performs more efficiently. The temperature leaving the precooler apparatus but before entering the condenser coil is indicated in Figure 82 by

$T_{dB, equivalent}$  which represents the temperature on the baseline curve that has a performance equal to that of the test result with the pre-cooler. The difference between  $T_{dB, test\ point}$  and  $T_{dB, equivalent}$  is the cooling delivered by the pre-cooler.

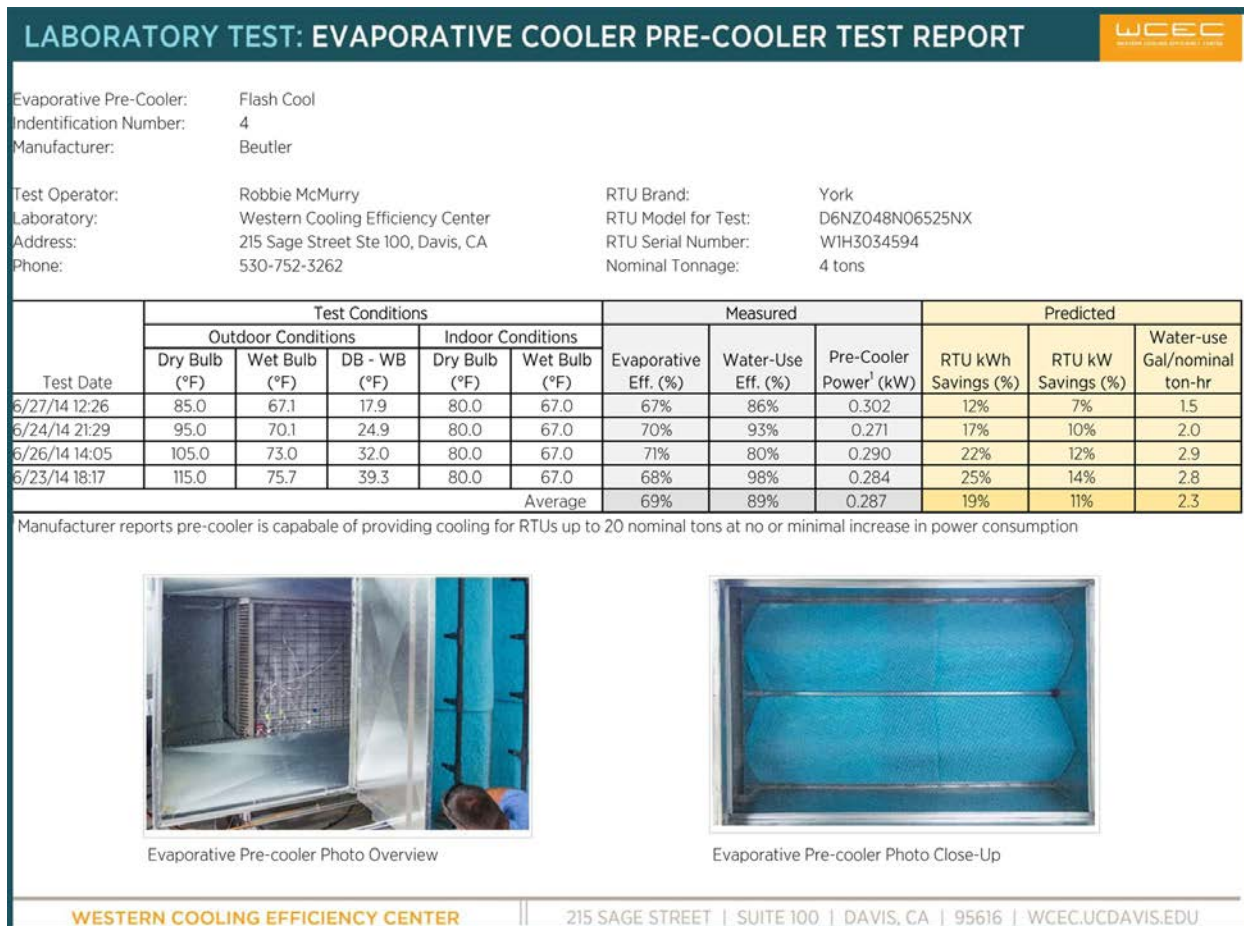
**Figure 82: Equivalent Performance Method**



Using this novel method to calculate the temperature delivered by the pre-cooler offers a high-accuracy objective method to compare pre-cooler performance. The pre-cooler results can be used to calculate potential energy savings using building energy consumption data and climate modeling.

The need for this type of research led directly to a large-scale project funded by Southern California Edison to construct a sophisticated environmental chamber at WCEC's new office location. The chamber's construction is now complete, and WCEC has already tested 4 different evaporative pre-cooler retrofits. Figure 83 below shows a preliminary test result for one of the pre-coolers tested at our new facility.

**Figure 83: Preliminary Test Result Page from One of the Precoolers Tested in the Laboratory Environment Chamber**



## 5.2 Swimming Pools as Heatsinks for Unitary Air Conditioners

*Project Status: This project is complete. Two academic journal papers were published based on this research.*

Model Validation Journal Paper:

<http://www.sciencedirect.com/science/article/pii/S0360132310002192>

Final Academic Journal Paper:

<http://www.sciencedirect.com/science/article/pii/S0378778812006871>

### 5.2.1 Problem Statement

The basic premise of this task is that simultaneously rejecting heat from condensers to the atmosphere, while burning natural gas to heat swimming pools is imprudent. Therefore, by rejecting condenser heat to a swimming pool, instead of ambient air, the energy is beneficially transferred instead of wasted. Furthermore, the reduction in sink temperatures seen by the condenser reduces compressor energy consumption during most hours of the day. The savings

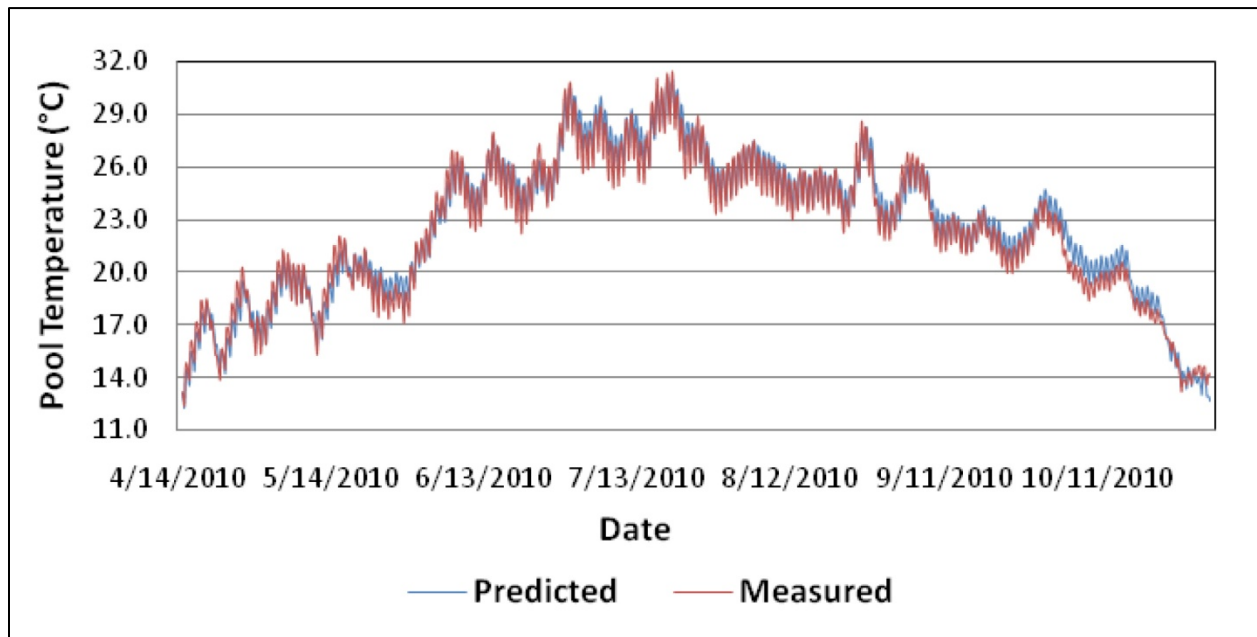
realized during peak conditions will be most significant since ambient air temperatures can exceed 100°F while pool temperatures stay relatively constant between 80-85°F.

Another advantage arises out of the improved heat transfer properties of water, which allow refrigerant temperatures to be only 20°F higher than the sink temperatures. For example, an analogous air cooled condenser requires the refrigerant temperature to be 35°F higher than the sink temperature. Therefore, rejecting heat to a swimming pool can reduce refrigerant temperatures by 30-35°F during peak conditions. The efficiency of R-410A increases by about 2% for every degree reduction in refrigerant temperature, which means these systems have the potential to improve overall vapor-compression efficiency by 70% during peak conditions.

### 5.2.2 Research Findings & Results

The model developed to simulate the thermal behavior of the pool has been validated through a demonstration at a home in Sacramento by two experiments: a passive test that looked at the natural temperature regulation of the pool and an active test that included external sources of heat delivered to the pool. The model development and first test are outlined in a paper published in the January 2011 edition of *Building and Environment Journal*. Figure 84 illustrates the current results for the active test.

**Figure 84: Comparison of Predicted and Measured Pool Temperatures in Sacramento, California.**



Multiple air conditioning system sizes were considered, along with various shading conditions and pool sizes to map the performance of a pool-coupled air conditioner in different scenarios. The results of the simulations are presented in greater detail in a paper recently submitted to *Energy and Buildings*. In light of the model validation, Figure 85 and Figure 86 present the energy savings and peak demand savings predicted for a 4-Ton water-source heat pump rejecting heat to a swimming pool in each of the climate zones considered. These results were

developed for pools that achieve a maximum hourly pool temperature of 90°F (i.e. the pool temperature reached a maximum of 90°F during one hour in the summer).

**Figure 85: Modeled Average Cooling Energy Savings in CA CZs 2, 9, 10, 12, and 13.**

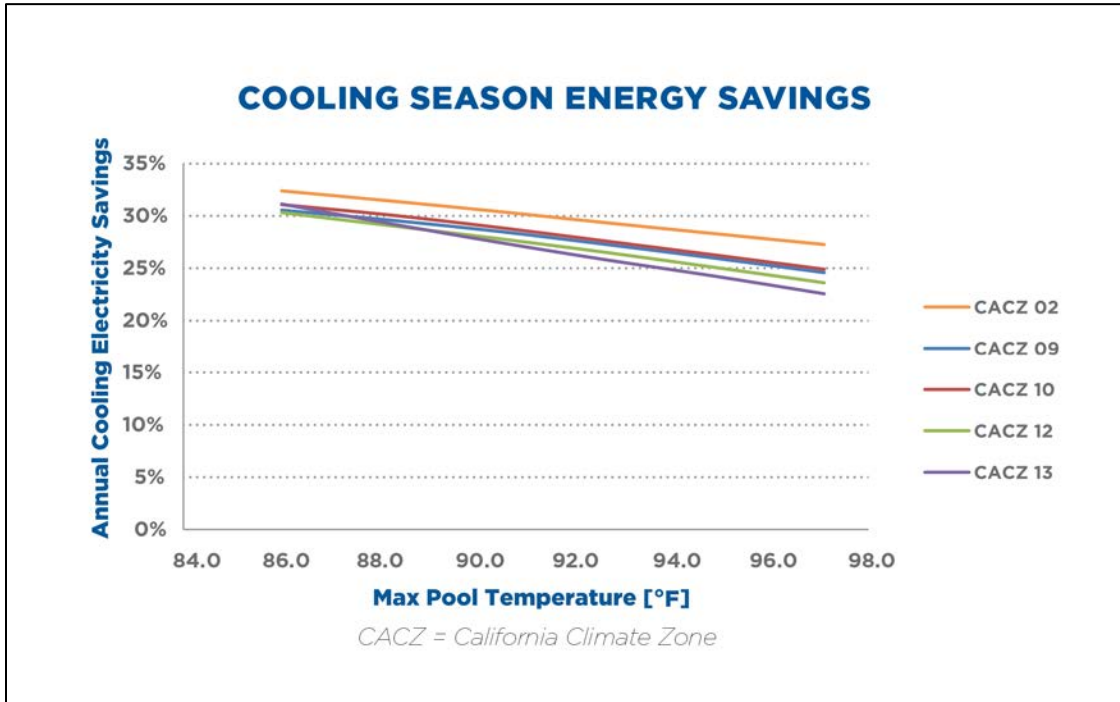
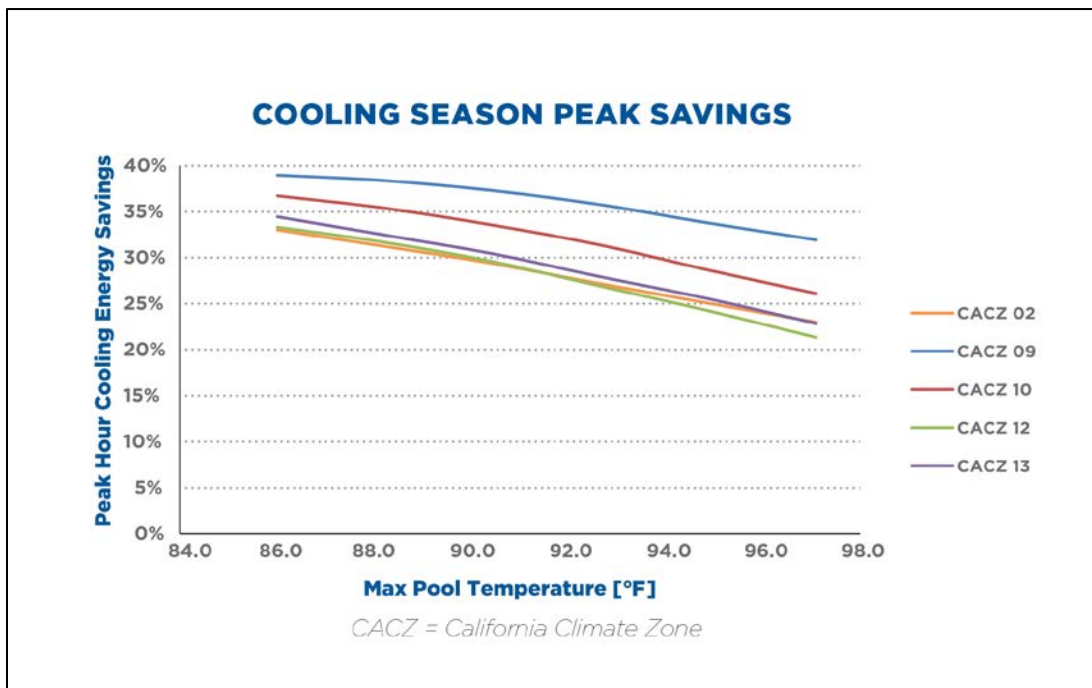


**Figure 86: Modeled Peak Cooling Energy Savings in CA CZs 2, 9, 10, 12, and 13.**



## 5.3 The Western Cooling Challenge

*Project Status: This project is ongoing and, after its initial seed funding from this IA Contract, has been funded by 3 major California utilities: Southern California Edison, Pacific Gas & Electric, and Sacramento Municipal Utility District*

### 5.3.1 Problem Statement

Cooling and ventilation can account for more than 50% of the summertime peak electrical demand from commercial buildings. Rooftop packaged air conditioners are predominantly responsible for this load. Energy saving features such as variable speed fans and multistage compressors promise substantial reductions for annual electricity consumption from rooftop air conditioners, however, since all components must operate at maximum effort during peak periods, they do not offer significant savings when electrical demand reduction matters most.

The Western Cooling Challenge advances development and commercialization of climate-appropriate air conditioning systems that capture substantial energy savings at peak. Recognizing the public benefits of reducing state wide peak electrical demand, The California Public Utilities Commission Energy Efficiency Strategic plan calls for a market shift toward climate appropriate air conditioners. Climate appropriate cooling technologies may take any format that works in concert with local meteorological conditions to achieve savings over code minimum equipment. However, all of the technologies currently advanced through the Western Cooling Challenge utilize some form of indirect evaporative cooling, usually in combination with a vapor compression system.

### 5.3.2 Research Findings & Results

The Western Cooling Challenge has been in motion since 2008, and quickly drew the first formal entry from Coolerado. That equipment, the Coolerado H80 surpassed Challenge performance requirements by a large margin – laboratory testing indicated 65% energy savings at peak cooling conditions.

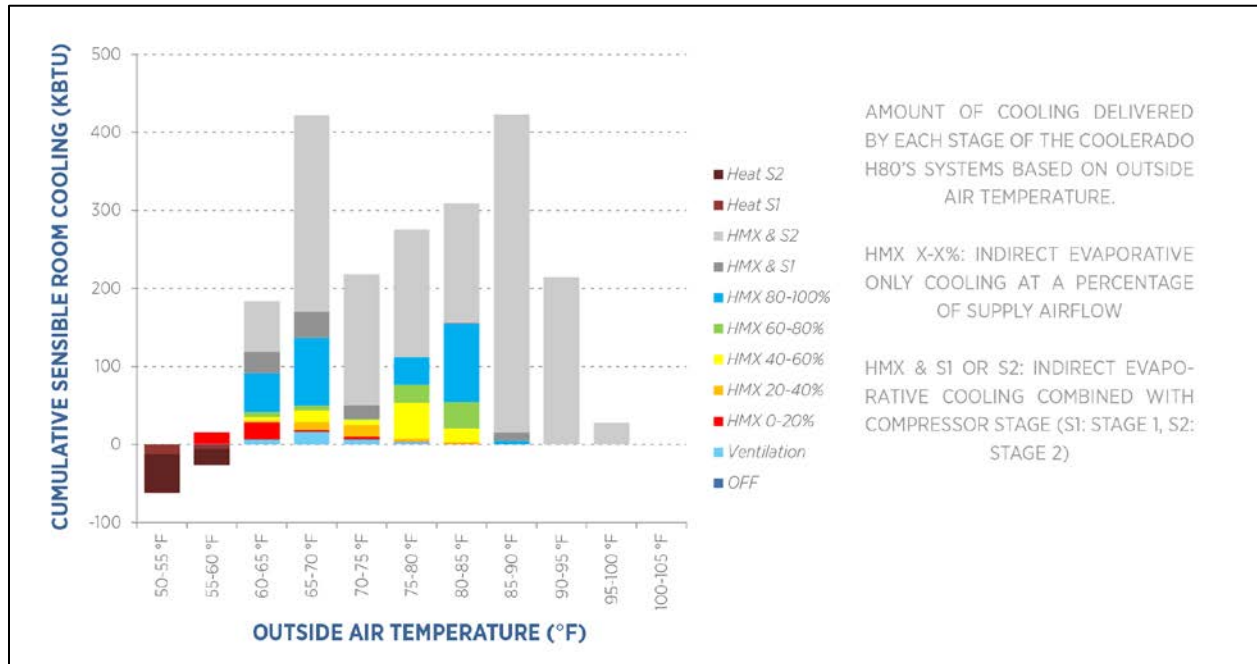
In 2012 and 2013, the Western Cooling Challenge made significant strides and saw growing participation from multiple manufacturers. Notably, WCEC has recently completed laboratory testing of hybrid unitary equipment from Trane and Munters. In collaboration with these and other manufacturers, WCEC is studying the performance of roughly 30 pilot systems installed with various customers throughout California. While the Challenge initially focused on characterizing performance for packaged hybrid rooftop units, the study has expanded to evaluate other climate appropriate methods for commercial cooling. This includes indirect evaporative dedicated outside air systems designed to cover the ventilation cooling load for a whole building, and indirect evaporative coolers installed as retrofit additions to existing rooftop air conditioners. The sections that follow outline a handful of our current work with specific technologies.

#### *Coolerado H80*

Two summers of data from the Coolerado H80 installed in light commercial settings show efficiency that is about 25% improved over baseline measurements when the outside air

temperature is above 95°F. Following installation of the first of these units, University of California Davis worked extensively with the manufacturer to troubleshoot a number of control related troubles, but since that time both systems have functioned reliably.

**Figure 87: Amount of Cooling Delivered by Each Stage of the Coolerado H80's Systems**



Notably, WCEC found that the indirect evaporative cooling component covered a significant portion of the total cooling load through the year. Figure 87 shows that for mild conditions (below 85°F), roughly 40% of the room cooling load was covered without compressor operation at all. When compressors did operate, indirect evaporative cooling provided 30-60% of the cooling capacity – a load that the compressors did not have to carry. Although the Coolerado H80 supplies more than the code minimum amount of fresh air, it was always able to carry the entirety of ventilation cooling loads, even at very high outside air temperatures.

The most significant operational difficulties observed through these pilots were related to unanticipated loss of cooling capacity after the indirect evaporative heat exchanger dried out. Coolerado's current systems require that if ever started from a dry state, the heat exchanger must be primed with a surfactant (dish soap) so that the surfaces will wick moisture properly. During the regular operating season, the heat exchanger must remain wet, even during periods when there is no call for cooling. If the heat exchanger dries out, it must be primed with surfactant again, or it will not perform adequately. On occasion, both installations experienced grid water outages of sufficient duration that the heat exchanger dried and lost its wicking prime. This water outage caused the system to operate with reduced capacity until service personnel reapplied surfactant. Coolerado's newest stand-alone indirect evaporative coolers will automatically recover from an unanticipated dry out event, as long as service personnel keep the soap reservoir filled in sequence with regular filter changes.

Overall, WCEC predicts that the H80 installed in Davis reduced annual electrical energy consumption for cooling by 10% compared to baseline measurements. This projected savings is significantly less than the savings predicted by Laboratory measurements. WCEC attributes the difference mainly to fan power measured for these installations, which was roughly twice what was recorded by NREL in the technical report “Coolerado 5 Ton RTU Performance: Western Cooling Challenge Results”<sup>13</sup> .

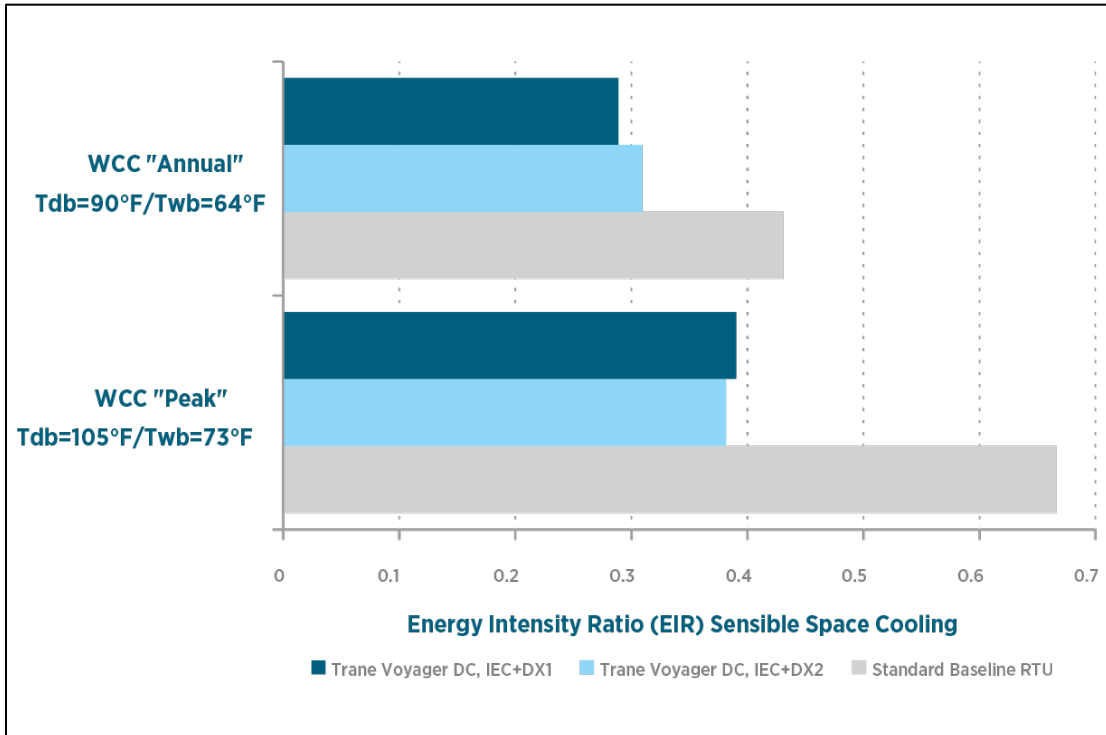
In Summer 2012, WCEC conducted laboratory tests of the Trane Voyager DC. The report, “Western Cooling Challenge Laboratory Results: Trane Voyager DC Hybrid Rooftop Unit” describes function of the factory-integrated hybrid rooftop unit, and documents peak demand savings of more than 40%. This equipment uses the DualCool technology, which provides direct evaporative precooling for condenser air, and circulates evaporatively cooled water through an air to water heat exchanger to cool ventilation air. This strategy reduces the ventilation cooling load for the vapor compression system, and improves operating efficiency by reducing condensing temperature.

Trane’s participation in the Western Cooling Challenge represents a major step toward California Public Utility Commission’s goals for climate appropriate HVAC. In the past months, WCEC has facilitated the installation of five Voyager DC systems for pilot study. Three 12-ton systems were installed in Southern California, one 25-ton system, and one 35-ton system were installed in Northern California. WCEC is logging performance data for these systems, and preliminary results indicate savings on the same order as was measured in laboratory tests, as shown in Figure 88. Importantly, these pilot installations are allowing an opportunity to learn about the broader range of operating characteristics for the system, in order to best understand annual energy savings potential. For example, while it is clear that DualCool provides significant savings at high outdoor air temperatures, WCEC aims to better describe the tradeoffs between these evaporative components and conventional economizer operating modes at lower outdoor temperatures.

---

<sup>13</sup> <http://www.nrel.gov/docs/fy11osti/46524.pdf>

**Figure 88: Energy Intensity Ratio for Trane Voyager DC Compared to Standard 1-Stage CAV RTU**



*Munters EPX 5000*



In collaboration with PG&E Applied Technology Services, UC Davis directed the laboratory testing of the Munters EPX 5000, a 5,000 cfm Dedicated Outside Air System, designed to cover the ventilation cooling load for large format commercial buildings. The equipment uses a polymer construction tube-in-flow indirect evaporative heat exchanger, in combination with a multistage vapor compression system to supply a constant volume of cooled fresh air ventilation to a space. Notably, the equipment can use return air from the space as working air for the indirect evaporative cooler. Since room air generally has a much lower wet bulb temperature than outdoors, this substantially improves wet bulb effectiveness for ventilation air cooling.



According to calculated comparisons from the laboratory experiments, using the Munters' technology for the entirety of ventilation air cooling in a large format commercial space should reduce whole building HVAC peak electrical demand by more than 20%. Following on the laboratory test, WCEC is monitoring two pilot field evaluations for the technology, both installed at grocery stores in California. Results will be published in the coming months.

## Hybrid Retrofits – Coolerado & Seeley Climate Wizard



In light of the fact that commercial HVAC equipment has a long operating lifetime, and that energy consumption for cooling is therefore entrenched within existing building infrastructure, the Western Cooling Challenge is seeking to advance climate-appropriate cooling technologies that can be installed as retrofits to existing rooftop packaged air conditioners. Beyond condenser air pre-cooler additions, WCEC are investigating a range of strategies to install indirect evaporative air conditioners that operate in sequence with existing commercial equipment. These indirect evaporative systems can serve cooled air into the ventilation air stream for a standard rooftop unit, or they can deliver air directly to the space in parallel with existing equipment. In both approaches, indirect evaporative cooling can cover ventilation loads very efficiently, and will cover a portion of the room cooling loads. The fraction of room cooling served without compressor operation will depend on the size and number of indirect evaporative coolers, compared to the total cooling capacity of conventional equipment on the rooftop.

The strategy employed for integrating these systems will significantly impact energy savings potential. For example, economizer function must be maintained, since this mode of cooling is still more efficient than indirect evaporative cooling at low temperatures. Through various pilot field studies, WCEC is collaborating with manufacturers, installers, customers, and utilities to explore and compare alternative application strategies. For a restaurant in northern California, WCEC facilitated installation of one Seeley Climate Wizard, installed with separate supply ductwork to operate in parallel with three existing conventional machines. A pre- and post-installation comparison by PG&E indicated that this retrofit reduced cooling energy consumption during occupied hours by 60%. WCEC is studying the system to characterize equipment performance explicitly, and to assess the implications and success of the installed control strategy.

In collaboration with Wal-Mart, WCEC directed the installation of three Coolerado M50 and three Seeley Climate Wizard CW-H15 systems at a store in Bakersfield. For this pilot, the indirect evaporative systems were installed to deliver chilled air through existing rooftop units, utilizing existing ductwork distribution. The equipment was selected to cover the total ventilation rate for the store, and allowed all other rooftop units to operate as recirculation only. To accomplish this, WCEC developed an inexpensive programmable controller that manages when each component in the combined system will operate. All six systems are controlled similarly, which provides an unmatched opportunity to compare field performance for these two innovative indirect evaporative air conditioners. The COP for each system can be seen in Figure 89 and the water consumption per hour is shown in Figure 90.

**Figure 89: Coefficient of Performance as a function of Outside Air Temperature (Based on Sensible System Cooling. Higher is better)**

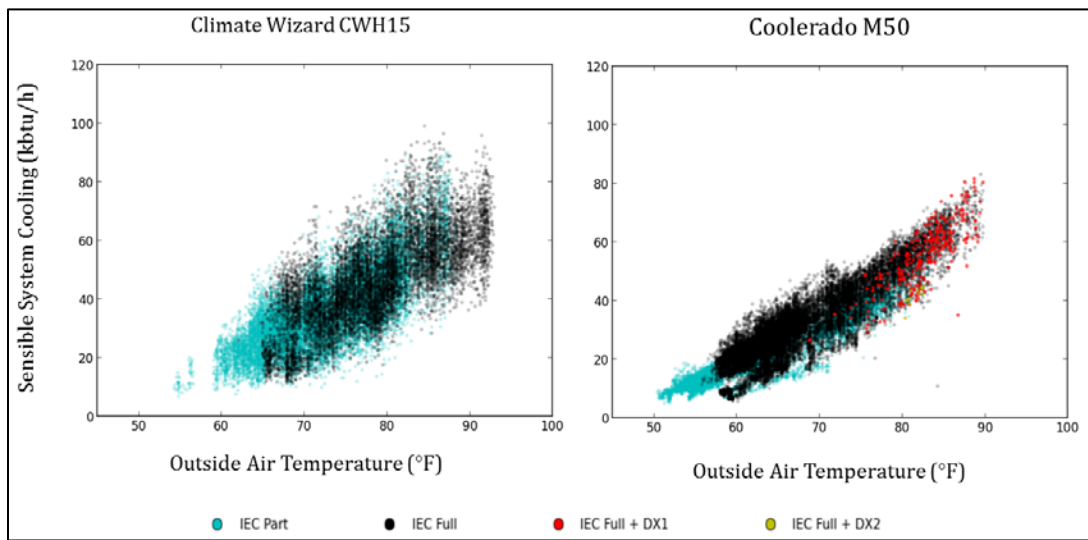
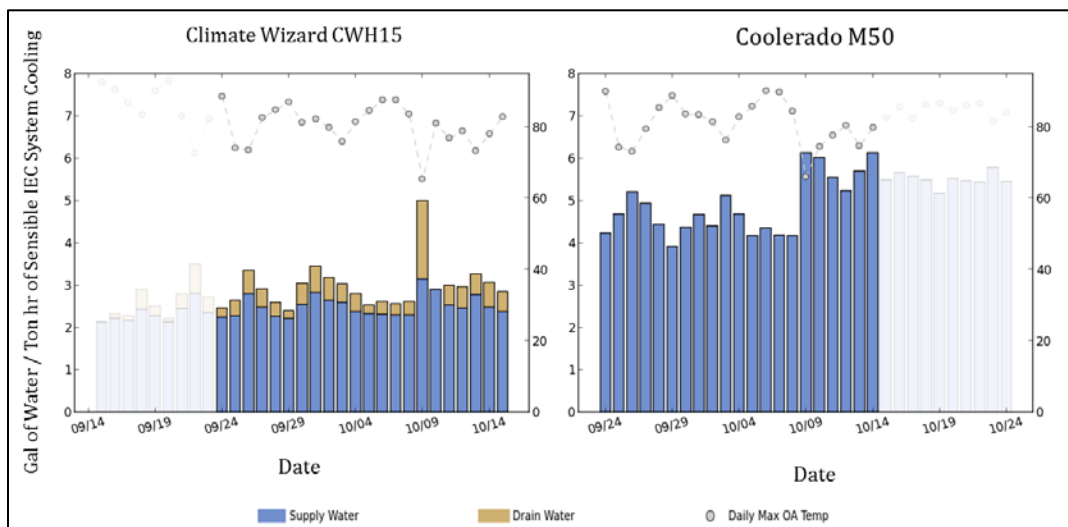


**Figure 90: Gal of Water Consumed Per Ton Hour of Sensible Indirect Evaporative System Cooling**



## *Moving Forward*

The Cooling Challenge has completed testing the Coolerado M50 and Seeley Climate Wizard. The results of this demonstration can be found in the report submitted to Southern California Edison.

The Challenge is actively installing even more Cooling Challenge equipment in demonstrations across the state of California. Some of the most valuable findings from the field are not the energy efficiency data, but the commissioning experience process involved in making these systems function at their optimum level. In light of this, WCEC has made recommendations to the Utilities to package rebate programs for these technologies with service agreements from licensed contractors that can properly commission this equipment. Likewise, WCEC also recommended to the manufacturers of these retrofits to work on creating a more complete solution that includes consistent, streamlined control systems and fault detection to ensure performance and reliability.

## **5.4 Hybrid Evaporative/DX Cooling Equipment First Principles Modeling**

*Project Status: This project is complete. It resulted in a Ph.D. thesis by a UC Davis student, and its results were published in a peer-reviewed journal.*

### **5.4.1 Problem Statement**

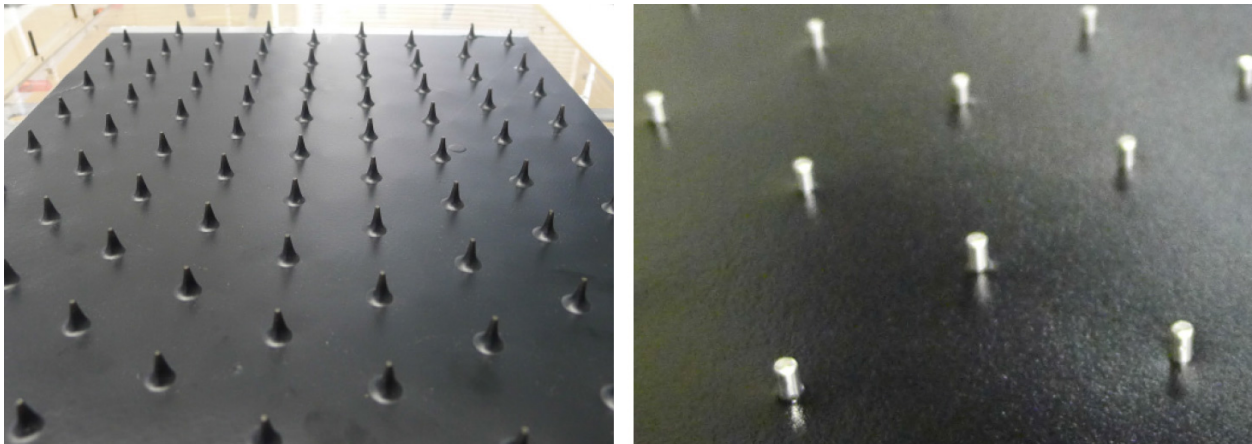
Indirect evaporative cooling (IEC) is attractive for space cooling in dry and hot climates due to its lower energy consumption (when compared to standard vapor compression air conditioners) and lack of humidification (when compared to direct evaporative cooling). The core technology, the IEHX (heat exchanger), is the most critical component in advanced IEC or hybrid IEC/DX systems. As such, the IEHX is the main focus of research for this study.

IEHX's can be configured in many ways, and their performance is heavily dependent on the operating conditions and the climate in which they are used. To characterize the thermal behavior of these coolers and to support their implementation by HVAC designers, a practical, accurate IEHX model is needed, preferably incorporated into building simulation packages (e.g. EnergyPlus). However, characterizing the performance of an IEC or hybrid IEC/DX system for cooling buildings in building simulation programs for different climates and different operating conditions, would take hundreds and even thousands of simulations. In this case, reduced computation time is crucial. This project attempts to address the above concerns by building a simplified IEHX model.

### **5.4.2 Research Findings & Results**

WCEC has continued to work on developing a model for indirect evaporative heat exchangers. The model is intended to be used for heat exchangers made using channels with thin plastic walls. The plates are kept apart, and the channels are kept from collapsing by pins, which also act as turbulence promoters. The simplest manufacturing technique is for the pins to be formed from the same sheet as the plate (Figure 91, left).

**Figure 91: (left) Heat Exchanger Wall with Tapered Pins. (right) Plate with Cylindrical Pins.**

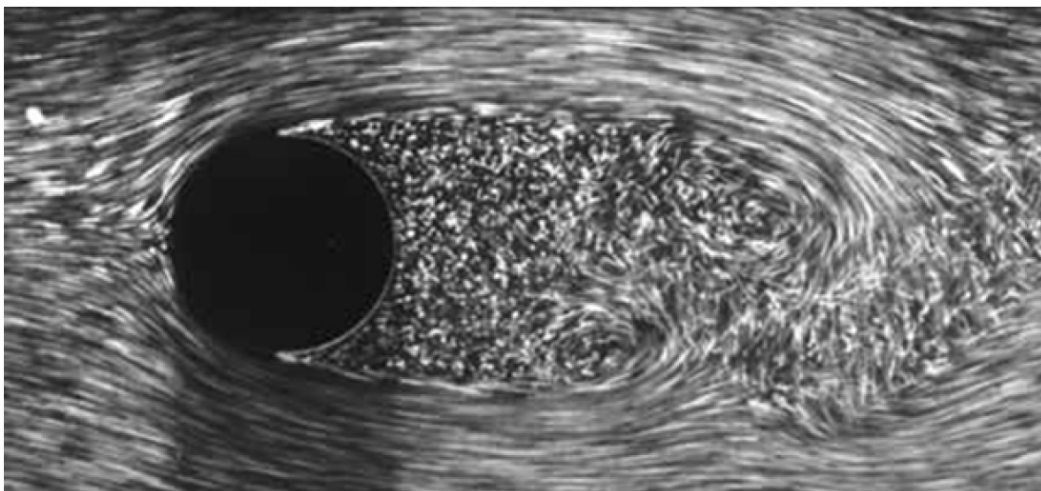


The pressure drop in the channels is caused by a number of effects, which are not independent. At this stage of our research, WCEC are keeping the channel height (spacing between the plates) and channel width constant to minimize the variables to study. In order to remove some of the variability in size/shape that were found in the tapered pins, WCEC have constructed plates with cylindrical pins (Figure 91, right) that are significantly more consistent.

#### *Effect of individual pins*

In a simple model, WCEC can divide the pressure drop into drag caused by two main components: the plates and the pins. The effect of the plates would be proportional to their surface area (all other things being equal) and the effect of the pins would be proportional to their cross sectional area. As the number and size of the pins increases, their effect becomes larger and the effect of the plates is reduced. However, this picture is complicated by the way in which the flow around the pins is disrupted (Figure 92).

**Figure 92: Typical Pattern of Fluid Flow Past a Cylindrical Pin**

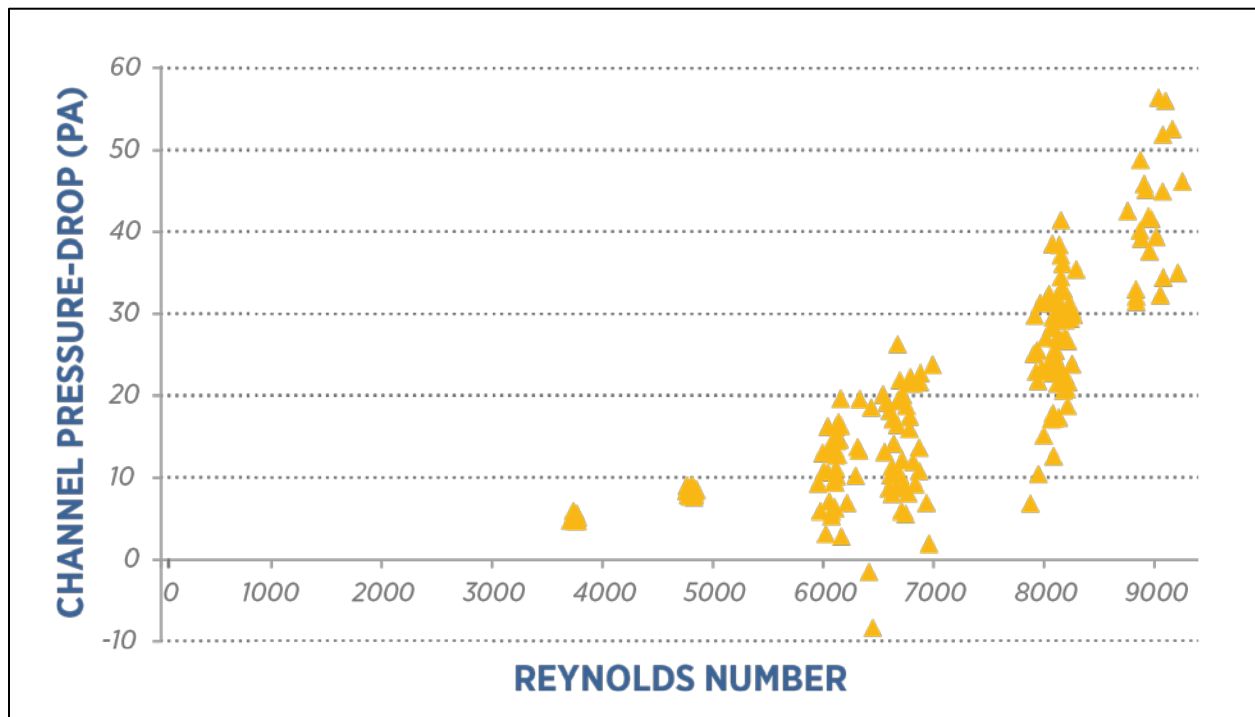


There is a quiescent area, or 'shadow', in the flow behind each pin, which will have the effect of reducing the effective area of plate surface over which the air is flowing. The size of this area will depend on the flow rate and the pin size. This effect is further complicated by the proximity of other pins: if the pin spacing is such that subsequent rows of pins fall in the shadow their effect on flow will be smaller than that of wider spaced pins. In order to understand the importance of this effect WCEC are measuring the pressure drop in channels with a range of pin sizes and separations. This aspect was started recently and the results are still being analyzed.

*Effect of water on pressure drop*

The wet channel has a flocked surface, which has a higher roughness than the smooth surface of the dry channel. Introducing water into the channel is necessary to provide cooling, but excessive water flow will disrupt the airflow in the channel. An example is given in the graph below, for a water flow rate of 60ml/min, the airflow is disrupted when the Reynolds number reaches 6000 (Figure 93).

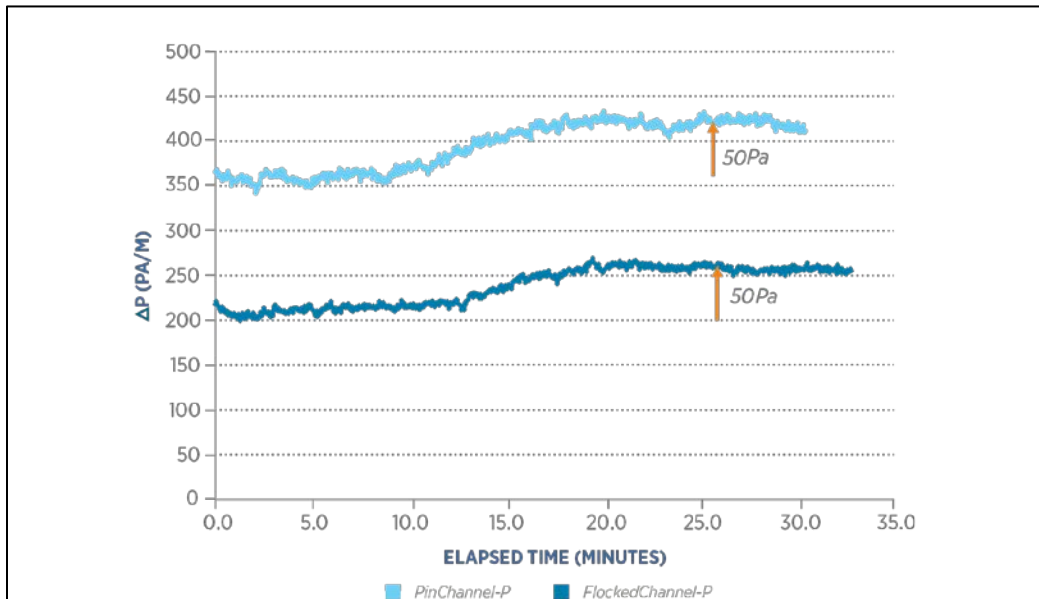
**Figure 93: Effects of Water on Pressure Drop**



More recent tests have focused on the low flow regime, to determine the effect of minimal water flow on the pressure drop. To study this, a channel was built with a flocked surface and water was flowed through the channel for several minutes to completely wet the surface. The water flow was then stopped and the pressure drop was monitored at a constant air flow rate. The test has been carried out for surfaces both with and without pins.

Figure 94 shows that in both cases the channel starts to dry after approximately 12 minutes, and is fully dry within 20 minutes. The difference in pressure drop between the wet and dry states is roughly 50Pa in both cases, even though the actual pressure drop is higher in the channel with pins, as would be expected. The similarity in the change in pressure drop suggests that the effect of drag on the plates can be de-coupled from the effect of the pins, which is promising for the development of our model.

**Figure 94: Pressure Drop Difference Between Wet and Dry States**



In addition to the experimental work and the modeling described, a separate model based on the effectiveness-NTU method was developed. Using some approximations, the governing differential equations that describe IEHX heat/mass transfer behavior were modified to produce a methodology that is analogous to the effectiveness-NTU method for sensible-only heat exchangers. The simplified set of equations can then be solved numerically. The model was compared to existing data from the literature and found to be in good agreement. This work was published in the journal HVAC&R Research<sup>14</sup>.

## 5.5 Optimized Hybrid Evaporative Cooling (Water-Use Efficiency)

*Project Status: This project was completed in 2009 and resulted in the publishing of an academic research paper<sup>15</sup>.*

<sup>14</sup> Zhijun Liu, William Allen, Mark Modera. *Simplified thermal modeling of indirect evaporative heat exchangers*. HVAC&R Research. Vol.19, Issue.3, 2013

<sup>15</sup> <http://www.sciencedirect.com/science/article/pii/S0378778810004019#>

### 5.5.1 Problem Statement

Evaporative cooling technologies are generally valued for their reduced energy consumption in comparison to compressor-based air conditioning systems. However, two concerns that are often raised with respect to evaporative cooling equipment are their on site water use and the impact of poor water quality on their performance. While compressor-based systems do not use water on site, they do consume water through their use of electricity, which consumes water through evaporation at hydroelectric power plants and cooling at thermal power plants. This research defines a water-use efficiency metric and a methodology for assessing the water use of various cooling technologies. The water-use efficiencies of several example cooling technologies are compared including direct evaporative, indirect evaporative in two different configurations, compressor-based systems, compressor-based systems with evaporative pre cooling of condenser inlet air, and hybrid systems that consist of an indirect evaporative module combined with a compressor-based module. Designing cooling systems for arid climates is entwined in the close relationship between water and energy and the scarcity of both resources. The analyses presented in this paper suggest that indirect evaporative and hybrid evaporative/compressor systems that significantly reduce peak electricity demand and annual energy consumption need not consume any more water than conventional systems.

### 5.5.2 Research Findings & Results

The cooling methods evaluated in this paper for water-use efficiency were:

1. direct evaporative cooling for supply air;
2. indirect evaporative cooling for supply air;
3. compressor-based air conditioning;
4. direct evaporative precooling of condenser air for compressor-based air conditioning; and
5. hybrid systems that combine indirect evaporative and compressor-based systems.

For numerical analyses, all cooling approaches are evaluated using outdoor air with 100°F dry bulb (DB)/69.2°F wet bulb (WB) (37.8°C DB/20.7°C WB) temperatures, and indoor air with 78°F DB/64°F WB (25.6°C DB/17.8°C WB) temperatures.

**Figure 95: Water-Use Efficiency of the Technologies Explored.**



Closer to 1 means greater efficiency.

The water-use efficiencies for all types of cooling equipment analyzed are summarized for side-by-side comparison in Figure 95. This comparison indicates that direct evaporative cooling has a competitive water-use efficiency, especially when water needs to generate electricity are high. However, the value of this efficiency is offset by the fact that the applicability of this technology is limited due to the elevated indoor humidity that it produces. On the other end of evaporative technologies, evaporative precooling of condenser air is one of the least efficient options, with a water-use efficiency of 0.09-0.18. This strategy is shown to be more advantageous for R-410A systems than for R-22 systems as R-410A performance is more strongly related to condenser air temperature. Even though precooling condenser air is not the most efficient water-use option, it has several advantages, namely that it is a relatively inexpensive retrofit that provides significant electricity savings and increased cooling capacity without impacting indoor humidity levels.

The most interesting results in Figure 5.5-1 involve indirect evaporative cooling, as it does not add any indoor moisture, yet its water use efficiency can be elevated above that of direct evaporative cooling by appropriate equipment design (i.e. incorporating this equipment with a compressor-based system). For the options that were analyzed, the water-use efficiency of indirect evaporative cooling is maximized when indoor return air is incorporated into the

intake air stream and the indirect-section exhaust is used as pre-cooled condenser inlet air for a properly-sized compressor-based system. When the water requirements for electricity generation are high, 4.15 gal/kWh (4.36 l/MJ<sub>e</sub>), an indirect evaporative cooler that recycles indoor air and recovers exhaust for a compressor-based system has a water-use efficiency of  $n = 0.30$ , which is actually more efficient than the standard-efficiency compressor-based system ( $n = 0.16$ ) and high efficiency R-410A compressor-based system ( $n = 0.26$ ). When the water requirements for electricity generation are low, 1.28 gal/kWh (1.35 l/MJ<sub>e</sub>), the high efficiency R-410A system has a water-use efficiency nearly two times greater than the most water-efficient evaporative system analyzed. In either case, the evaporative system significantly reduces peak electricity demand and annual energy consumption. It is clear that pinpointing the quantitative water-use efficiency results relies very heavily on the water use for hydroelectric electricity generation, which varies by state. Without knowing the “exact” answer, it is clear that evaporative technologies that are superior from an energy efficiency standpoint can be competitive from a water-use efficiency standpoint as well.

The comparative results shown assume that the required ventilation for the building is 33% of the total supply air. However, the direct and indirect systems with no recovery of indoor air actually provide 100% ventilation air. The indirect system with recovery of indoor air analyzed provides a supply air stream that is 56% ventilation air. The sensible cooling provided by the evaporative cooler (Equation [2]) only receives credit for the required 33% ventilation. If the required ventilation is higher, the water-use efficiencies for the evaporative cooling systems will increase. If the required ventilation is lower, the water-use efficiencies for the evaporative cooling systems will decrease. The water-use efficiency for compressor-based systems is not a function of ventilation rate. Therefore, evaporative systems are even more attractive for buildings with high ventilation requirements, or in buildings with multiple cooling units, where particular units can be dedicated to providing additional ventilation.

Another issue that will need to be addressed for evaporative coolers in some regions is the effect of hard water on the maintenance of the system. Hard water can cause mineral buildup on wet-side heat exchange surfaces. Initial experiments indicate that the mineral build up does not appear to reduce evaporative effectiveness, but that it does increase flow resistance and, therefore, capacity and efficiency. Typically, manufacturers drain sump water and/or use extra water to wash the media on a regular basis to prevent and remove mineral buildup. Use of extra maintenance water is not considered in the analysis and will reduce water-use efficiency. The amount of maintenance water required based on mineral content is not well understood, but “rule of thumbs” are in the range of 5-50% of the evaporated water. Potential options to reduce maintenance water consumption include pretreating the water supply to remove minerals or changing evaporative media on a periodic basis when mineral buildup reaches an unacceptable level.

One other consideration when comparing the water use efficiencies of various cooling-equipment alternatives is the difference between localized water use and power-plant water use. On the negative side for evaporative equipment is the fact that it takes energy to transport water to the local cooling equipment. On the positive side for evaporative equipment is that there are localized water sources that are suitable for evaporative cooling purposes, but which

currently cannot be used for drinking. These include air-conditioner condensate, captured rainwater, and grey water. Along a similar line, purge water from evaporative coolers can potentially be used for gardens, thereby eliminating maintenance-water use from the equation.

Designing cooling systems for California's climate is entwined in the close relationship between water and energy and the relative scarcity of both resources on both peak and annual bases. It is clear that a rationale basis is needed for comparing cooling-system alternatives. This research has presented a possible framework for such comparisons, as well as example applications of that framework to a number of cooling alternatives.

This work suggests that there exist viable alternatives for reducing energy consumption and peak electricity demand that do not significantly increase overall water use. One such solution may be in designing hybrid evaporative-plus-compressor systems that significantly reduce peak and annual electricity demand while making efficient use of on-site water. WCEC also suggests that additional research on water quality impacts and local water management strategies could prove to be valuable.

## **5.6 Fault Detection & Diagnostics**

*Project Status: The policy changing scope of this project was completed in 2011 and resulted in the Title 24 change that requires all new RTUs to have a useful, base level of fault detection and notification system.*

### **5.6.1 Problem Statement**

Maintenance for rooftop packaged air conditioners (RTUs) is rarely a preventative practice. Generally, service calls are limited to emergency response to major system failures that impact occupant comfort. Even in the case of equipment maintained by regular service contracts, technicians normally only detect and diagnose severe and obvious faults since their procedures typically only involve routine qualitative assessments. This failure means that nonemergency faults that cause significant energy waste can go unnoticed for years.

### **5.6.2 Research Findings & Results**

There are many common occurrences that significantly reduce RTU system efficiency. The range of faults includes sensor failures, poorly commissioned control set points and calibrations, airflow restrictions, and mechanical component failures. These faults result in a number of different inefficiencies such as failed or inappropriate economizer operation, low thermodynamic efficiency, reduced cooling capacity, and increased fan energy use. Recent research into the prevalence and energy-use penalty of various failures has helped to inform how automatic fault detection and diagnostic (AFDD) tools should prioritize the importance of nonemergency faults, and what types of capabilities Title 24 codes should require of these tools. Table 12 describes the efficiency impact of various common faults, the probability that these faults occur within a normal equipment lifetime, the likelihood that such a failure would be noticed with and without AFDD tools, and the average energy savings that could be had from repairing the faults. Figure 96 shows the overall percentage prevalence of various RTU faults.

**Table 12: Faults that impact energy performance of RTUs**

| FAILURE MODE  | EFFICIENCY PENALTY                  | PROBABILITY OF FAULT (15 YEARS) | PROBABILITY OF DETECTION W/AFDD | PROBABILITY OF DETECTION W/O AFDD | AVG. KWH/TON-YR SAVINGS OVER (15 YEARS) |
|---|-------------------------------------|---------------------------------|---------------------------------|-----------------------------------|---|
| Low airflow: 300 <i>cfm/ton</i>   | 5%                                  | NA                              | NA                              | NA                                | not modeled for Title 24 code change    |
| Evaporator heat exchange problem, incl. low airflow (50% coil blockage)           | 5%                                  | 74%                             | 75%                             | 25%                               |   |
| Refrigerant charge: 80% of nominal charge   | 15%                                 | 85%                             | 75%                             | 50%                               |   |
| Performance degradation: 30% condenser blockage, 300 <i>cfm/ton</i> , -10% charge | 21%                                 | NA                              | NA                              | NA                                |   |
| Refrigerant line non-condensables   | 8%                                  | 50%                             | 75%                             | 25%                               |   |
| Condenser heat exchange problem (50% coil blockage)                               | 9%                                  | 48%                             | 75%                             | 25%                               |   |
| Compressor short cycling  | 10%                                 | 30%                             | 75%                             | 25%                               |   |
| Refrigerant line restrictions/TXV problems  | 56%                                 | 62%                             | 75%                             | 25%                               |   |
| Air temperature sensor failure  | not a comparable efficiency penalty | 2%                              | 75%                             | 25%                               | 9.5                                     |
| Non-optimal economizer set point (55°F instead of 75°F)                           |                                     | 30%                             | 75%                             | 75%                               | 448                                     |
| Economizer damper failure   |                                     | 24%                             | 75%                             | 25%                               | 535                                     |
| Excess outside air  |                                     | 24%                             | 75%                             | 25%                               | 136                                     |

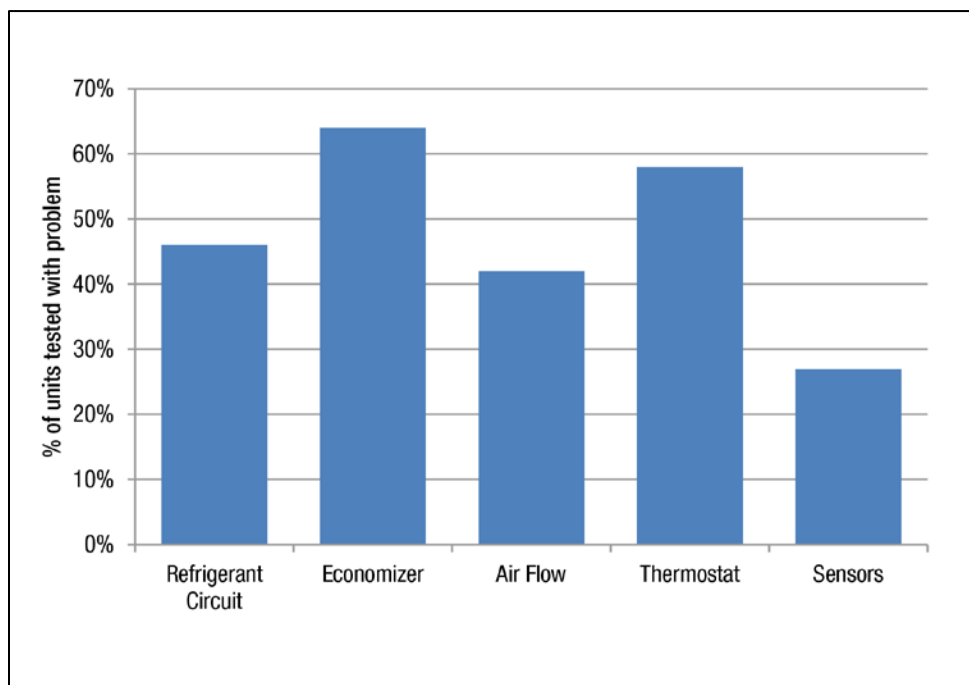
The failures considered here include:

1. *Air temperature sensor failure.* Damage, disconnected wiring, or mis-calibration of air temperature sensors can cause a rooftop unit to operate in inefficient modes, such as failing to actuate an economizer when outside air is appropriate to provide cooling, or remaining in a high-capacity mode in an attempt to maintain supply air temperature when a more energy efficient stage could provide adequate cooling.
2. *Sub-optimal refrigerant charge.* Refrigerant charge is one of most common faults with rooftop air conditioners. It occurs either because of improper installation or service practices, or due to leaks in the refrigerant circuit or refrigerant valves. While a system may still be able to provide adequate cooling capacity, low or high refrigerant charge results in decreased efficiency. A system that is charged 20% lower than manufacturer’s nominal recommendations can result in a 15% efficiency degradation.
3. *Low airflow.* Low supply airflow occurs when fan speed is not appropriately commissioned, or when there is some airflow restriction, such as a blocked coil, dirty filter, or major point of resistance in the air distribution system. Airflow below 300 *cfm/nominal-ton* can cause significantly reduced cooling capacity, and increased compressor power. If airflow is low enough it can cause an evaporator coil to ice, could allow liquid refrigerant to pass through the compressor, and might cause short cycling of the compressor.

4. *Condenser or evaporator coil heat exchange problems.* This occurs when there is low airflow through the evaporator or condenser coil, generally caused by coil blockage, or fan failure. Low airflow through the evaporator coil can cause incomplete refrigerant vaporization and results in liquid flooding the compressor which wastes energy and will damage the compressor.
5. *Refrigerant line contaminants.* When noncondensable contaminants such as air and water vapor become entrained in a refrigerant circuit, the system operates less efficiently because heat transfer surface is reduced, and compression power increases. This is most commonly caused by leaks, or poor service practices such as failing to completely evacuate refrigerant lines when charging equipment.
6. *Refrigerant line restrictions.* Flow constriction due to blockage in the refrigerant line causes flow resistance, which impacts system operating pressures, and starves flow to system components. This causes reduced cooling capacity as refrigerant flow is reduced, and increases compressor power as additional pressure drop must be overcome. When a restriction is present in the liquid line, it can cause a larger than normal vapor expansion pressure which may cause freezing on the evaporator coil. These restrictions can be caused by dirty suction filters, dirty expansion devices, dirty liquid line filter/dryers, a joint partly filled with solder, or bent or crimped refrigerant lines resulting from physical damage. According to research by the Texas A&M Energy Systems Laboratory, liquid line restriction can reduce EER by 56%, while other restrictions can impact performance by 25%.
7. *Compressor short cycling.* Compressor short cycling can be caused by coil blockage, equipment oversizing, and poor thermostat location, among other reasons. It is characterized by repeated run times shorter than three minutes. Since it takes at least 3 minutes for an RTU to achieve steady state and full cooling capacity, short cycling can result in a significantly decreased average efficiency, even if there are no physical failures in the equipment. According to AEC's Small HVAC System Design Guide, short cycling can cause efficiency penalty of approximately 10%. In addition to the energy cost, short cycling is one of the most common causes for early equipment failures, as the undue cycling impacts several components adversely.
8. *Sub-optimal economizer setpoint.* Economizer damper actuation is controlled by an outdoor air temperature set point which returns the outdoor air damper to a minimum ventilation position when the outside air is too warm to provide cooling. An economizer set to changeover at 55°F significantly limits the number of hours for economizer operation compared to a 75°F set point, as Title 24 recommends for most California climate zones. Some economizers have adjustable set points, while others do not, but it is common that set points are not selected optimally. The opposite problem can occur as well. When a setpoint is higher than recommend or when an outside air damper is stuck open, there may be an unnecessary increase in heating and cooling energy.

9. *Economizer damper failure.* Often, economizers fail to actuate at all. This can be due to a motor failure, link failure, or jammed damper blade. The failure results in significant energy inefficiency, either because of an undue addition of heating and cooling load when stuck open, or a missed opportunity for free cooling when a damper is stuck closed.
10. *Excess outside air.* When an economizer damper is stuck open, or when a system is commissioned with a higher than necessary ventilation rate, it causes an energy penalty because of additional heating and cooling load. The energy penalty of this fault differs by climate zone, but can dramatically increase energy use for heating and cooling.

**Figure 96: Prevalence of Various Fault Types in RTUs (NBI 2004)**



There are various technical strategies to detect and diagnose faults. Each method takes a different approach on what points to measure in a system, and how to interpret measurements as distinct indication of particular faults. Some fault detection strategies measure refrigerant circuit variables only, such as temperatures and pressures, to alarm when there is an identifiable problem. Some monitor the air-side of the system to detect deficiencies. Other strategies use electric power measurements, or vibration as a proxy to identify various operating modes, and can identify the presence of faults based on operating history, and signal patterns compared to nominal expectations. Some methods are able to diagnose faults and their underlying causes explicitly, while others are designed to send alarm signals when there is a clear degradation in system performance. Each strategy has different cost effectiveness implications, and technical energy savings potential according to what faults it is able to

capture. In 2010 and 2011 the Western Cooling Efficiency Center installed and evaluated several different fault detection technologies in an effort to understand and characterize their range of capabilities. Table 2 compares nine different specific AFDD technologies by their technical ability to measure particular faults.

#### *California Title 24 Requirements for AFDD*

Since 2008 AFDD for RTUs has been a Title 24 compliance option, but the requirements for fault detection capabilities were not explicitly defined, and the technology has not been broadly applied. The research results presented in this case study informed the recent Title 24 requirement for AFDD as a mandatory measure for all new commercial unitary DX systems with an economizer and mechanical cooling capacity larger than 4.5 tons. This includes split systems, and variable refrigerant flow systems with economizers. Development of the requirement was supported by a broad industry stakeholder collaboration through the Western HVAC Performance Alliance. The mandatory requirements become effective January 1, 2014. An evaluation of cost effectiveness and potential energy savings for the range of technology capabilities resulted in prioritization of the most important faults to detect. The code language requires AFDD to detect and communicate the following faults:

1. Air temperature sensor failure/fault
2. Not economizing when it should
3. Economizing when it should not
4. Damper not modulating
5. Excess outdoor air

Compliance will require laboratory testing for certification of fault detection technologies, and in-field verification of AFDD functionality for all new RTUs. In parallel to the Title 24 code change, the Western HVAC Performance Alliance AFDD Committee has launched a Project Committee for ASHRAE Standard 207.P to define a protocol for certification of AFDD technologies.

While there are several third-party AFDD tools available, it is anticipated that OEM's will begin to include these fault detection capabilities within standard production models, since many new RTU's already have alarm codes associated with certain faults. The most important shift will be toward communicating faults off-board so that they are actually addressed. Title 24 code requires AFDD technologies to annunciate faults detected to some form of fault management tool, the zone thermostat, or appropriate facility personnel. When applied universally for all new RTUs in California, it is estimated that annual energy use for RTUs would be reduced by 12%, amounting to more than 30 Million kWh savings across California over the next 15 years.

**Table 13: Comparison of Capabilities for Several AFDD Technologies**

|                            | FDSI INSIGHT V.1 PRODUCTION | SENSUS MI | CLIMACHECK | SMDS | NILM | LOW COST NILM | SENTINEL/INSIGHT BETA TESTING | VIRTJOULE | LOW COST SMDS |
|----------------------------|-----------------------------|-----------|------------|------|------|---------------|-------------------------------|-----------|---------------|
| Low Airflow                | ●                           | ●         | ●          |      | ●    | ●             | ●                             | ●         |               |
| Low/High Charge            |                             | ●         | ●          |      | ●    | ●             | ●                             | ●         |               |
| Sensor Malfunction         | ●                           | ○         | ●          | ●    |      |               | ●                             | ○         |               |
| Economizer non Functioning | ●                           | ○         | ○          | ●    |      |               | ●                             | ●         |               |
| Compressor Short Cycling   | ●                           | ○         | ●          |      | ●    | ●             | ●                             | ●         | ●             |
| Excessive Operating Hours  | ●                           | ○         | ●          |      |      |               | ●                             | ●         | ●             |
| Performance Degradation    |                             | ●         | ●          | ●    | ●    | ●             | ●                             | ●         | ●             |
| Insufficient Capacity      | ●                           | ○         | ●          |      |      |               | ●                             | ○         | ●             |
| Incorrect Control Sequence | ●                           | ○         | ●          |      | ●    | ●             | ●                             | ●         |               |
| Lack of Ventilation        | ●                           | ○         |            | ●    |      |               | ●                             | ○         |               |
| Unnecessary Outdoor Air    | ●                           | ○         | ○          | ●    |      |               | ●                             | ○         |               |
| Control Problems           | ●                           | ○         | ●          | ●    |      |               | ●                             | ●         |               |
| Failed Compressor          | ●                           | ●         | ●          | ●    | ●    | ●             | ●                             | ●         |               |
| Stuck Damper               | ●                           | ●         | ●          | ●    |      |               | ●                             | ○         |               |
| Slipping Belt              | ●                           | ●         | ●          |      | ●    |               | ●                             | ●         |               |
| Leaking Valves             |                             |           | ●          |      | ●    |               | ●                             | ○         |               |
| Unit Not Operational       | ●                           | ○         |            | ●    | ●    | ●             | ●                             | ●         | ●             |

●=STANDARD CAPABILITY ○=EXTENDED CAPABILITY

## 5.7 Industry Support & Outreach

Figure 97: WCEC Tour



Mark Modera explains the aerosol envelope sealing technology with the State Secretary for Infrastructure & Environment, the Netherlands

WCEC has been involved in numerous activities to support industry in advancing energy-efficient HVAC technologies. WCEC was able to participate and influence the progress on a number of efficiency measures through a host of technical meetings, conference and other outreach speaking engagements. WCEC participated and chaired technical committees at ASHRAE to help shape Title 24 policy with regards to Fault Detection & Diagnostics; wrote the standard protocol for properly evaluating evaporative cooling retrofits; as well as involvement with numerous committees involved in HVAC efficiency including (but not limited to) ACCA QH Standard 12 Advisory Committee, ASHRAE SPC 207P, TC 6.3 and TC 7.5.

Also of note, WCEC has met with and consulted on energy efficiency strategies for a large number of prominent businesses in California including (but not limited to) Wal-Mart, Target, and Wells Fargo. WCEC also met with many representatives from HVAC manufacturing, contractors and a diverse group of policymakers from Jordan, the United Arab Emirates, Australia, and even with Wilma Mansveld, State Secretary for Infrastructure & Environment for the Netherlands (Figure 97).

## REFERENCES

- Carrie, F.R.; Modera, M.P. (1998). "Particle Deposition in a Two-Dimensional Slot from a Transverse Stream." *Aerosol Science and Technology*, 28, pp. 235-246.
- Committee, A.S., ASHRAE HANDBOOK: Fundamentals 2013. 2013, ASHRAE.
- Data Taken From U.S. Energy Information Administration (EIA) ; Available from:  
<http://www.eia.gov/consumption/residential/>
- Drinking Water Treatability Database: Ozone, EPA.
- Emmerich, et. Al. Investigation of the Impact of Commercial Building Envelope Airtightness on HVAC Energy Use. National Institute of Standards and Technology. 2005. Ppg. 27
- Guidelines for Rainwater Harvesting. 2010; Available from: <http://www.ci.berkeley.ca.us/>
- P. Griffiths and P. C. Eames, "Performance of chilled ceiling panels using phase change material slurries as the heat transport medium," *Applied Thermal Engineering*, vol. 27, pp. 1756-1760, 2007.
- Health, C.D.o.P.; Available from: [www.cdph.ca.gov](http://www.cdph.ca.gov).  
[http://www.epa.gov/waters/tmdl/docs/33596\\_draftmdl\[1\].pdf](http://www.epa.gov/waters/tmdl/docs/33596_draftmdl[1].pdf)
- Liu, Zhijun, Allen, William, Modera, Mark. Simplified thermal modeling of indirect evaporative heat exchangers. HVAC&R Research. Vol.19, Issue.3, 2013.
- Managing Wet Weather with Green Infrastructure Municipal Handbook: Green Infrastructure Retrofit Policies. US Environmental Protection Agency, 2008
- McKenzie, E.R., et al., An investigation of coupling evaporative cooling and decentralized graywater treatment in the residential sector. *Building and Environment*, 2013. 68(0): p. 215-224.
- Wiley. Engineering, H., Handbook of Public Water Systems. 2002.
- Yu-sen E. Lin, R.D.V., Janet E. Stout, and Victor L. Yu, Negative Effect of High pH on Biocidal Efficacy of Copper and Silver Ions in Controlling *Legionella pneumophila*. 2002.
- Sherman, Max and McWilliams, Jennifer. Air Leakage of US Homes: Model Prediction. Lawrence Berkeley National Laboratory, 2007.

## GLOSSARY

| <b>Term</b>       | <b>Definition</b>  |
|-------------------|--|
| ACH               | Air changes per hour   |
| AFDD              | Automated fault detection and diagnostics                                  |
| AHU               | Air handling unit  |
| ASHRAE            | American Society of Heating, Refrigerating, and Air-conditioning Engineers |
| BTU               | British Thermal Unit   |
| °C                | Degrees Centigrade   |
| Ca                | Calcium  |
| CaCO <sub>3</sub> | Calcium carbonate  |
| CAHP              | California Advanced Homes Program  |
| ccm               | Cubic centimeters per minute   |
| CDD               | Cooling degree days  |
| CFM               | Cubic feet per minute  |
| CFU               | Colony forming units   |
| CoP/COP           | Coefficient of Performance   |
| CO <sub>2</sub>   | Carbon dioxide   |
| CZ                | Climate zone   |
| DCW               | Domestic cold water  |
| DHW               | Domestic hot water   |
| DO                | Dissolved oxygen   |
| DOC               | Dissolved organic carbon   |
| EC                | E. coli  |
| EER               | Energy efficiency ratio  |
| Energy Commission | California Energy Commission   |

|                 |   |
|-----------------|---|
| EPA             | United States Environmental Protection Agency |
| EPIC            | Electric Program Investment Charge            |
| EWT             | Entering water temperature                    |
| °F              | Degrees Fahrenheit                            |
| ft <sup>2</sup> | Square feet                                   |
| FC              | Fecal coliforms                               |
| GHE             | Ground heat exchanger                         |
| gpm             | Gallons per minute                            |
| GSHP            | Ground Source Heat Pump                       |
| GSHP            | Ground Source Heat Pump                       |
| HDD             | Heating degree days                           |
| HDPE            | High density polyethylene                     |
| HERS            | Home Energy Rating System                     |
| HH              | High hardness (water)                         |
| HVAC            | Heating, ventilation and air conditioning     |
| IEC             | Indirect evaporative cooler                   |
| IECC            | International Energy Conservation Code        |
| IEHX            | Indirect evaporative heat exchanger           |
| kg              | Kilograms                                     |
| kJ/kg/°C        | Kilojoules per kilogram per degree Centigrade |
| kW              | Kilowatts                                     |
| kWh             | Kilowatt hours                                |
| LDEB            | Large Diameter Earth Bore                     |
| LH              | Low hardness (water)                          |
| LISST           | Laser in-situ scattering and transmissometry  |
| LWT             | Leaving water temperature                     |
| mPCM            | Microencapsulated phase-change materials      |

|                 |   |
|-----------------|---|
| μs/cm           | Microsiemens per centimeter (measure of conductivity)   |
| Mg              | Magnesium   |
| mg/l            | Milligrams per liter  |
| mM              | Millimolar  |
| MPN             | Most Probable Number method   |
| MPN/100ml       | Most probable number per 100 milliliters  |
| NG              | Natural gas   |
| NH <sub>3</sub> | Ammonia   |
| NTU             | nephelometric turbidity unit  |
| Pa              | Pascals   |
| PCM             | Phase Change Material   |
| PG&E            | Pacific Gas and Electric Company  |
| PO <sub>4</sub> | Phosphate   |
| ppb             | Parts per billion   |
| ppm             | Parts per million   |
| PVDF            | Polyvinylidene difluoride membrane filter   |
| RD&D            | Research, development and demonstration   |
| RTD             | Resistive temperature device  |
| RTU             | Rooftop unit  |
| Smart Grid      | Smart Grid is the thoughtful integration of intelligent technologies and innovative services that produce a more efficient, sustainable, economic, and secure electrical supply for California communities. |
| SMUD            | Sacramento Municipal Utilities District   |
| TC              | Total coliforms   |
| TOU             | Time of use   |
| VFD             | Variable frequency drive  |
| WCEC            | Western Cooling Efficiency Center   |
| ZNE             | Zero net energy   |

